Acknowledgment

This thesis, which was carried out at the University of Stavanger in spring 2016, is the final product that concludes my master's degree in Mechanical and Structural Engineering with the specialization of Offshore Construction. My supervisor, associate professor S.A. Sudath Siriwardane, suggested the subject of this, which sounded fascinating and got me motivated to start working with it.

I would like to thank S.A. Sudath Siriwardane, who consistently offered valuable feedbacks and guidance with the challenges that I faced with the thesis. I would also thank Senior Engineer Samdar Kakay for his precious advice and guidance with the finite element analysis software Abaqus/CAE, and also for offering a helping hand whenever I needed.

Stavanger, 15th June 2016

Hikmat Saaid Saleh

Abstract

Lifting is an essential part of almost every offshore operation, which includes a variation of structures with different sizes, shapes and weights. To ensure safe lifting operations, lifting equipment must be utilized. Among these lifting equipment, pad eyes and shackles play a significant role. These pad eyes must have high safety, reliability and appropriate costs. To test and analyze the capacity of pad eyes, traditional checking methods, such as laboratory testing are usually used, which can be exhausting, time-consuming and somewhat expensive. Therefore, a simpler, equally precise, less time consuming and more cost effective would be a proper alternative solution. This alternative approach to the traditional checking methods would be the FE simulation software, Abaqus/CAE. The purpose of this thesis is to compare the FE simulation results of the capacity of the pad eyes, with the experimental and theoretical results of the pad eye capacity obtained from the previous study "Offshore Hook-up Project Management"[1].

To conduct the simulation analyses of the design load capacity of pad eyes, several tests had to be made. Theses tests included different pinhole sizes in the pad eyes, different strain directions of pad eye pinholes, and different loads that acted on the pad eyes. The purpose of this is to check the importance of following the requirements given in related standards. Each of the simulation tests that were carried out in two different cases. The first case was when the pad eye was without a plate, while the second was when the pad eye was firmly welded to a base plate. The purpose of this was to see how the addition of the plate to the pad eye affected the load capacity of the pad eyes.

The results that were obtained showed that the addition of the plate to the pad eyes increased the capacity of the pad eyes. They further showed that the larger the pinhole size, the less capacity the pad eye had, which indicates the importance of following standard's requirements. It was also observed that a reduction of the load capacity was recognized for angled loading relative to the vertical loading case, even though theoretical capacities provide the same for both cases. Finally, when the results were compared, it revealed that some of the simulation results were close to the experimental and the theoretical results, while others were somewhat far from them. Some factors, including the uncertainty of material behavior, may have caused these deviations.

v

Table of Contents

List of figures

List of tables

Abbreviations

CAE   Complete Abaqus Environment

SWL   Safe Working Load

FEM   Finite Element Method

FE   Finite Element

FEA   Finite Element Analysis

2D   Two-Dimensional

3D   Three-Dimensional

BC   Boundary Condition

MPa   Mega Pascal

NDT   None Destructive Testing

UTS   Ultimate Tensile Strength

Symbols

f_y	Tensile yield strength, [N/mm^2]
$\gamma_{m,1}$	Partial safety factor
t_{eff}	Effective thickness of a plate, [mm]
E	Elasticity Modulus [N/mm^2]
σ	Stress [MPa]
ε	Strain
υ	Poisson's ratio
N	Newton
mm	Millimeters
σ_{Mises}	Von Mises stress [MPa]
U$_2$	Vertical displacement
kgf	Kilogram-force
σ_{von}	von Mises stress
ε_p	Plastic strain
σ_{YS}	Tensile Stress
σ_u	Ultimate Tensile Stress

1 Introduction.

1.1 Background and motivation.

Lifting operations in the Norwegian Continental Shelf include a variation of structures with different sizes, shapes and weights, and most of those structures weigh under 50 tonnes. These structures are lifted from the sea to the platform (or from the platform to the sea) using platform cranes. Over two hundred different lifting operations can occur in a single vessel. We usually divide the lifting operations into five phases:

- The lift-off from the deck.
- Lifting in the air.
- Crossing the splash zone.
- Lowering the structure through the sea water.
- The landing of the structure on the seabed.

To ensure that these lifting operations are carried out safely, lifting equipment must be utilized, among which pad eyes and shackles play a significant role. In this thesis, we focus on the capacity of pad eyes in the subsea lifting operations. To test and analyse the ability of pad eyes to withstand external loads, we usually use traditional checking methods such as laboratory testing. However, the problem with that type of approaches is that it can be exhausting, time-consuming and somewhat expensive. Therefore, a simpler, equally presice, less time consuming and more cost effective would be a proper alternative solution to the traditional checking methods.

1.2   The "offshore hook-up project management" thesis

The previous study [1] was about the offshore hook-up project management where different issues and various parts of the hook-up project were addressed, such as testing the capacity of pad eyes in the laboratory, risk analysis, the importance of safety and overall project management. The offshore field, which that thesis was based on, was Ekofisk, and in particular, the platform Ekofisk 2/4 L.

The approach that was used in the "offshore hook-up project management" project was based on comparing the theoretical results with the experimental results to investigate the difference between them. To be able to compare the results, the theoretical calculations were carried out first and then several tests were done to analyze the experimental load capacities of the pad eyes and to study their plastic stress behavior.

1.3   Objective

In this thesis, we will use a different approach than the one utilized in [1]. Engineers around the world in many major oil and gas companies are efficiently using this method, namely the FE software Abaqus/CAE. The primary objective of this master's thesis is to compare the simulation results of the capacity of 3.25-ton pad eye, when subjected to different load magnitudes in different directions, to the experimental and theoretical results of the pad eye capacity, from the previous study [1]. That table contained ten tests, which we are considering only six of them (marked with red in the table below).

Table 1.1 – Comparison basis from [1] and [2]

Table 2. Comparison of test results with design load capacities

Test Specimen	Hole diameter (mm)	Direction of load	Shackle SWL (Tons)	Load capacity (Tons)		Remarks
				Theoretical	Experimental	
1	22	Vertical	3.25	26.2	>21.0	0.5mm displacement
2	32	Vertical	9.25	20.7	>21.0	1.5mm displacement
3	32	Vertical	3.25	20.7	>21.0	3.5mm displacement
4	42	Vertical	3.25	15.3	14.5	Large deformation of shackle
5	22	Angled	3.25	26.2	>14.0	Large deformation
6	32	Angled	3.25	20.7	>15.0	Large deformation
7	42	Angled	3.25	15.3	>14.5	Large deformation
8	22	Vertical	3.25	26.2	>25.5	Large deformation
9	32	Vertical	3.25	20.7	24.2	Large deformation of shackle
10	42	Vertical	9.25	15.3	18.0	Large deformation of shackle

1.4 Scope and limitations

In many cases, offshore structures can only be lifted by cranes with the help of slings and shackles, which are attached to the pad eyes, which are formed on the structure. These pad eyes must have high safety, reliability and appropriate costs. Transporting accidents have occurred in the past because of the breakage of the pad eyes in the construction process in many shipyards. Because of the lacing of a simple, safe and yet accurate method for stress and strain analysis in pad eyes, designers are forced to use cumbersome and somewhat unsafe methods for pad eye analysis and design [3]. A simpler method for the determination of stresses in pad eyes is essential for promoting the safety of pad eyes, which would be the finite element analysis software Abaqus/CAE.

The scope of this thesis we will be to use the finite element analysis software Abaqus/CAE to verify the capacity of a 3.25-ton pad eye. We will test the pad eye three times where we increase the hole diameter each time to see how the growth in hole diameter in the pad eye affect its capacity and its plastic behavior.

1.5 Overview of the Thesis

The introduction to this thesis is described in chapter one while chapter two and three will present the theoretical part and the relevant standard guidelines, which is the basis for the analysis of the 3.25-ton pad eye used in this thesis.

In chapter four, the methods employed to outline how the modelling and analysis of the pad eye in Abaqus/CAE, are performed. This chapter will also include the FE simulation results.

Chapter five will present the comparison and discussions of the results while Chapter Six will describe the conclusion and recommendations for future work.

2 Lifting Equipment – Pad eyes

2.1 Introduction:

In this chapter, we will cover the theoretical part of this thesis. In it, the terms "pad eyes" and "shackles" will be explained, we will describe the conceptual approach to design load capacity, and the pad eye analysis will be presented. We will also describe different types of pad eyes and their relationship with shackles. And finally, the material properties of the pad eye will be described.

2.2 Lifting equipment guidelines

It would be of great advantage and necessity if lifting operations would be in accordance with standardized calculations. In 2012, NORSOK provided a new standard, R-002 "Lifting equipment" [4]. The purpose of this design code is to make sure that there is a reasonable and acceptable level of safety to human lives and injuries, environment and assets in the petroleum industry, by providing technical requirements and regulations for lifting equipment, which are in alignment with lifting operation requirements on the Norwegian Continental Shelf. Pad eyes and shackles are two very important parts of lifting equipment.

2.3 Padeyes and Shackles

A **pad eye** (also called lug) is a device made of steel, which is used in both offshore and onshore applications, as an attachment point, and is welded or fixed on a part (usually to the deck or the hull) of the vessel. In offshore applications, pad eyes are typically used to assist a safe lifting operation, which is done by connecting the slings to the pad eyes by shackles.

Figure 2.1 – the 3.25-ton pad eye [1]

Shackles are U-shaped metal pieces which are secured with a bolt to prevent unwanted openings of the shackles. They are the main connecting links in all subsea lifting operations, from different types of vessels to industrial crane rigging, as the quickly can be connected and disconnected.
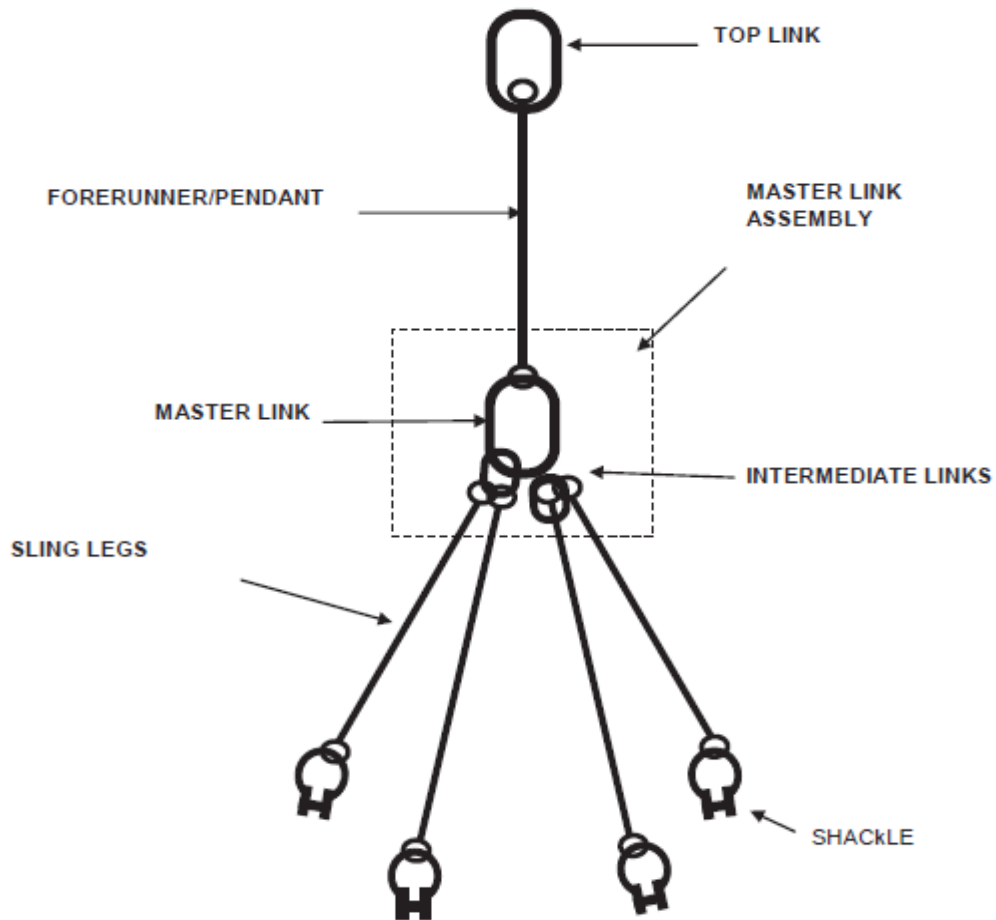
Figure 2.2 - A demonstration of the lifting set terminology [4]

2.3.1 Types of pad eyes:

There are three main types of pad eyes with different design geometries [4]:

- Type 1: The basic type manufactured from one single plate.
  Typical for shackles with WLL $\leq$ 8.5 tonnes and load angle between $-90^o \leq \alpha \leq 90^o$.

- Type 2: Has one cheek plate fillet welded on each side of the plate.
  Typical for shackles with WLL $\leq$ 55 tonnes and load angle between $-90^o \leq \alpha \leq 90^o$.

- Type 3: Has a boss partly welded to the plate with full penetration weld.
  Typical for shackles with WLL $\leq$ 55 tonnes and load angle between $-90^o \leq \alpha \leq 90^o$.
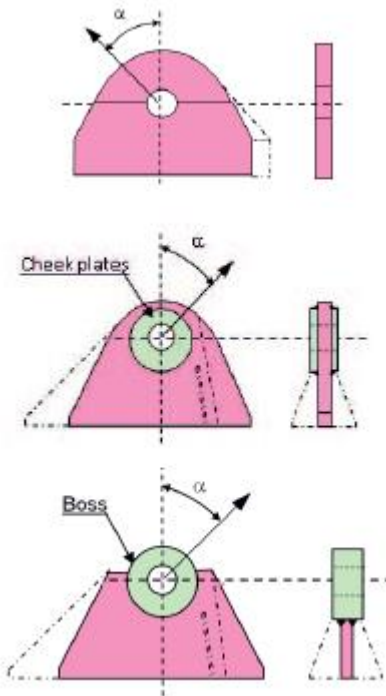
Figure 2.3: Pad eyes type 1, 2 and 3 (Dotted lines indicate alternative designs) [4]

2.3.2 Padeye and shackle accommodation

According to NORSOK R-002 [4], "Lifting lugs (pad eyes) should be designed to match the relevant standard shackle dimensions, and to account for tolerance deviation between the different shackle types. The selected shackle shall house both lifting lug and selected sling or hook", (see Figure 2.4 and Table 2.1); this means that the design of the pad eye must take the size and the shape of the shackles into consideration. Once we create the pad eye, there will be only one size of shackle, which will fit. Therefore, the designer should determine the size of it and all of its details, before designing the pad eye. In this thesis, we will neglect "Type 2" and "Type 3" and only focus on "Type 1" of the pad eye types given in Figure 2.3.
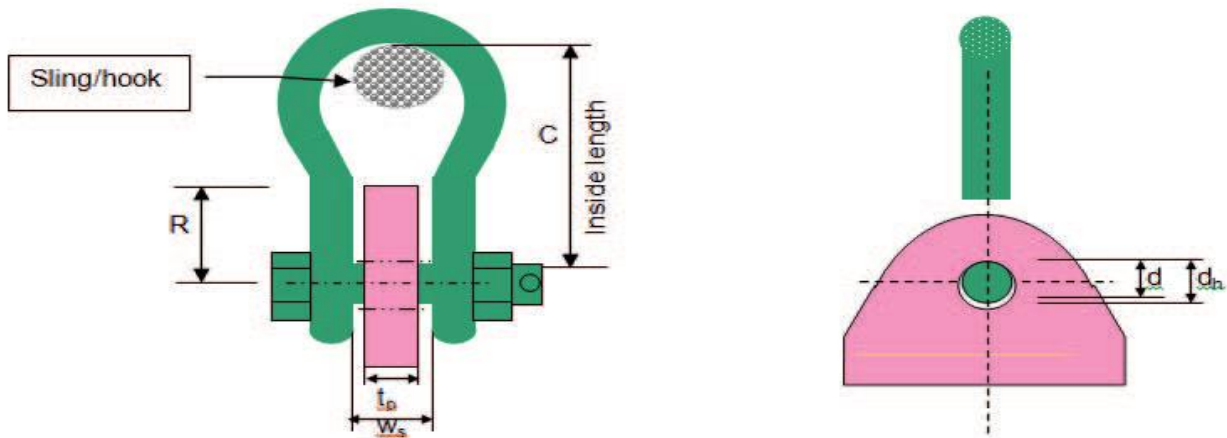
Figure 2.4 - Padeye vs. shackle interface. Type 1 lifting lug shown. [4]

Table 2.1 - Type 1 - single plate, relationship between shackles and pad eyes [1]

SWL	dh	tp	R	h	L	k	aw
tonn	mm	mm	mm	mm	mm	mm	mm
2	19	15	30	45	110	15	6
3,25	22	20	35	50	120	20	7
4,75	25	25	35	55	140	25	7
6,5	28	30	40	65	160	30	8
8,5	31	35	50	70	180	35	9
9,5	35	35	50	80	200	35	9

3 Theories and design guidelines of pad eyes

In this chapter, the theoretical part and the standardized regulations and guidelines about pad eyes and shackles will be covered. In it, the material properties of the pad eye steel used in this thesis, in reference to DNV will be described, and also the stress – strain relationship will be explained. The measuring of stresses and strains will also be described. Finally, the theoretical and experimental approaches from [1], to design the load capacity of pad eyes, will be reviewed, as they are an essential part of this thesis.

3.1 Pad eye modelling according to DNV standard

3.1.1 General

The demand for non-linear, plastic analysis has increased in recently. Therefore, the first requirement is that the selected material model should be able to represent the non-linear behavior of the steel when we both increase and decrease loading so that it can describe the structural response of the material sufficiently [5].

To obtain the correct representation of the non-linear behavior of the pad eye steel in this thesis, the time-independent elastic-plastic model in Abaqus/CAE has to be used. The main component in this case for such time independent elastic-plastic model is the yield surface, which shows when the plastic strains are generated in the pad eye after we run the simulation. We usually use the von Mises yield function for capacity analysis of steel structures.

3.2 Stress - Strain Relationships

When a pad eye is placed in a tension-compression-testing machine, each time the axial load gets increased, the elongation over the gauge length is measured, this continuous until it reaches the failure. This procedure describes the stress-strain relationship, which is important because it allows us to derive the load-stress and load-displacement for the pad eyes considered in this thesis. The relations are utilized to study the elastic and plastic material behaviors. The stress-strain relationship is usually described by the stress-strain diagram, which varies for different materials [6].

3.2.1   Material properties

A stress-strain diagram is typically used to determine some specific material properties of a structure or a part of that structure. Let us consider a tensile specimen which is subjected to strain, resulting from a load. If the strain in the specimen and the load which caused that strain, returns to zero at the same time, then the material is within its elastic limit (no permanent deformation, see part 0A in Figure 3.1 (a)). However, if the load produces a stress that exceeds the elastic limit (stress at point J in Figure 3.1 (a)), the strain does not disappear when the load returns to zero (curve JK in Figure 3.1 (a)). The material has exceeded the elastic limit and is now in the plastic zone, which means that the steel specimen is permanently deformed.
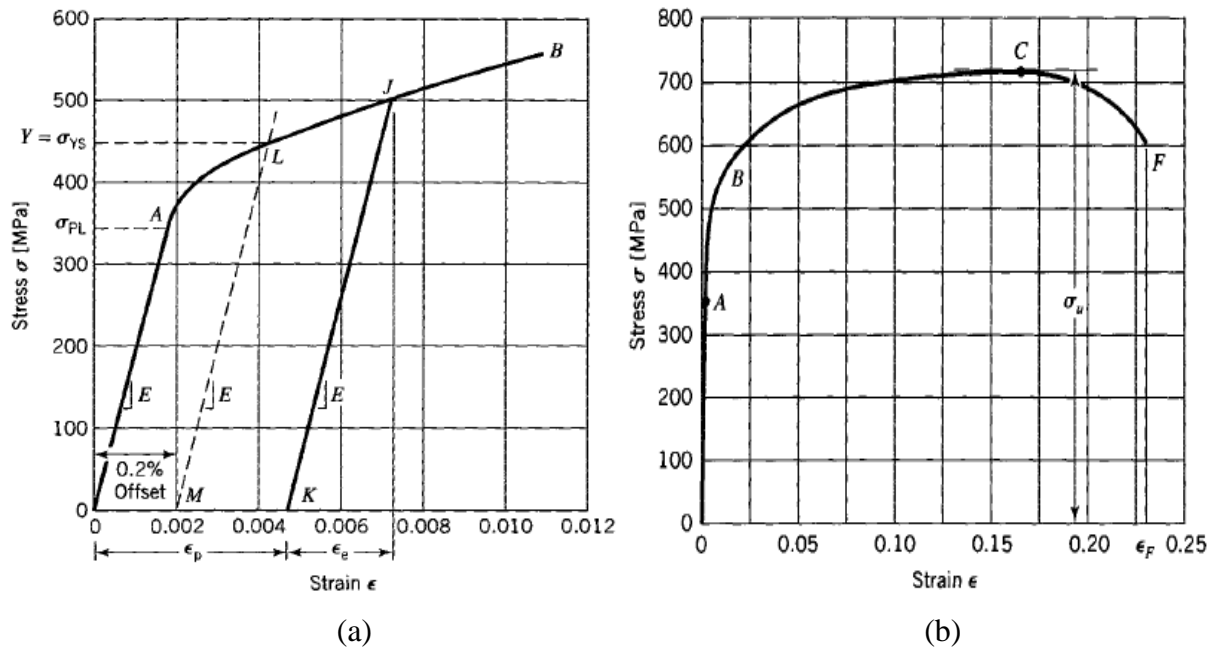
Figure 3.1 – Engineering stress-strain diagram of a tension steel specimen [7]

A critical parameter from the stress-strain relationship is called **yield strength** (point L in Figure 3.1), which is the stresses that lead to a specific amount of deformation. Another critical parameter is called **ultimate tensile strength,** which determines the strength of a material and it's ability to withstand external loads, [6] (point C in Figure 3.1 (b)).

In this thesis, we will steel type S355, which is widely used in structural applications. Note that higher steel class gives higher yield strength. For example S355 has higher yield strength than S235, see Tables Table A.2 in APPENDIX A. The material properties of the pad eye used in this thesis are based on the previous study [1] and DNV-RP-C208 [5], (see Table A.2)

Table 3.1 - Non-linear properties for S355 steel (Engineering stress-strain) [5]

Thickness [mm]	20
E [MPa]	210000
σ_{prop} [MPa]	310.5
σ_{yield} [MPa]	345
σ_{yield2} [MPa]	348.4
σ_{ult} [MPa]	470
ε_{p_y1}	0.004
ε_{p_y2}	0.02
ε_{p_ult}	0.15

The following graph explains the parameters in Table 3.1
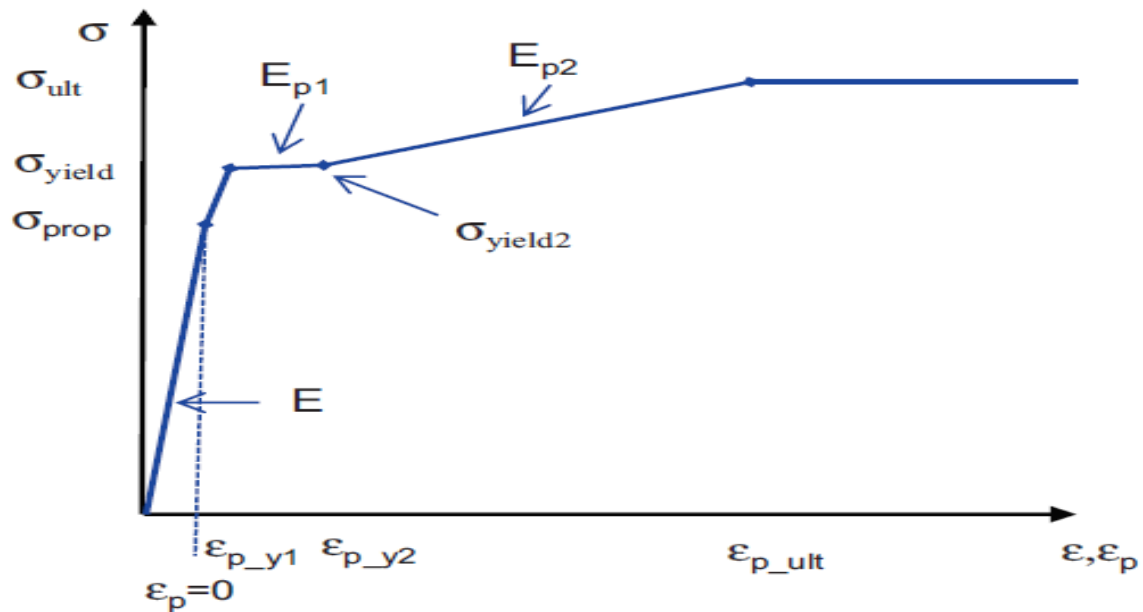
Figure 3.2 - Parameters in stress-strain curve [5]

12

3.2.2 Cyclic stress–strain curves

Cyclic stresses and strains are the distribution of stresses and strains that change over time in a repetitive manner. It is required that we apply the cyclic stress-strain curves of the materials. We can use the true stress-strain curves from Figure 3.3, unless we know the actual cyclic behavior of the material. The curves in Figure 3.3 are described according to the Ramberg-Osgood relation [5]:

$$\varepsilon = \frac{\sigma}{E} + \left(\frac{\sigma}{K}\right)^{10}$$

Where K is a constant that depends on which material we are considering, the value of K is given in the following table:

Table 3.2 - Value of coefficient K [5]

Table 5-3 Ramberg-Osgood parameters for base material	
Grade	*K (MPa)*
S235	410
S355	600
S420	690
S460	750

The curves in the following figure are based on Table 3.2, are given below:
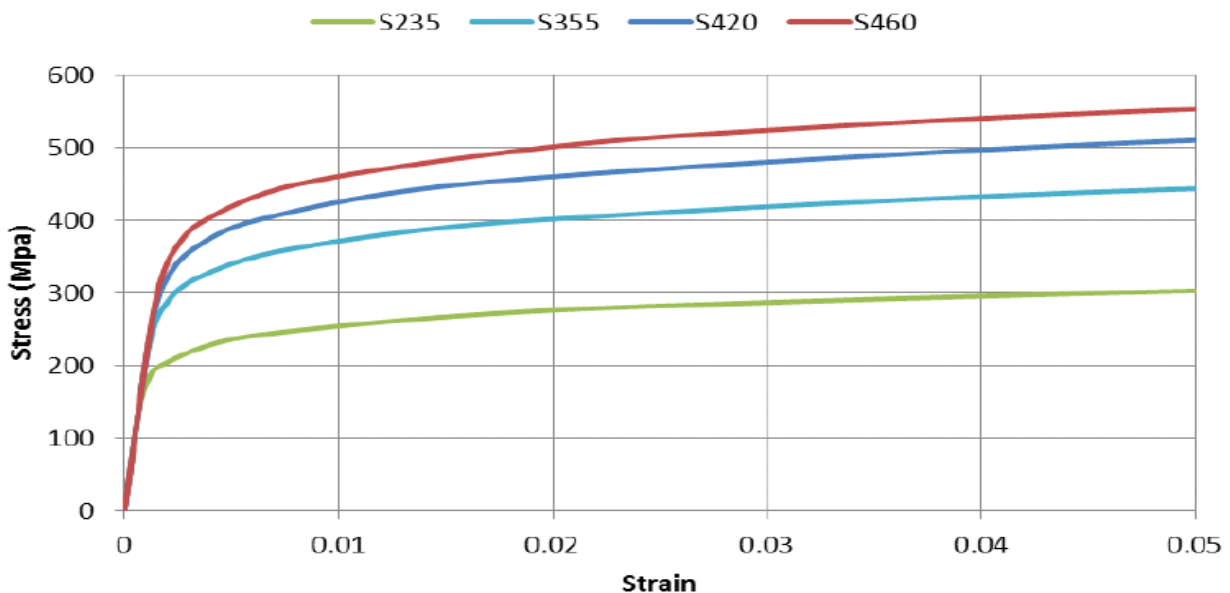
Figure 3.3 - True cyclic stress-strain curve for typical offshore steel grades [5]

13

3.2.3   Stress and strain measures

We can measure stresses and strains in several ways, but the two most important ways applicable in our case are:

- Engineering stress
- True stress

Let us assume that we place the pad eye a tension-compression-testing machine, the load that is divided by the cross-sectional area is stress. Before we started pulling the pad eye we had a particular cross section, the **Engineering stress** is the load divided by this original cross section. While the tension-compression-testing machine is pulling the pad eye, deformations occur and geometries changes, at any load, the load divided by the cross-sectional are at that instant is called **True stress [8].** When we test materials, the results are often given as "Engineering" stress-strain, while the FE software input is often "True" stress-strain. We will focus only engineering stress and strain in this thesis.

3.3 Design load capacity – Theoretical Approach

The theoretical pad eye analysis was an essential part of the previous study [1], and since we are going to compare our simulation results to the theoretical (and the experimental) results from that thesis, it is important to have a brief review of it.

The analysis of pad eyes is complicated to some extent because several interacting failure modes are affecting the pad eye simultaneously. Those failure modes occur in different areas of the pad eye, see Figure 3.4.
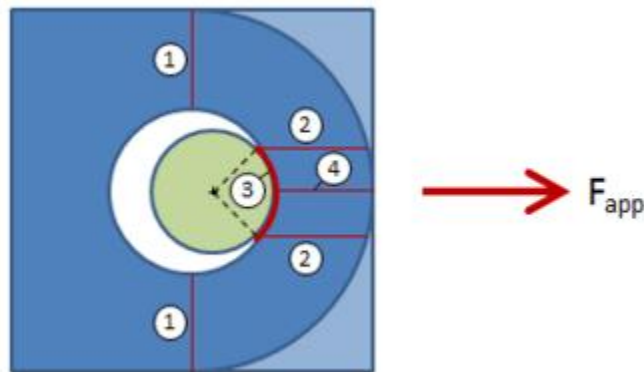
Figure 3.4 - Different failure modes in a pad eye [9]

As shown in Figure 3.4 - Different failure modes in a pad eye [9]above, several failure modes occur in a single pad eye under loading; the numbers corresponds to the numbered sections, which we have listed below:

1. Tension failure
2. Tear-out failure
3. Bearing failure
4. Hoop tension failure

In this section, we focus only on the tear-out failure and the bearing failure, which are both essential and very commonly used design criteria for prediction of load capacities of pad eyes and shackles.

3.3.1 The design of tear-out loads of pad eyes

Here we describe the design load capacity of pad eyes without their cross sections being subjected to tear out. The design tearing-out load can be derived as [2]:

$$P_t = 2\,\tau_{Rd}A_{sh}$$

Where:

$\tau_{Rd} = \dfrac{f_y}{\gamma_{m,1}}\sqrt{3}$ is the design shear strength.

f_y is the tensile yield strength of plate material.

$y_{m,1}$ is the partial safety factor and is defined by Table 3.3.

$A_{sh} = (R - \dfrac{d_h}{2})t_p$ is the tearing-out area.

R is the outer radius.

d_h is the hole diameter of the pad eye plate.

t_p the thickness of the plate.

Table 3.3 - Material safety factors section 6.1 from [10]

Type of calculation	Material factor 1)	Value
Resistance of Class 1,2 or 3 cross-sections	γ_{M0}	1.15
Resistance of Class 4 cross-sections	γ_{M1}	1.15
Resistance of member to buckling	γ_{M1}	1.15
Resistance of net section at bolt holes	γ_{M2}	1.3
Resistance of fillet and partial penetration welds	γ_{Mw}	1.3
Resistance of bolted connections	γ_{Mb}	1.3

3.3.2   The design of bearing load of pad eyes

Here we describe the design load capacity of pad eyes without them being subjected to bearing failure. The design-bearing load can be derived as [2]:

$$P_b = f_{b,Rd} t_{eff} d$$

Where

$f_{b,Rd} = 1.5 \dfrac{f_y}{\gamma_{m,1}}$ is the design shear strength.

f_y is the tensile yield strength of plate material.

$y_{m,1}$ is the partial safety factor.

$t_{eff} = t_{p\,is}$ the effective thickness of the plate.

d is the diameter of the shackle bolt as shown in Figure 2.4

3.4   Design Load Capacity- Experimental Approach

The other essential part of the previous study [1] was the experimental approach for the determination of the load capacity. Ten different tests of pad eyes were made in the laboratory. The majority of them (eight) were pad eyes with the Safe Working Load (SWL) of 3.25 tons, while only two of the ten tests were pad eyes with SWL of 9.25. The ten pad eye specimens differed in the pinhole size, the SWL and the load direction (Quasi-static load test), which acted on the pad eyes.

The pad eyes were then welded to the plates by using full penetration welding technique. To ensure that the pad eyes were firmly and correctly welded to the plates, some NDT techniques were utilized. The capacity of the pad eye specimens was then tested in combination with the shackles, the tension cylinders, and the dynamometer (measure the force on the samples), see Figure 3.5.
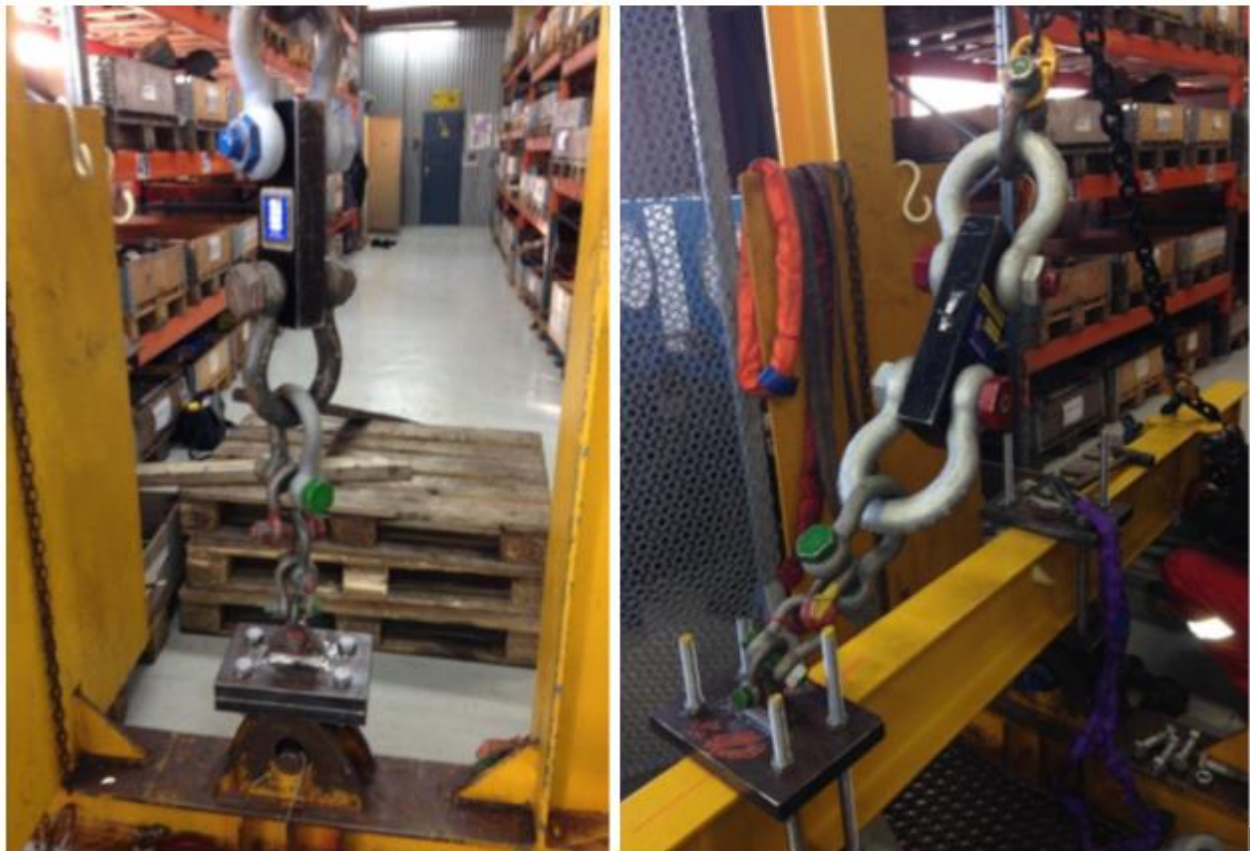
Figure 3.5 – Test set-up of the vertical and angular strain test [1]

4 Design Load Capacity – Simulation Approach

4.1 Introduction – FE Analysis of pad eyes

After the capacities of the pad eye specimens were determined by using the theoretical and experimental approaches in the previous thesis [1], the design load capacity will be taken a step further. In this chapter, the load capacity of the pad eyes will be determined by the FE simulation approach, the FEA software Abaqus/CAE. Before going on with the procedure, it is important to have an idea about the finite element method, as it is an essential term in this thesis.

In the current modern and technological world, the engineers are challenged to accomplish increasingly complicated and costly projects, which are expected to have a high level of safety and reliability. These projects exist in some of the most important fields in our modern world, such as structural engineering applications, space travel, automobile industry, the airline industry, etc., where the safety and reliability are of immense importance. To be able to understand those complicated systems, the analysis needs numerical techniques so that they can simulate the behavior of those physical systems.

Some engineering tools (mechanics of solids, thermodynamics, etc.) are used to describe the behavior of physical systems in the form of partial differential equations, which are complicated non-linear equations that describes the nature of those systems. One of the most commonly used tools to solve such equations is FEM [11].

In other words, FEM is a way that engineers invented to solve engineering differential equations, for example, structural equations. Those differential equations may solve/answer questions like:
- What are the stresses in a bridge if a big truck drives across that bridge?
- If a large structure is in motion due to external forces such as the wind, what are the stresses in that structure and will it withstand those external forces?
- Can a ship with specific geometries and material types withstand storms at sea?
- What are the stresses and displacements in a pad eye under a particular external force and can this pad eye withstand this loading?

To be able to apply this method (FEM) we must use computer software. These types computer software can solve several types of problems such as linear and non-linear regions in both one-, two and three-dimensions. The proposed alternative solution, in this project, to the traditional checking methods, is a finite element software known as Abaqus/CAE. We can find the regulations for the finite element methods (FEM) in DNV-RP-C208 "Determination of Structural Capacity by Nonlinear FE Analysis Methods" [5].

4.1.1 The FEA software Abaqus/CAE

Abaqus/CAE is an engineering simulation software based on finite element methods that provide a simple, yet highly efficient way of analyzing and simulating the behaviors of a wide variety of some of the most common materials used in engineering applications such as metals, rubber, polymer, reinforced concrete, etc. Those material behaviors might be both linear and non-linear. Although we will mainly use Abaqus/CAE in this thesis for analyzing stress and displacements of the pad eye, it can also be used to study several other problems than mechanical problems (stress, strain, deflections, elasticity, plasticity, etc.). Those problems might be thermal (conductivity, heat generation, heat fractions, etc.), electrical/magnetic (electrical conductivity, magnetic permeability, etc.) and other problems such as mass diffusion, pore fluid, etc. With Abaqus/CAE, we can practically model any geometry, accurately and efficiently. [12]

Abaqus/CAE provides a simple approach for creating, submitting, observing and then evaluating results from Abaqus/Standard and Abaqus/Explicit simulations. The difference between Abaqus/Standard and Abaqus/Explicit is that Abaqus/Standard can solve simple finite element models, for example examining a static response of a model under loading. While Abaqus/Explicit is more suited for complex problems such as studying the dynamic response of a model under immediate loading [13].

Abaqus/CAE provides a practical and systematic approach to the modelling process to get the results for our inputs. This systematic process contains several modules that start from **Part, Property, Assembly, Step, Interaction, Load** (which also includes **Boundary Condition**), **Mesh, Optimization, Job, Visualization** and then ends with **Sketch.** We will describe these modules in details later in this chapter.

4.1.2 A simple Abaqus/CAE example.

To get acquainted with the finite element analysis (FEA) software Abaqus/CAE, modelling a simple design was carried out before starting with the pad eye modelling. This model was a plate with an elliptical hole in the middle with a major axis 2a, and the minor axis 2b, see **Feil! Fant ikke referansekilden.**.

A uniform tensile stress of 1000 N/mm² is applied at the top end of the plate, 150 mm above the centre of the ellipse, and distributed tensile stress is directed perpendicularly to the major axis 2a. See Figure 4.1
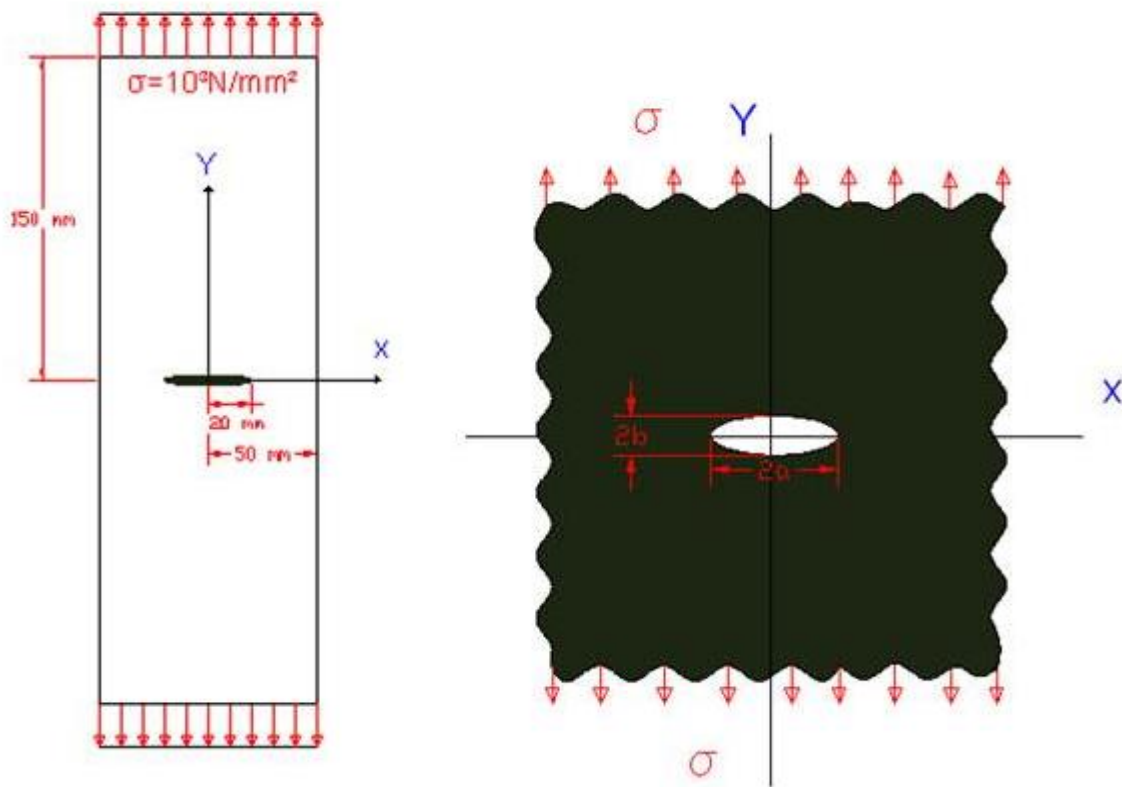
Figure 4.1 - Geometries of the plate with ellipse

The magnitude of the stress at the ends of the major axis of the ellipse will be calculated, which logically will be the most critical zone (zone with highest stresses). Those magnitudes will be determined by the following formula [14]:

$$\sigma_{\beta\beta(\text{max})} = \sigma\left(1 + 2\sqrt{\frac{a}{\rho}}\right)$$

Where

ρ is the radius of the curvature of the ellipse at the end of the major axis and is deined by:

$$\rho = \frac{b^2}{a}$$

Where a and b are the major and the minor axis of the ellipse.
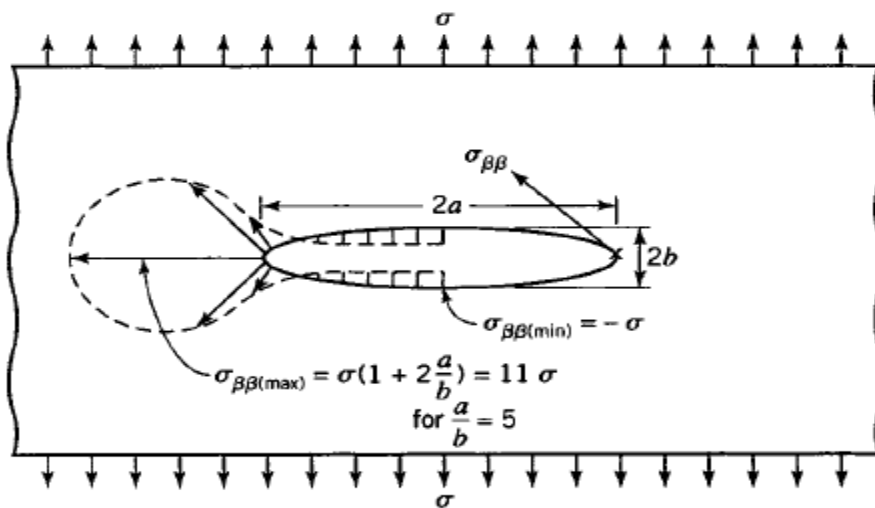
Figure 4.2 – Distribution of $\sigma_{\beta\beta}$ around an elliptical hole in an infinite plate [14]

From the above formulas we get:

$$\rho = \frac{b^2}{a} = \frac{2.0^2}{20} = 0.2$$

Hence:

$$\sigma_A = \sigma\left(1 + 2\sqrt{\frac{a}{\rho}}\right) = 1000\,{}^N/_{mm^2}\left(1 + 2\sqrt{\frac{20mm}{0.2mm}}\right) = 21000\,{}^N/_{mm^2}$$

Now we module the plate in Abaqus/CAE with elastic analysis to find the critical zone of the plate.

Material properties:

Material behavior: Elastic

Modulus of Elasticity, E = 210000 MPa

Poisson's ratio, v = 0.3

Boundary Condition is fixed at the bottom end.

Load is equal 1000 N/mm2

And for the **meshing** it is important to note the by changing the element size, both globally (of the hole plate) and the locally (at areas of interest, which is the elliptical hole in this case) slightly different results will be obtained.

After putting the data above in Abaqus/CAE, the following results in Figure 4.3 were determined:
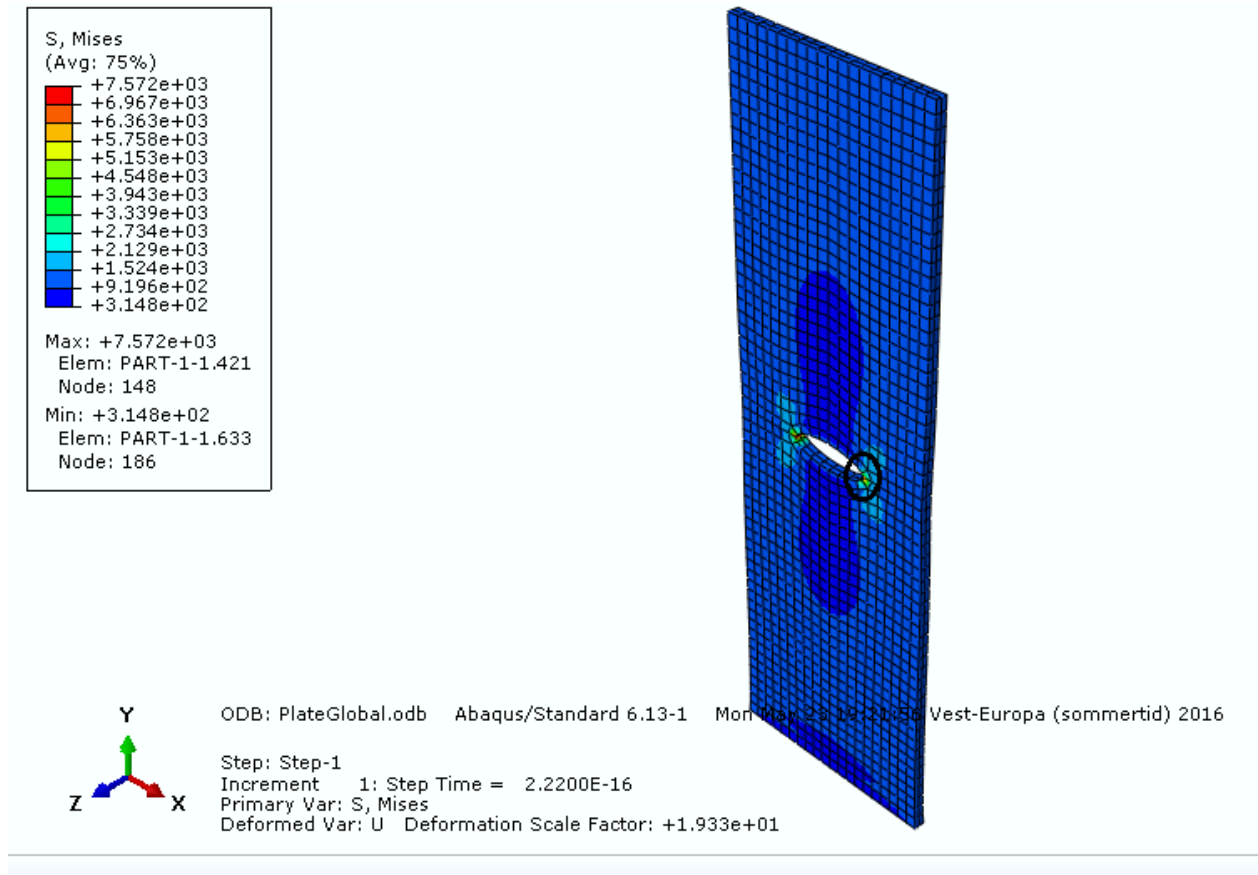
Figure 4.3 - Global meshing

In **Feil! Fant ikke referansekilden.** only the global meshing size was applied, which means the same element sizes for all of the nodes at the plate. It is also obvious from the figure above that the highest stress magnitude is at the end of the major axis of the ellipse, in the black circle (same stress at both ends because of symmetry) as we assumed. The results obtained was $\sigma = 7572\ MPa$, which is much lower than the theoretical result $\sigma_{\beta\beta(\text{max})} = 21000\ MPa$.

Now, more local elements will be added around area of interest, which is the ellipse, to see how that affects the stress magnitudes:
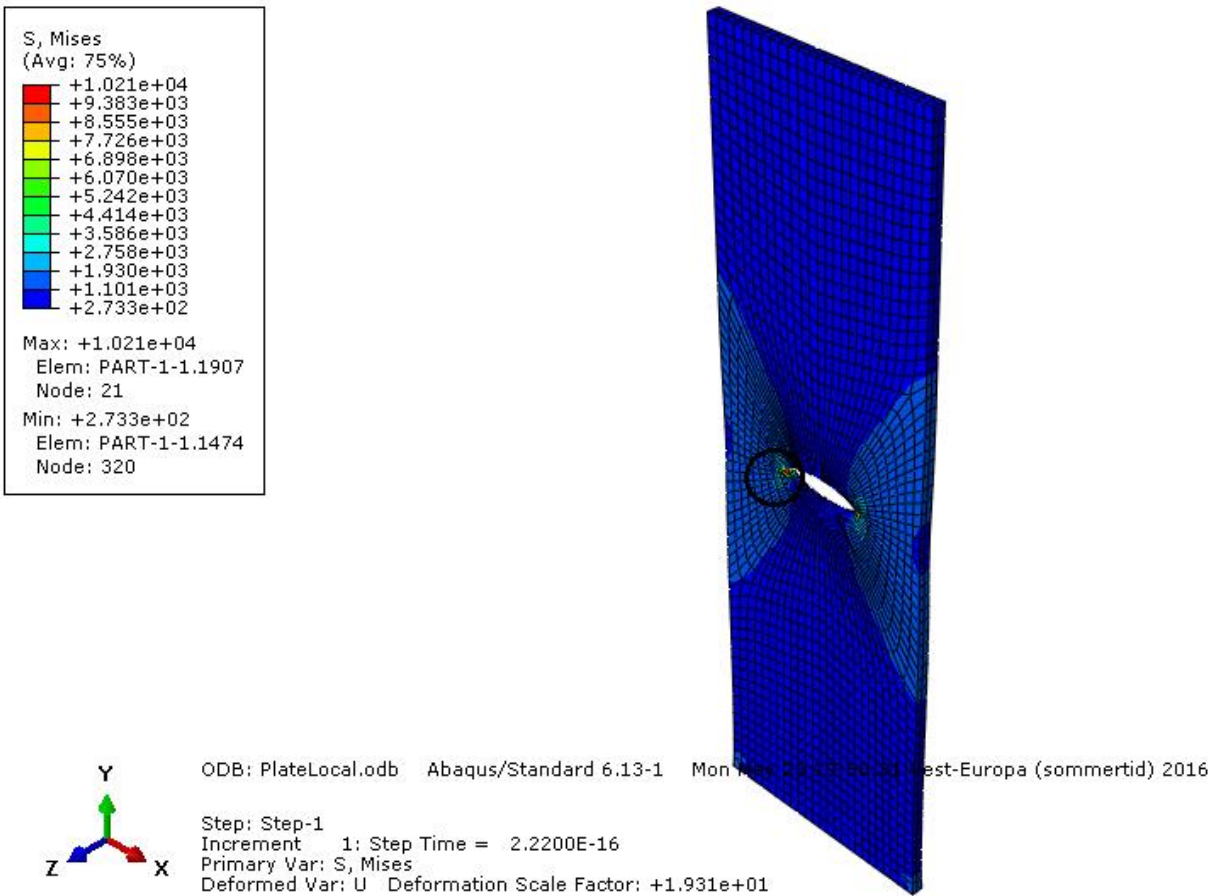
Figure 4.4 - Global and local meshing

As seen from Figure 4.4, the change in element size leads to a change in the stress magnitude that we get, which is more exact. The highest stress is at the end of the major axis of the ellipse (black circle), which $\sigma = 10\,210\,MPa$ and is closer to the theoretical result which we got which was $\sigma_{\beta\beta(\text{max})} = 21000\,MPa$.

4.1.3 The modelling procedure

The process of modelling the 3.25-ton pad eye will be divided in two different cases:

The first case: The pad eye is welded firmly to a structure at the bottom end, without the use of a plate. See   Figure 4.5.
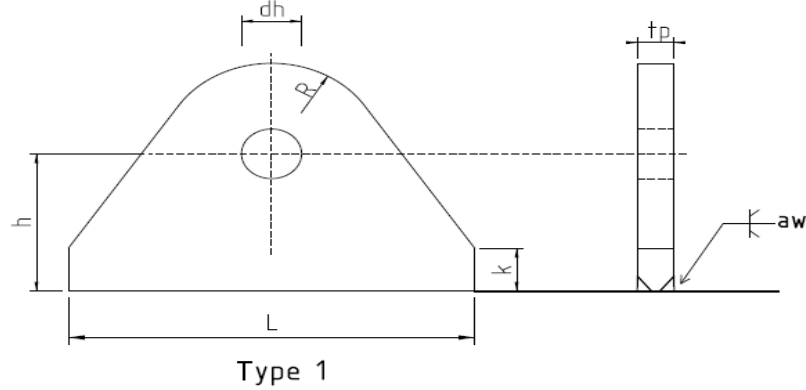
Figure 4.5 - Pad eye without plate

The second case: The 3.25-ton pad eye will be welded to a 20 mm thick plate with full penetration welding [15]. The plate consists of four bolt-holes through which four bolts of 26 mm diameter will be placed.
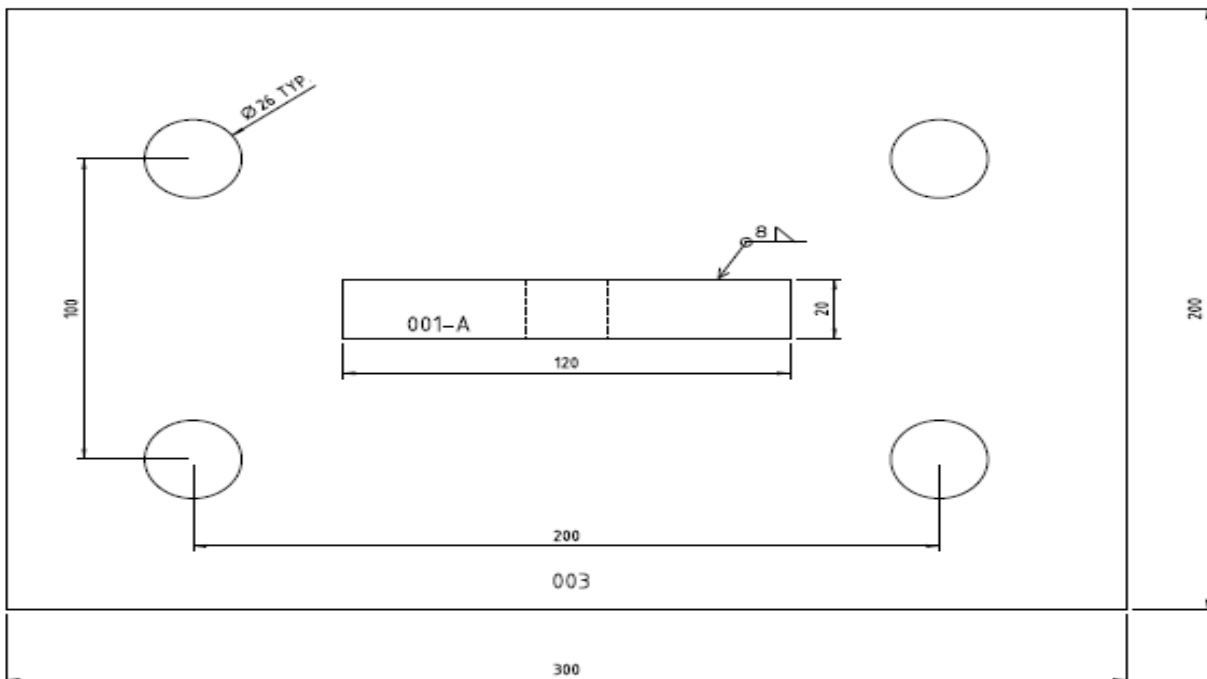
Figure 4.6 – The pad eye with the plate (view from above) [1]

The reason that the pad eye is designed with and without the plate is to see how the addition of a plate to the pad eye changes the global deformation of the pad eye. Each case (with and without the plate) will be done with three different hole sizes and in each case, both the elastic and plastic behavior of the pad eye will be studied. Abaqus/Standard will be applied for elastic behavior while Abaqus/Explicit will be utilized for the dynamic behavior.

As mentioned in section 1.4 of this thesis, the pad eye will be tested three different times where the pinhole diameter will be increased each time (see Table 4.1) to see how the growth in hole diameter in the pad eye affect its capacity and its plastic behavior.

Table 4.1 - Geometries of the different Type 1 pad eye tests [1]

SWL [Tonnes]	Hole diameter, d_h [mm]	Plate thickness, t_p [mm]	Radius, R [mm]	Height, h [mm]	Length, L [mm]	Height 2, k [mm]	Weld, a_w [mm]
3.25	22	20	35	50	120	20	8
3.25	32	20	35	50	120	20	8
3.25	42	20	35	50	120	20	8

4.1.4 Some simplifications

To be able to simplify the modelling of the pad eye in Abaqus/CAE without affecting the quality of the results, the following assumptions are made:

- Instead of including complicated interaction between the pad eye and the bolt in this model, distributed pressure on the upper half of the pin hole will be applied.
- The pressure variation around the pinhole will not be considered, and instead, we use a uniform pressure.
- The weld a_w (see Table 4.1) will be neglected when interacting the pad eye to the plate, which may cause larger stresses around the interaction area between the pad eye and the plate, but this will not affect results obtained at the upper part of the pinhole.

4.2 The elastic analysis of the pad eye using Abaqus/Standard

In this section, the focus will be on the elastic behavior of the pad eyes in all of its forms, both with and without the plate and with all of the three different pinhole sizes. However, since the pad eyes in this, thesis are identical, except the pinhole sizes, only the pad eye with the pinhole diameter of 22 mm will be viewed (the other models will be viewed in the appendixes) for simplicity's sake (except the Meshing Visualisation modules). In each module; both, the pad eye with and without the plate will be considered. For details on how the modulus work and for further understanding of them see [13].

4.2.1 The Part module

This step creates the entire analysis model for this problem. The first phase of modelling is defining the geometries. A 3D deformable part, with a solid and extruded base feature, will be created. First, the 2D profile of the pad eye will be sketched, and then it will be extruded with the depth of the model. In Abaqus/CAE, the units which are going to be used has to be decided.The SI system of millimeters, megapascal, and kilogrammes.are utilized.

The first case (pad eye without plate): In this step, the pad eye model with three different hole sizes will be designed, starting with the 22 mm diameter and then move on to 32 mm diameter and 42 mm diameter. The geometries of this pad eyes are based on Table 4.1.

The second case (pad eye with plate): We will create the pad eye plate, the geometries of the pad eye plate are based on Figure 4.6 – The pad eye with the plate (view from above)

4.2.2 The Property module

The second step in creating the model is to define and assign the material and section properties to the pad eye. Our pad eye model has to be referred to a section property, which includes the material properties of the pad eye that we defined. We will create an elastic material with a Young's modulus of E=210000 MPa and a Poisson's ratio of $v = 0.3$. Both the pad eye and the plate consists of the same material properties. See Table 3.1.

4.2.3 The Assembly module

The assembly module contains the parts of the finite element model. Each part of the model is oriented in its coordinate system and is independent of the other parts of the model. Even though a model may contain several parts, it only contains one assembly. We define the geometry of an assembly by creating instances of a part and then directing them toward each other in a global coordinate system. An instance can be either dependent or independent. We mesh independent part instances individually while we mesh dependent part instances in association with the mesh of the original part.

The first case (pad eye without plate): We only have one single part instance, the pad eye. See APPENDIX B for the pad eyes without the plate.

The second case (pad eye with plate): We have two part instances, the pad eye, and the pad eye plate, which we are going to include in our model. We will direct and move those two part instances in the right positions to each other so that the pad eye is located in the middle of the plate. To obtain that we utilised the tool "create constraint: face to face" in the Assembly module tool set.
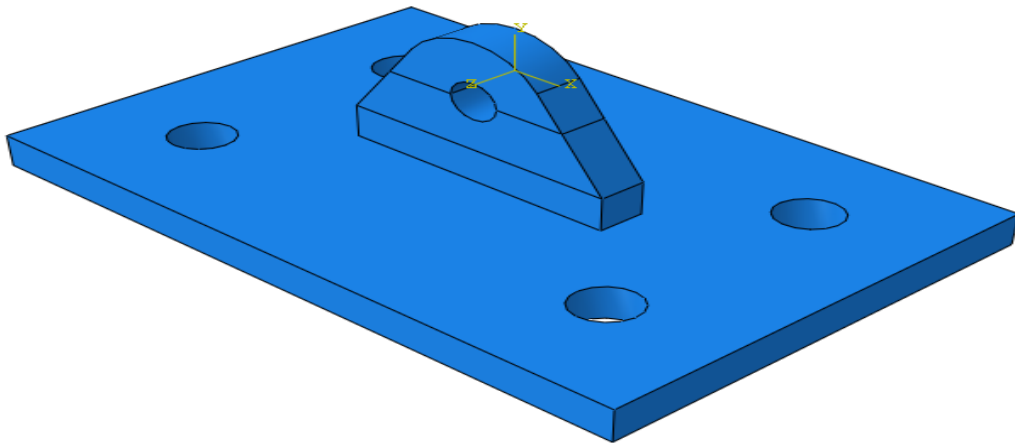
Figure 4.7 - Pad eye with 22 mm pinhole diameter connected to the plate

For the cases where the pinhole diameter is 32 mm and 42 mm, see APPENDIX B

4.2.4 The Step module

Now that we have created our assembly, we can arrange our analysis by starting to define our analysis steps. Since both interactions, loads and boundary conditions are step-dependent; we must determine the analysis steps first before we specify them. In this module, we will also determine our output requests in the "Edit Field Output Request" window for this analysis for each step that we want so that we can have the desired values in areas of interest from our model, in a report.

The first case (pad eye without plate): Since this is a single event, we will define a single static, general step for this simulation. In the "Edit step", we set the setting to default. Thus, we will have two phases in our analysis:

- An initial step, which Abaqus/CAE generates automatically, where we will apply BC.
- An analysis step, where we will implement the load.

The second case (pad eye with plate): Since this is also a single analysis step, the same points from above are applicable.
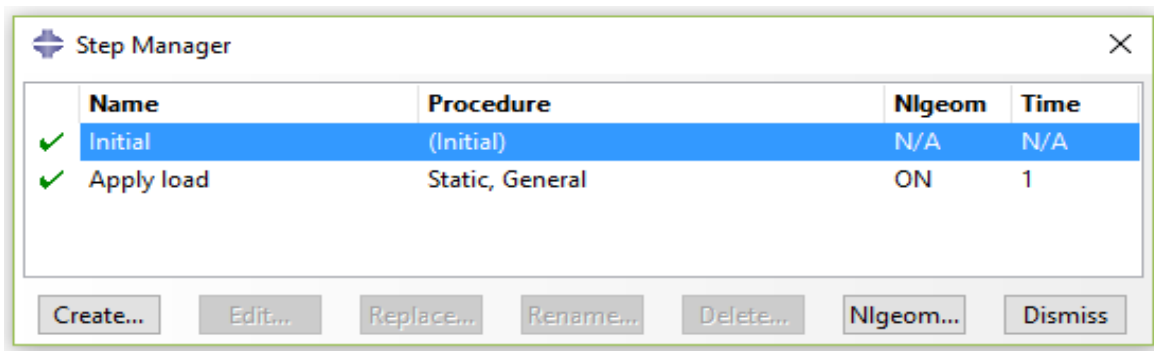
Figure 4.8 – Analysis steps

4.2.5 The Interaction Module

In this module, we can interact to or more parts so they can be a permanent part of the same model and behave as one part. In the first case, when we only have the pad eye without the plate, which means we only have one part and therefore do not need the application of "Interaction.".

The second case (pad eye with plate): In section 3.2.2 "The Assembly module", we assembled the pad eye to the plate and connected them into one piece. However, that connection is not sufficient to firmly "weld" the pad eye to the plate and make them two inseparable parts of the same model. To obtain a firm connection between the two parts, we first defined the surfaces which we want to connect, (see Figure 4.9), and then we utilised the "Constraint" tool.
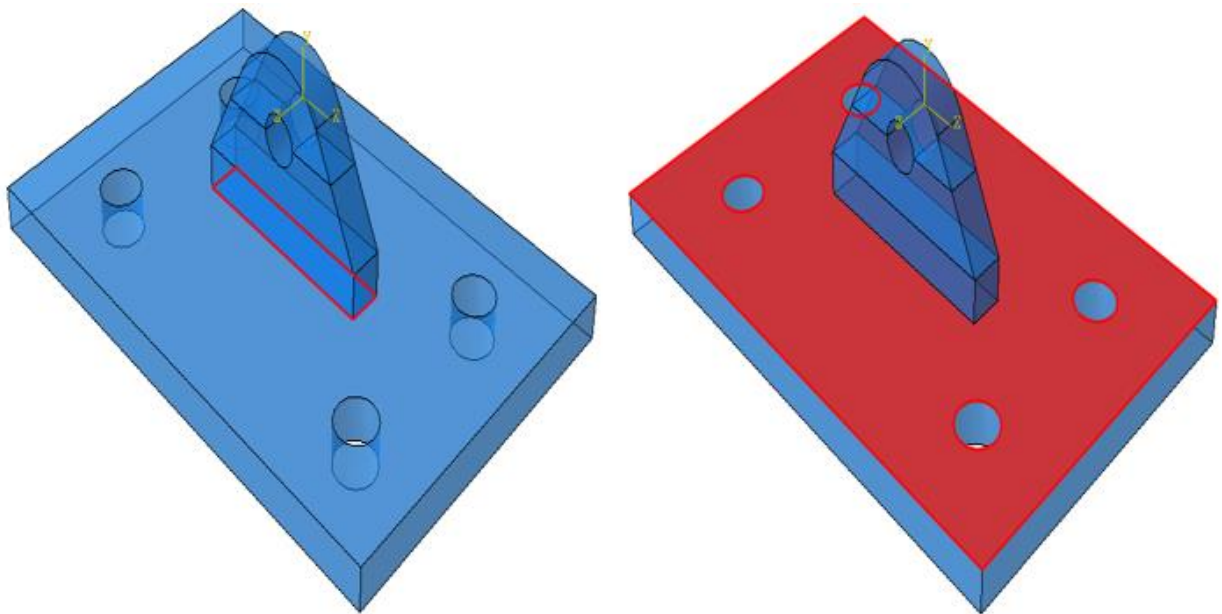
Figure 4.9 – The surfaces which we want to connect firmly together (22 mm pinhole diameter)

For the surfaces in the pad eyes with 32 mm and 42 mm pinhole diameter, see APPENDIX B

The constraint type used in this analysis is "Tie" which can be a restriction against both translational (x,y and z-axis) and rotational (rotations in all directions) degrees of freedom in the contact area between the bottom surface of the pad eye and the upper face of the plate. In another word, the tie constraint will function as a fixed boundary condition in all directions. Figure 4.10 shows the constraint utilised for connection between the pad eye and the plate.
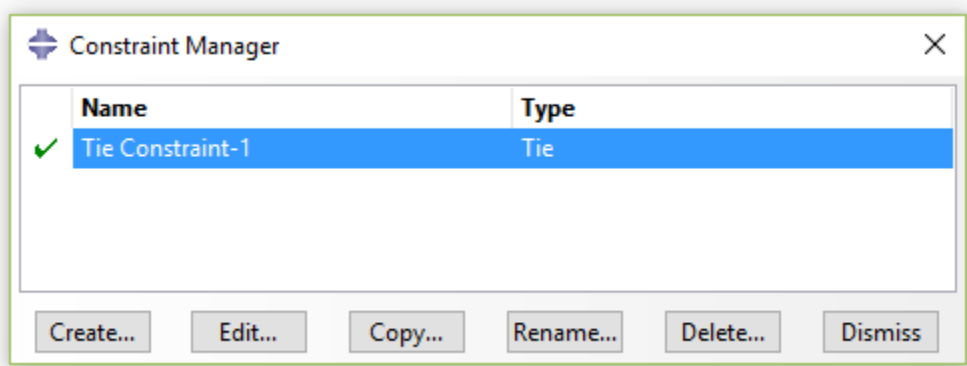
Figure 4.10 – Constraint Manager

4.2.6 The Load Module

In this module, we can define several types of loads and boundary conditions for an assembled model. The loads, which we are considering, are both vertical and angled loads which pulling the pad eye upward. We will consider the following loads and directions for this analysis, and then later we compare our simulation results to the theoretical and experimental load from Table 4.2 below.

Table 4.2 – Basis of our load (only 3.25-ton shackles) and load direction choices [1]

Test number	Pinhole diameter of the pad eye [mm]	Load direction	Theoretical load capacity [Tonnes]	Experimental Load capacity [Tonnes]
1	22	Vertical	26.2	> 21
3	32	Vertical	20.7	> 21
4	42	Vertical	15.3	14.5
5	22	Angular	26.2	>14
6	32	Angular	20.7	>15
7	42	Angular	15.3	>14.5

The pulling load, which is given as tones, is considered as a concentrated load, pulling the pad eye from the upper part of the pinhole upward in both vertical and angled (45º) directions. This kilogram-force, given as tons, will be converted to uniform pressure, which is working on the upper half of the pinhole [7]

The vertical strain:
$$P = \frac{F}{D*t}$$

Where

P   is the internal pressure acting upwards on the top horizontal half of the pinhole.

F   is the force

D   is the diameter of the pinhole

t   is the thickness of the pad eye

The angular strain:
$$P = \frac{F}{0.85*D*t}$$

Hence, the uniform pressures that we get for the different tests from Table 4.2 are as follows:

Table 4.3 – Input load in Abaqus/CAE

Test number	Pinhole diameter of the pad eye [mm]	Load direction	Input unifrom pressure in Abaqus/CAE [MPa]
1	22	Vertical	500
3	32	Vertical	350
4	42	Vertical	169.3
5	22	Angular	400
6	32	Angular	300
7	42	Angular	250

For calculations, see 1.a)i)(1)(a)APPENDIX B

Boundary Conditions (BC)

In structural analysis, the boundary conditions are applied to the regions of the model where the displacements and/or the rotations are known. We may consider remaining these areas fixed (having zero displacements and rotations) during our simulation, or may allow some particular non-zero displacements and/or rotations in some regions.

The first case (pad eye without plate): In this instance we will apply the pressure on the top of the pinhole in "Test 1" from Table 4.2 in the "Edit load window, see Figure 4.11.
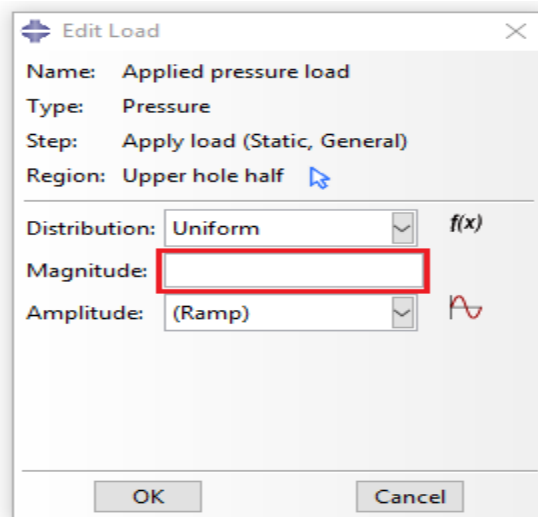
Figure 4.11 – Determination of loads

Moreover, regarding the boundary conditions, we will fix the bottom surface of the pad eye:
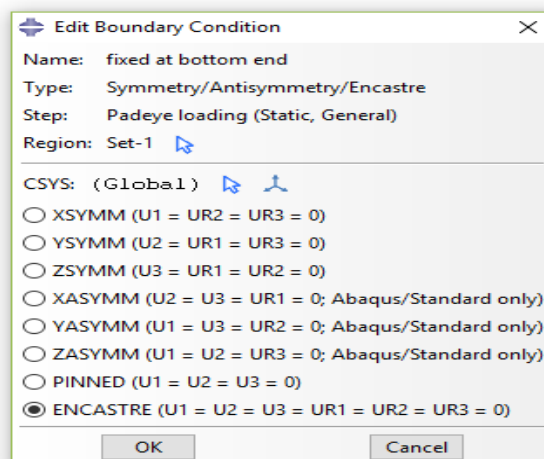
Figure 4.12 – Fixed BC

36

We illustrate Figure 4.11 and Figure 4.12 with the following illustration:

(a)   (b)
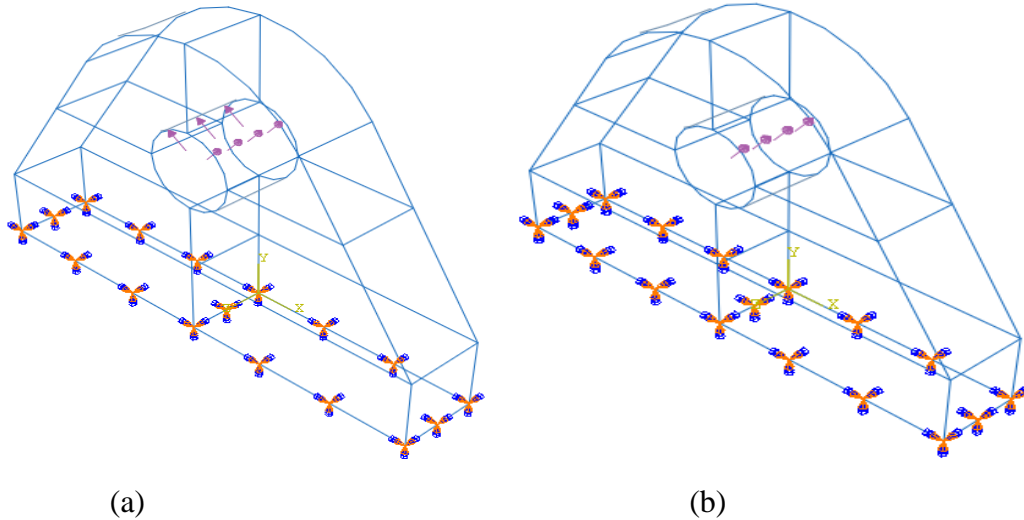
Figure 4.13 – Fixed pad eye subjected to (a) vertical and (b) angled uniform pressure (22 mm pinhole diameter)

The second case (pad eye with plate):

The only difference between this case and the first one is that here we will fix the holes in the plate so that the neither move translationally nor rotationally, while in the first case we fixed the bottom of the pad eye. The fixed holes represent the bolts. See Figure 4.14.
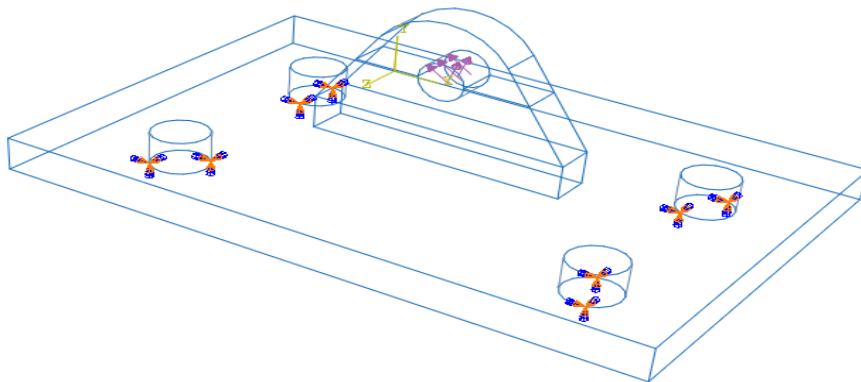
Figure 4.14 – The vertically applied pressure and fixed BC on the pad eye with the plate (22 mm pinhole diameter)

For the models with 32 mm and 42 mm pinhole diameter, for both cases (with and without the plate) see FIGURES in APPENDIX B

4.2.7 The Meshing Module

We will now create the finite element mesh. This module enables the designer to generate meshes in the whole model or parts of the model, which we assembled in the assembly module. We can choose the meshing technique, the element shape, and the element type to create the mesh. First, we need to consider the element type that we are going to use before we start building the mesh for a particular problem. In this analysis, we will use an Abaqus/Standard since we only are interested in the static response. We will use 20-node hexahedral elements with reduced integration. The selections made in Figure 4.15 are based on DNV-RP-C208 [5].
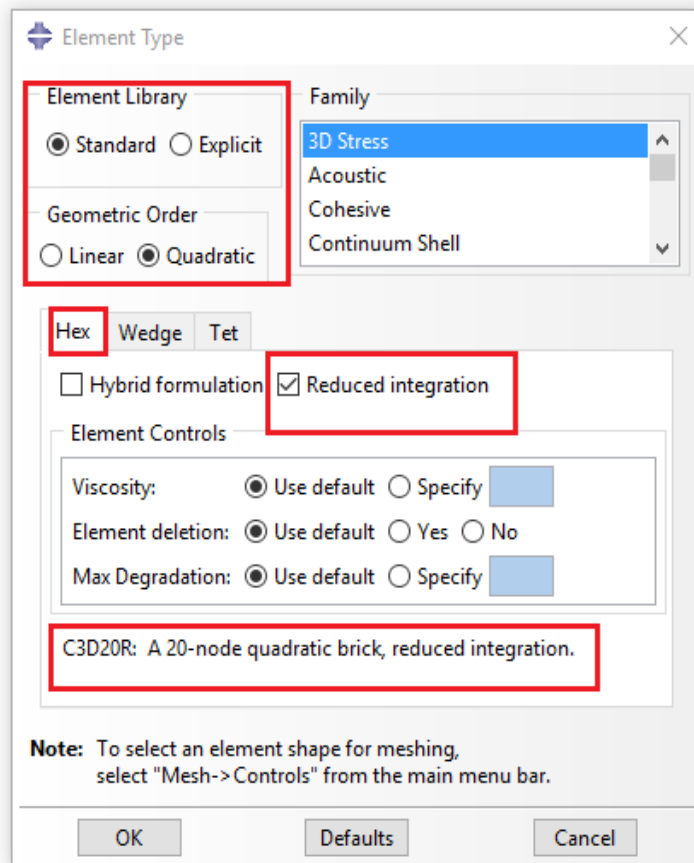
Figure 4.15 – Choosing element type

Mesh density

Now that we have chosen the element type, we can start the design for the pad eye. The most important decision regarding the mesh design for this analysis is how many element we are going to use around the pinhole. We distinguish between global seeds and local seeds; see Figure 4.16. Global seeds mean the element sizes in the whole model, while the local seeds mean the local element sizes in some specific areas of interest in which we want to have finer mesh.

For both the ductility and stability evaluations, we should have a sufficient number of elements (both local and global elements) to have good strain estimates and to capture failure modes. This information is based on section 4.5 "Mesh density" in DNV-RP-C208 [5].
To be more specific, we choose the "Approximate global size" to be between three and four for all our pad eye cases, while the "Number of elements" in the "Local Seeds" window increases with the size of the pinhole.
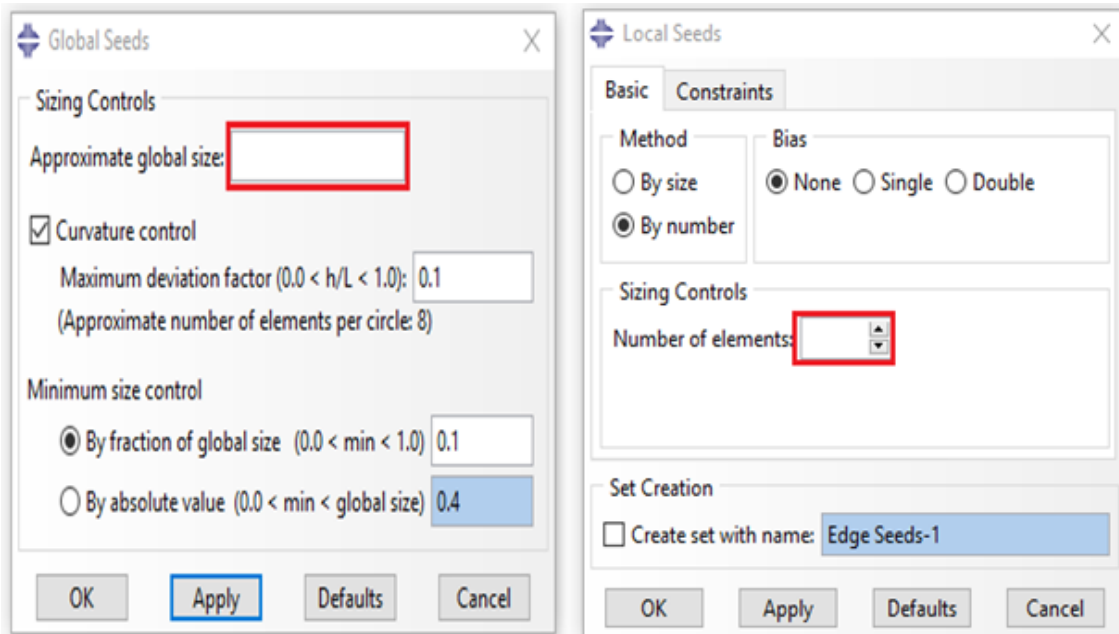
Figure 4.16 – Global and Local seeds

The following figure, will show an illustration of what global and local seeds are, which will be a further understanding of the text and figures in section 0. The black circles at the edges of the pad eye are the "Global Seeds", which determine the size of the elements in the whole model. While the pink circles, around the upper half in the pinhole, are the "Local Seeds", which we use to have sufficiently accurate results in areas of interest.
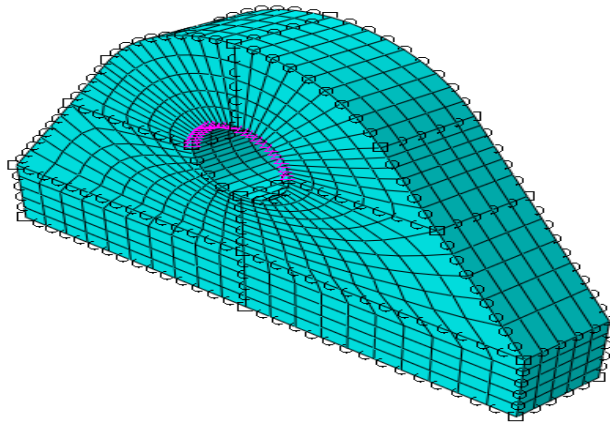
Figure 4.17 – Global and local seed elements

Meshing techniques

Abaqus/CAE suggests several meshing techniques to mesh models with different topologies. These different meshing techniques offer varying stages of automation and user control. Figure 4.18 shows the four types of meshing techniques.
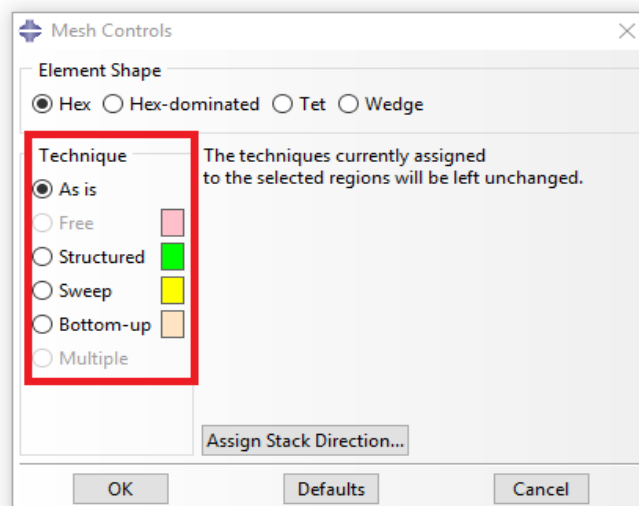
Figure 4.18 – Meshing techniques

40

Free meshing: This is the most flexible meshing technique that uses no pre-established mesh patterns and can be applied to almost every model.

Structured Meshing: We must portion complex models into simpler regions to use this technique.

Swept meshing: Abaqus/CAE creates swept meshes by internally generating the mesh on an edge (or a face), and then sweeping it along a sweep path, or resolves it around an axis of revolution. Swept meshing is also limited to models with distinct topologies and geometries, like structured meshing.

Bottom-up meshing: This technique uses the part geometry as a guideline for the outer bounds of the mesh.

When we enter the mesh model, Abaqus/CAE automatically colors the regions of the model according to the methods it will use to produce a mesh. These colors have the following meanings:

- The green color of the region means that the region can be meshed with structured meshing.
- The yellow color of the region means that the region can be meshed with swept meshing.
- Pink color of the region means that the region can mesh with free meshing.
- Orange color means that a region in the model can not be meshed using the default assignment of the element shape and it has to be portioned more.
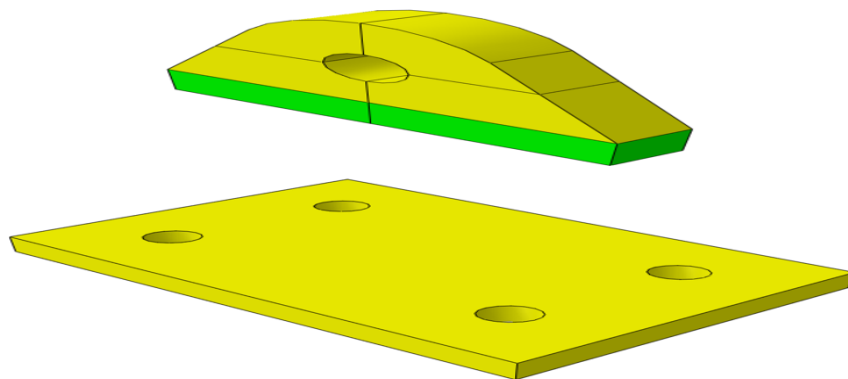
Figure 4.19 – Portioning process

As we can see from Figure 4.19 – Portioning processe has regions with both yellow and green color, which means that the swept meshing and the structured meshing technique will be utilized. The horizontal line at the middle of the pinhole is drawn to portion the pinhole in two in the horizontal direction so that we can be able to apply the uniform pressure at the upper part of the pinhole. While the vertical line is drawn to simply get a better mesh.

Viewing the meshed models:

In this section, we will view all of the pad eye models that we have meshed in this chapter, both with and without the plate and in all diameter sizes.

First case (pad eye without plate):

Figure 4.20 shows the pad eye without plate meshes of the pinhole diameters of **(a)** 22 mm, **(b)** 32 mm and **(c)** 42 mm:

(a)   (b)   (c)
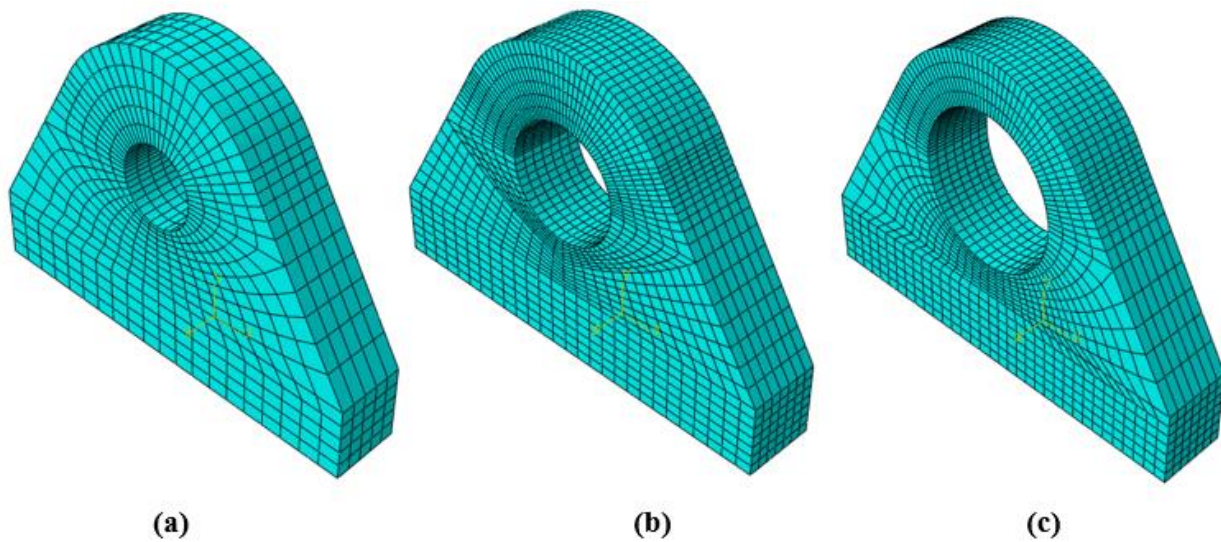
Figure 4.20 – Meshes of pad eyes without plate

First second (pad eye with plate):
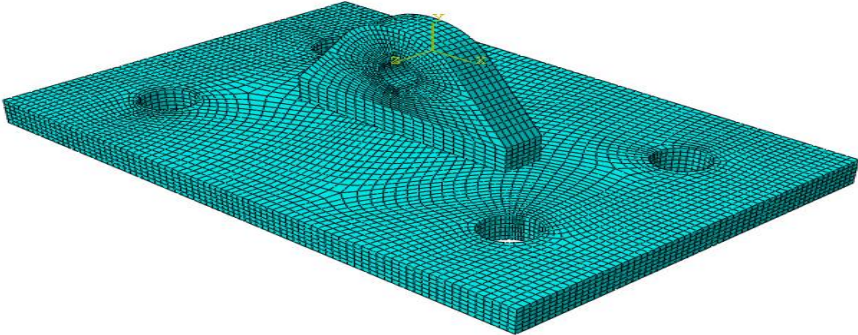
Figure 4.21 – Meshing of the whole model (22 mm pinhole diameter)
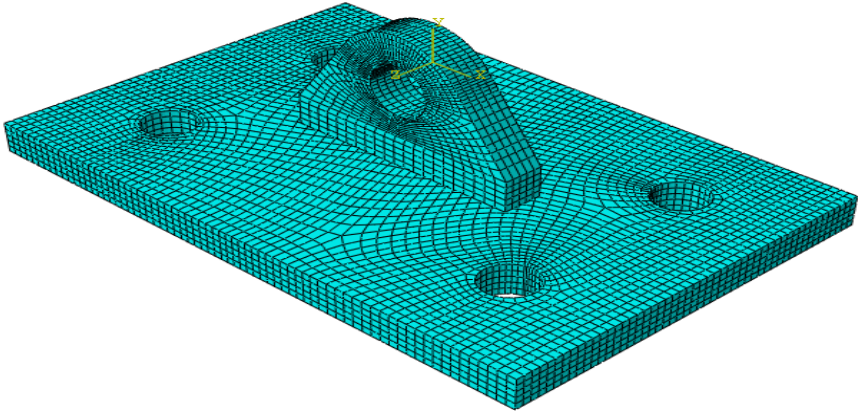
Figure 4.22 - Meshing of the whole model (32 mm pinhole diameter)
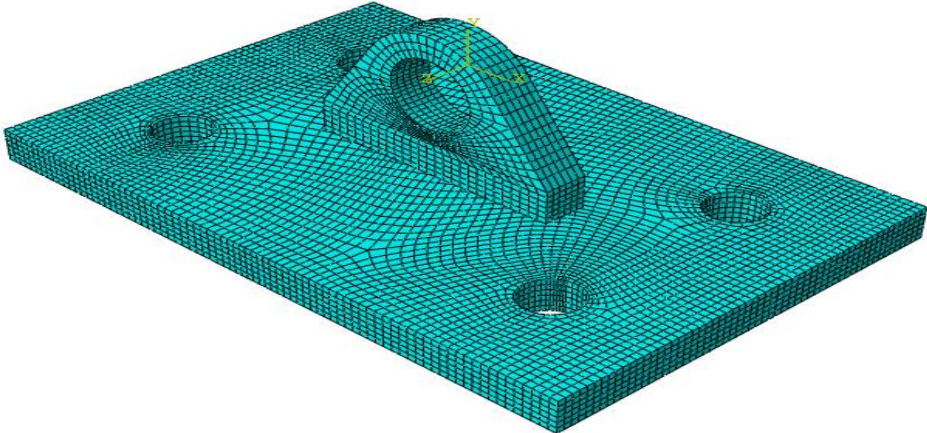
Figure 4.23 - Meshing of the whole model (42 mm pinhole diameter)

4.2.8 The Job Module

Now we have come to the stage where the only task remaining to complete the simulation is to define the job. We can then submit the job in Abaqus/CAE. The software then monitors the simulation progress interactively.

4.2.9 Simulation results of the elastic analysis of the pad eye.

In this section, we will view the results of the procedure in section 4.2 "The static analysis of the pad eye using Abaqus/Standard", which are given in the Visualization Module. The idea is to identify the critical zones (the zones with maximum stresses, which are about to yield) in every pad eye (with different pinhole sizes, with and without the plate). Abaqus/CAE generates automatically the output data for the entire model, but we are only interested in the upper part of the pad eye pinhole, which we will call our "area of interest" (see. To be able to view the stresses in the areas of interest, we use the tool "Display Groups" in the Results tree, to highlight and isolate those areas. This tool will help us to neglect the stresses (and other variables) in the areas we are not considering.
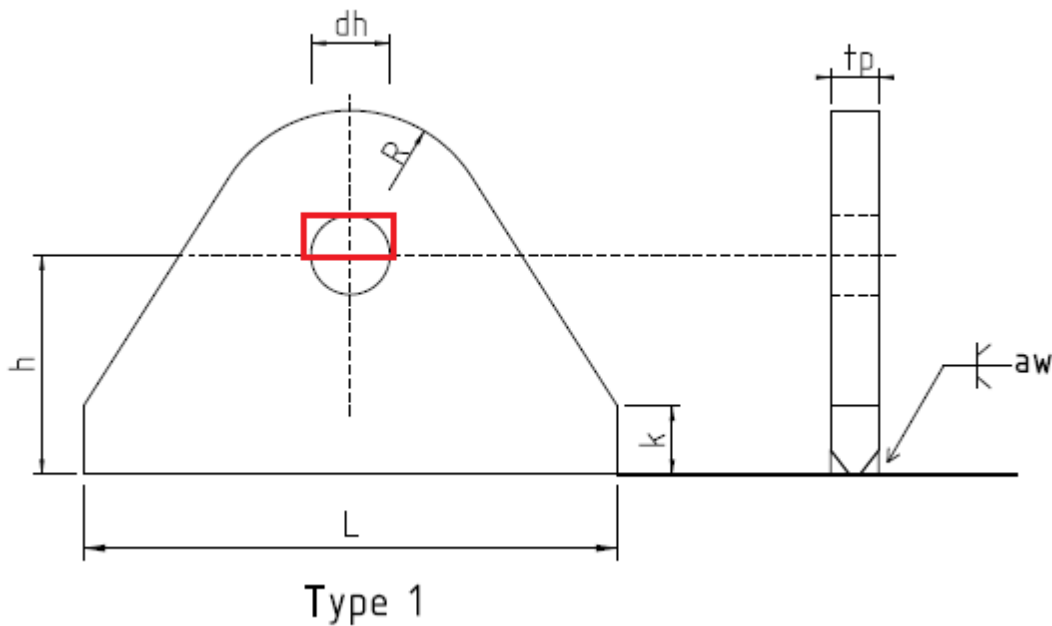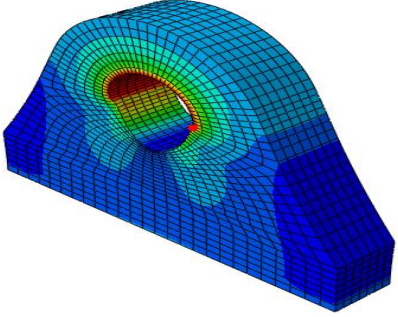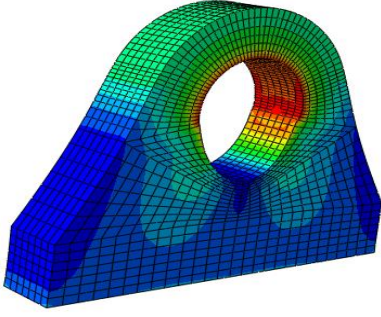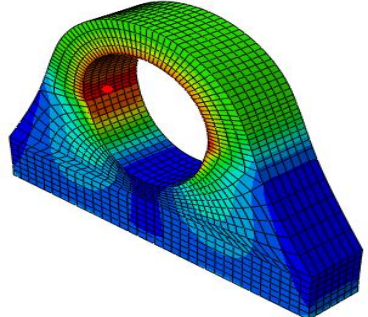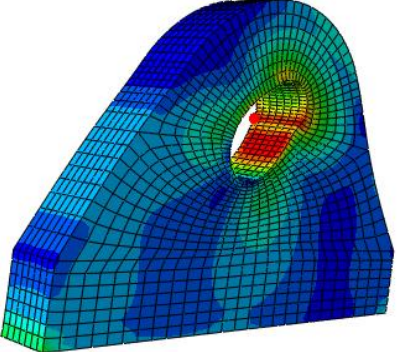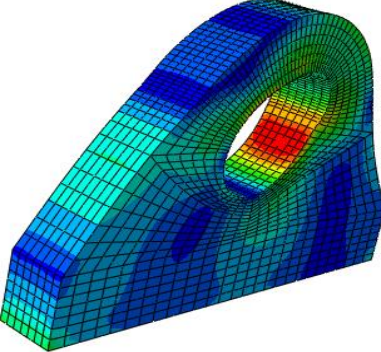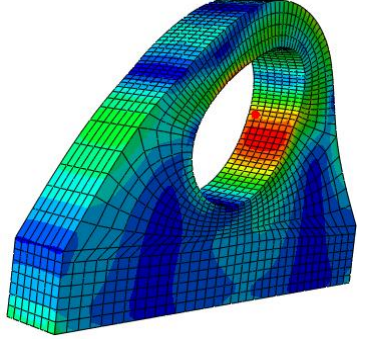
Figure 4.24 – Our area of interest (red marking) [1]

First case (pad eye without the plate):

To find the critical zones in our area of interest, we search for the nodes which have the highest stresses in that area. Those nodes with the corresponding stresses are shown in.

1.a)i)(1)(a)APPENDIX C We obtained the following results of the static simulation from Abaqus/Standard:

Table 4.4 - Critical zones (red dots) in the pad eyes without the plate

(a)

(b)

(c)

(d)

(e)

(f)

- Figure (a) shows the pad eye without plate from Test 1 (from Table 1.1 – Comparison basis from [1] and [2]
- Figure (b) shows the pad eye without plate from Test 3
- Figure (c) shows the pad eye without plate from Test 4
- Figure (d) shows the pad eye without plate from Test 5
- Figure (e) shows the pad eye without plate from Test 6
- Figure (f) shows the pad eye without plate from Test 7

Second case (pad eye with the plate):

Similarly, as the first case, we search for the nodes which have the highest stresses in our area of interest in the pad eyes with the plates, to find the critical zones. Those nodes, with the corresponding stresses are shown in 1.a)i)(1)(a)APPENDIX C , We obtained the following results from Abaqus/CAE:

Table 4.5 - Critical zones (red dots) in the pad eyes with the plate

(g)

(h)

(i)

- (g) represents the pad eye with the plate from Test 1
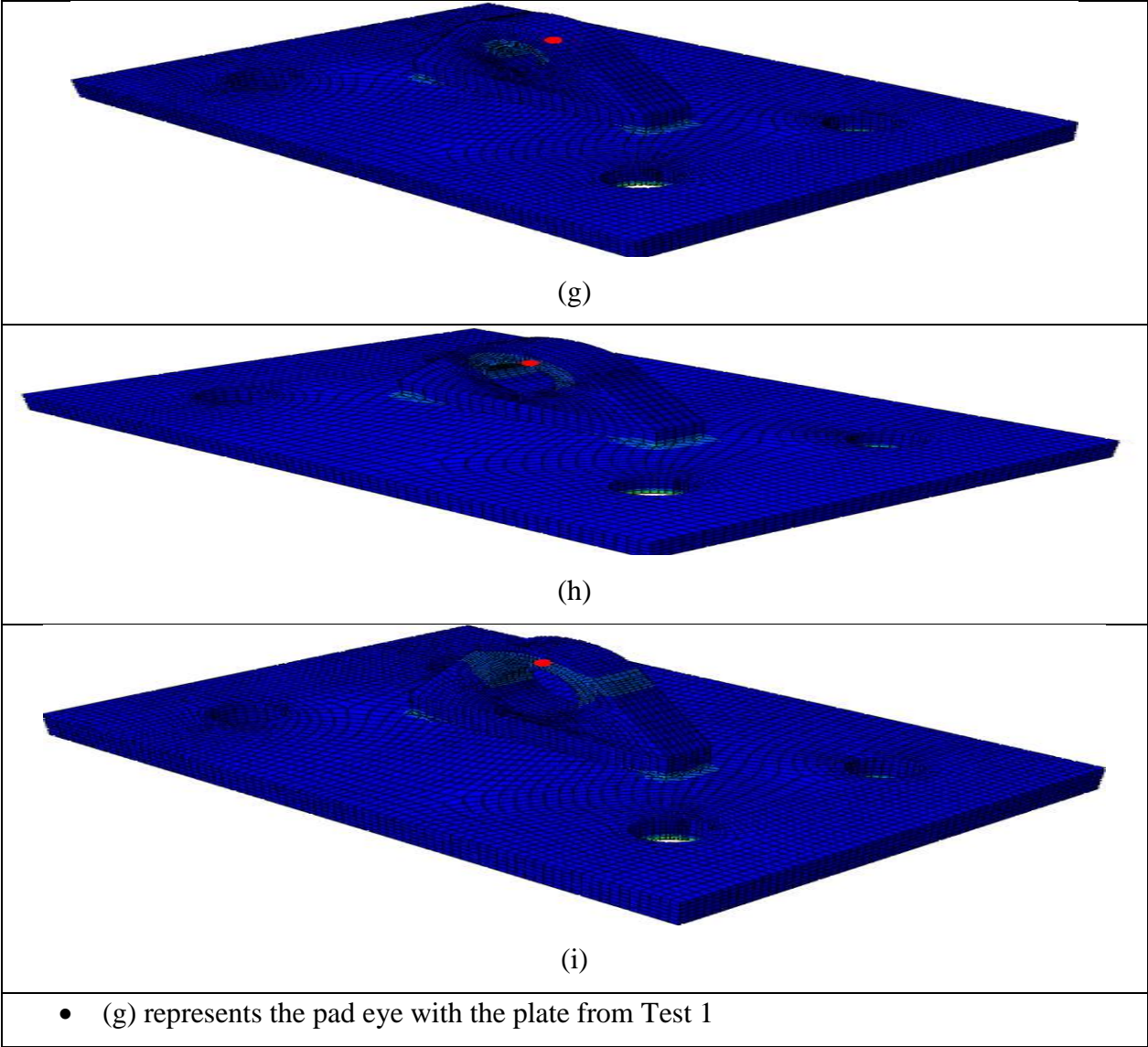
- (h) represents the pad eye with the plate from Test 3
- (i) represents the pad eye with the plate from Test 4

4.3   The elastic-plastic analysis of the pad eye using Abaqus/Explicit

In this section, we will focus on the elastic-plastic response of the 3.25-ton pad eye, when the same loads (which was used in the static response simulations) varies with time. The results in this section will be our comparison basis with the theoretical and experimental results from [1]. The same procedure used in Section 4.2 "The elastic analysis of the pad eye using Abaqus/Standard." will again be used here, expect some small modifications, which are:

- **Material Properties:** In the "Property Module", we will add the density (in kg/mm^3) and the plastic material behavior of steel S355. The plastic material behavior contains the addition of a hardening model, which defines how the plastic strain affects the yield surface of steel S355. A combination of both isotropic hardening (adding hardening to the material to expand the yield surface) and kinematic hardening (useful for the cyclic behavior of S355) is utilized in this case. [5] and [16]
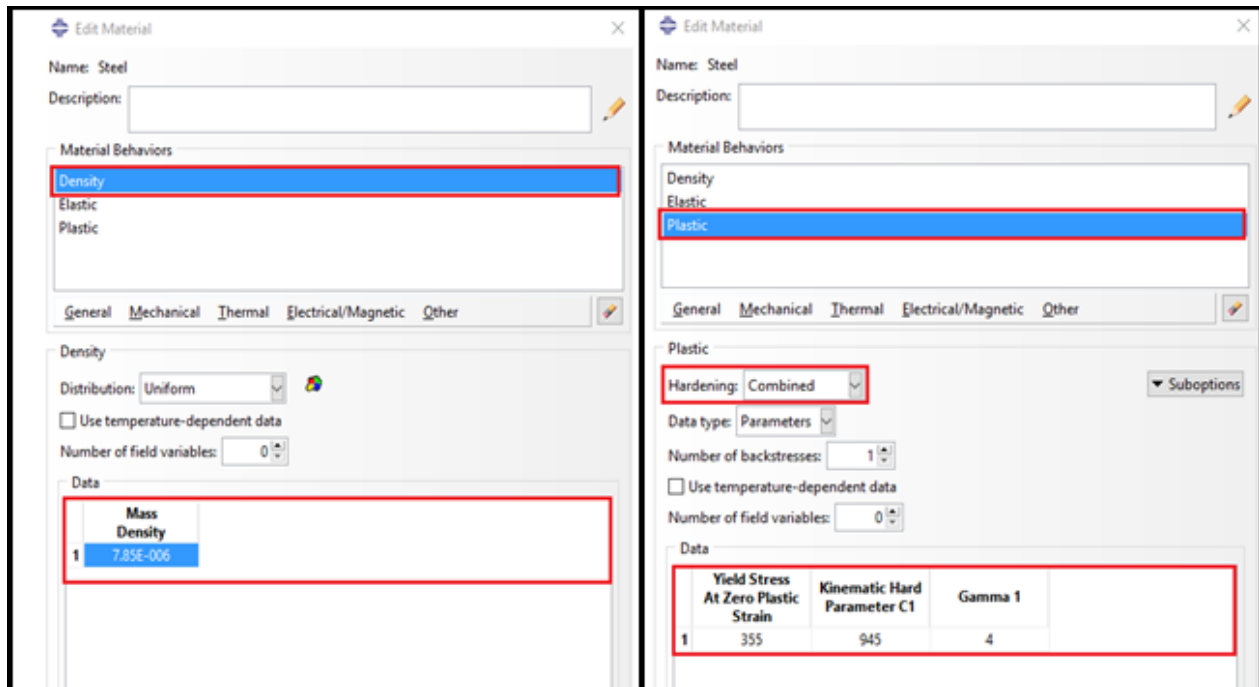
Figure 4.25 – Material properties for dynamic behavior

- **Step:** In the "Step Module", we will replace the Abaqus/Standard to Abaqus/Explicit. In addition to that, we will enter the "time period", which is the total duration of a particular step, while the "Increment size" is the time period of each iteration during that particular step.

- **Load:** In the "Load module" we use the "Amplitude toolset" to specify the time or frequency variations of the applied load throughout a step. This tool is utilized in correlation with "Time Period" and "Incrimination" tools. We choose the "Tabular" type of amplitude in the "Create Amplitude" window.

- **Mesh:** In the "Mesh Module" we change the element type used in the model. The following selections are based on [5] and my trials of finding out which selections would give me the best results.
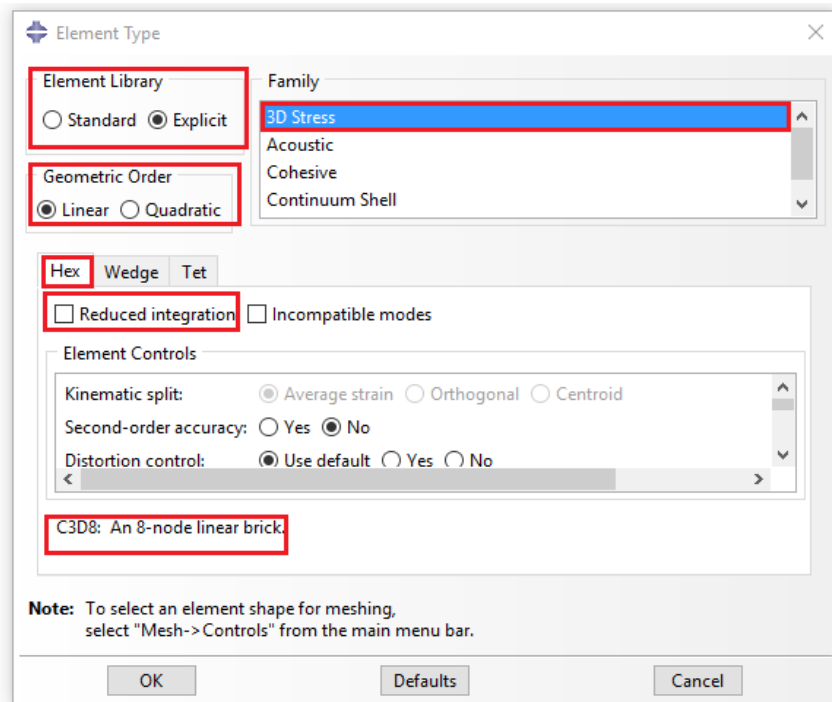
Figure 4.26 – Element type selections in Abaqus/Explicit

4.3.1 Simulation results of the elastic-plastic analysis of the pad eye.

In the static analysis, which was performed with Abaqus/Standard, the critical zones in the pad eye were identified. In this section, we will take it a step further. First, the critical zones will be identified, and then the force which will lead to failure will be determined. That Failure force will be the capacity of the pad eye, which later will be compared to the experimental and theoretical results from the previous thesis. To be able to identify the failure force, the ultimate yield strength criteria for steel S355 [5] must be utilized. The criteria is defined as:

$$\sigma_{von} \leq \sigma_{ult} = 470 \, MPa$$
$$\varepsilon_p \leq \varepsilon_{ult} = 0.15$$

This will be done with the aid of graphs. Theses graphs will be used to identify the pressure failure loads (which we will convert to the failure forces) at the points where the ultimate von Mises stress and ultimate plastic strain are located. In addition to that, the corresponding displacements will also be determined. Since we will obtain to different failure forces, from both pressure-stress curve and pressure-plastic strain curve, we will use the smallest one of those to values, as our failure force:

$$F_{failure} = Min \begin{bmatrix} F_{max\,1} \\ F_{max\,2} \end{bmatrix}$$

The failure force will be determined by the following formula (see section 4.2.6):

Vertical strain: $\qquad\qquad P_{max} = \frac{F_{max}}{D*t} \rightarrow F_{max} = P_{max} * D * t$

Angular strain: $\qquad\qquad P_{max} = \frac{F_{max}}{0.85*D*t} \rightarrow F_{max} = 0.85 * P_{max} * D * t$

This procedure will be used for all of the tests of the pad eyes described below (with and without plate). The numbering of the tests below is based on the tests given in Table 4.2. For the details about the critical zones and node numbers, which describes the maximum von Mises stress and the corresponding equivalent plastic strain and displacements, in each of the tests below, see APPENDIX D

Test 1: Pad eye <u>without</u> plate.

Table 4.6 - Data diagrams of pad eye without plate from Test 1

Table 4.6 shows that the capacity ($F_{failure}$) of the pad eye in "Test 1", in the case of pad eye without plate is equal to <u>25.575 tons,</u> and the corresponding vertical displacement (U2) is equal to <u>0.060 mm.</u>

For details, see APPENDIX D section "Test 1 (pad eye without plate)".

Test 1: Pad eye <u>with</u> plate.

Table 4.7 - Data diagrams of pad eye with the plate from Test 1

Table 4.7 shows that the capacity ($F_{failure}$) of the pad eye in "Test 1", in the case of pad eye with plate is equal to <u>26.247 tons,</u> and the corresponding vertical displacement (U2) is equal to <u>0.250 mm.</u>

For details, see APPENDIX D section "Test 1 (pad eye with plate)".

Test 3: Pad eye <u>without</u> plate.

Table 4.8 - Data diagrams of pad eye without plate from Test 3

Pressure vs. Stress

Pressure [MPa] vs von Mises stress [MPa]

Pressure vs. Strain

Pressure [MPa] vs Equivalent Plastic Strain [MPa]

Pressure vs. Displacement

Pressure [MPa] vs Vertical displacement U2 [mm]

Stress vs. Strain

von Mises stress [MPa] vs Equivalent plastic strain PEEQ

From Table 4.8 it is observed that the capacity ($F_{failure}$) of the pad eye in "Test 3," in the case of pad eye without the plate is equal to <u>22.179 tons,</u> and the corresponding vertical displacement (U2) is equal to <u>0.180 mm.</u>

For details, see APPENDIX D section "Test 3 (pad eye without plate)".

Test 3: Pad eye <u>with </u>the plate.

Table 4.9 - Data diagrams of pad eye with the plate from Test 3

From Table 4.9 it is noticed that the capacity ($F_{failure}$) of the pad eye in "Test 3", in the case of pad eye with the plate is equal to <u>24.464 tons,</u> and the corresponding vertical displacement (U2) is equal to <u>0.750 mm.</u>

For details, see APPENDIX D section "Test 3 (pad eye with plate)".

Test 4: Pad eye <u>without</u> plate.

Table 4.10 - Data diagrams of pad eye without the plate from Test 4
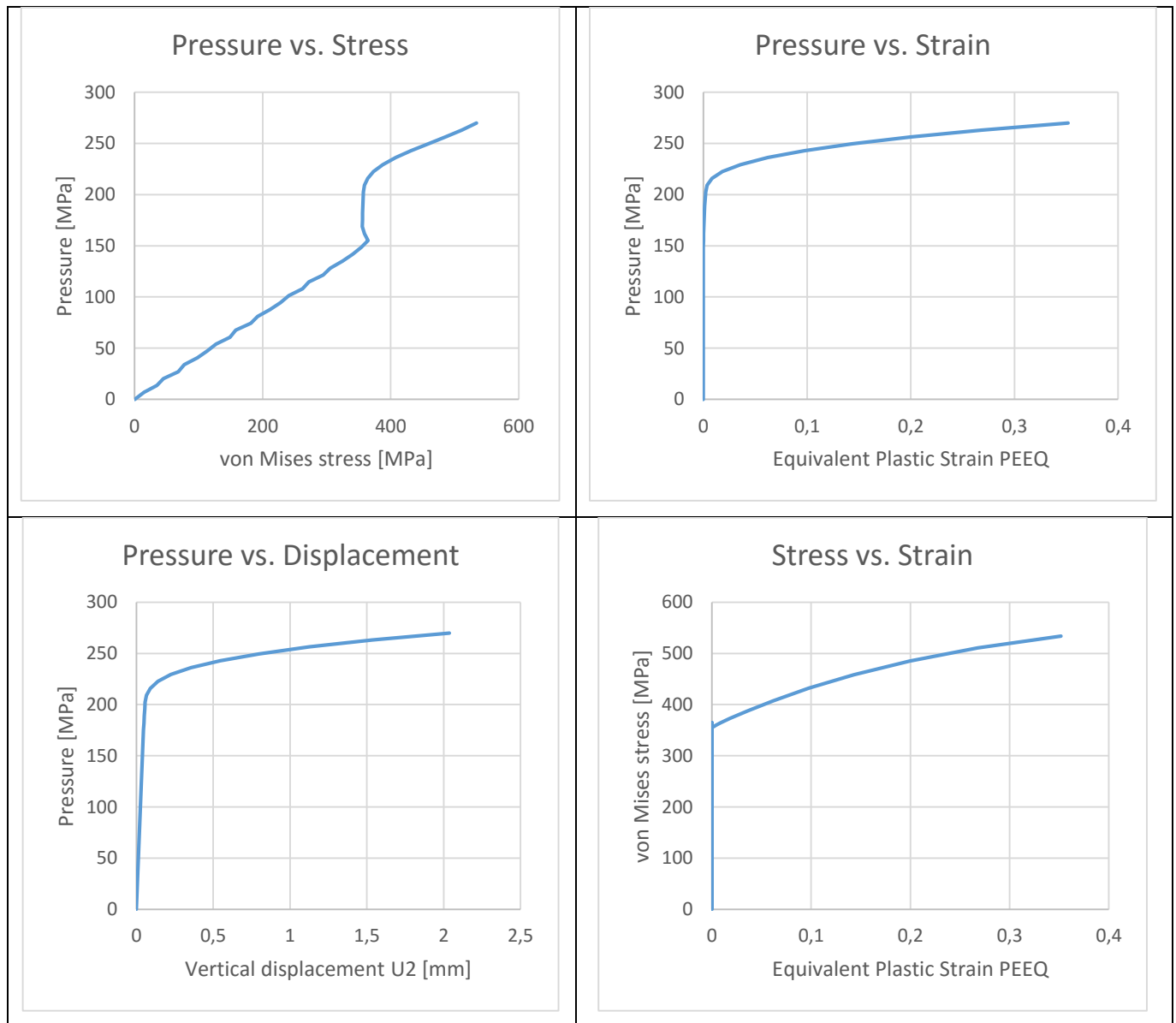
Table 4.10 shows that the capacity ($F_{failure}$) of the pad eye in "Test 4", in the case of pad eye without plate is equal to <u>21.406 tons,</u> and the corresponding vertical displacement (U2) is equal to <u>0.800 mm.</u>

For details, see APPENDIX D section "Test 4 (pad eye without plate)".

Test 4: Pad eye with the plate.

Table 4.11 - Data diagrams of pad eye with the plate from Test 4
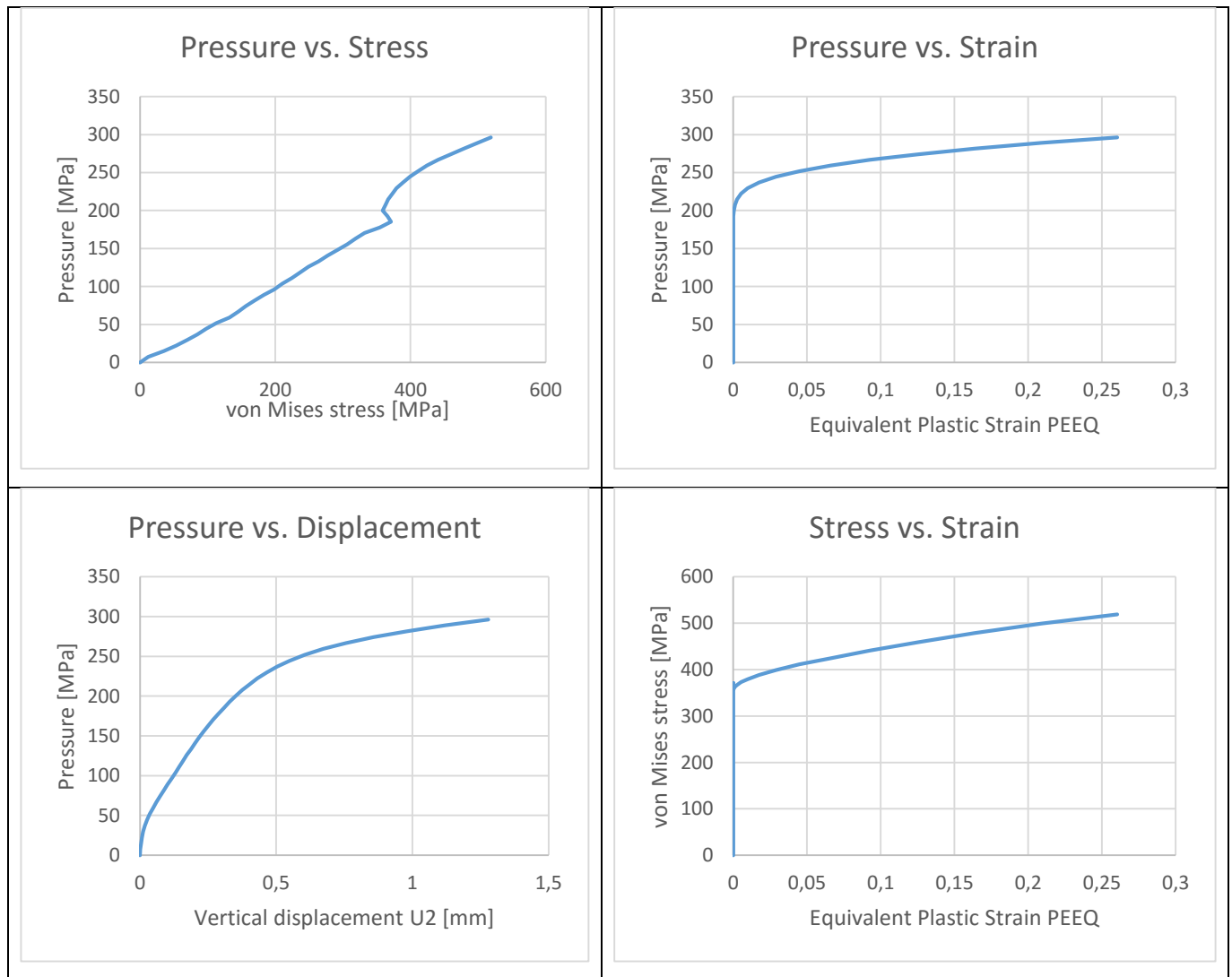
Table 4.11 illustrates that the capacity ($F_{failure}$) of the pad eye in "Test 4", in the case of pad eye with the plate, is equal to 23.547 tons, and the corresponding vertical displacement (U2) is equal to 0.850 mm.

For details, see APPENDIX D section "Test 4 (pad eye with plate)".

Test 5: Pad eye <u>without</u> the plate.

Table 4.12 - Data diagrams of pad eye without the plate from Test 5
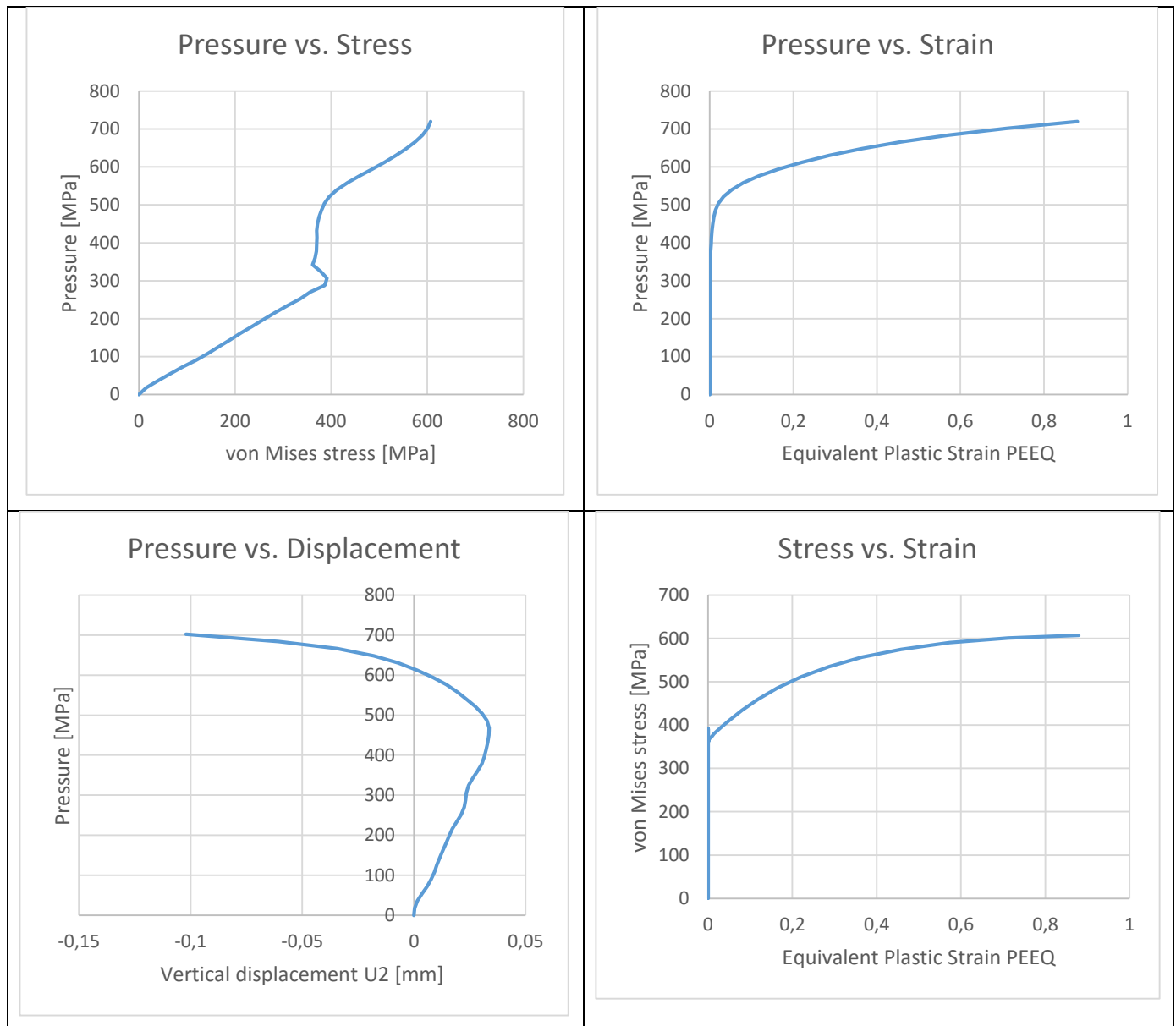
Table 4.12 illustrates that the capacity ($F_{failure}$) of the pad eye in "Test 5," in the case of pad eye without the plate, is equal to <u>22.493 tons,</u> and the corresponding vertical displacement (U2) is equal to <u>0.0085 mm.</u>

For details, see APPENDIX D section "Test 5 (pad eye without the plate)".

Test 6: Pad eye <u>without</u> plate.

Table 4.13 - Data diagrams of pad eye without the plate from Test 6
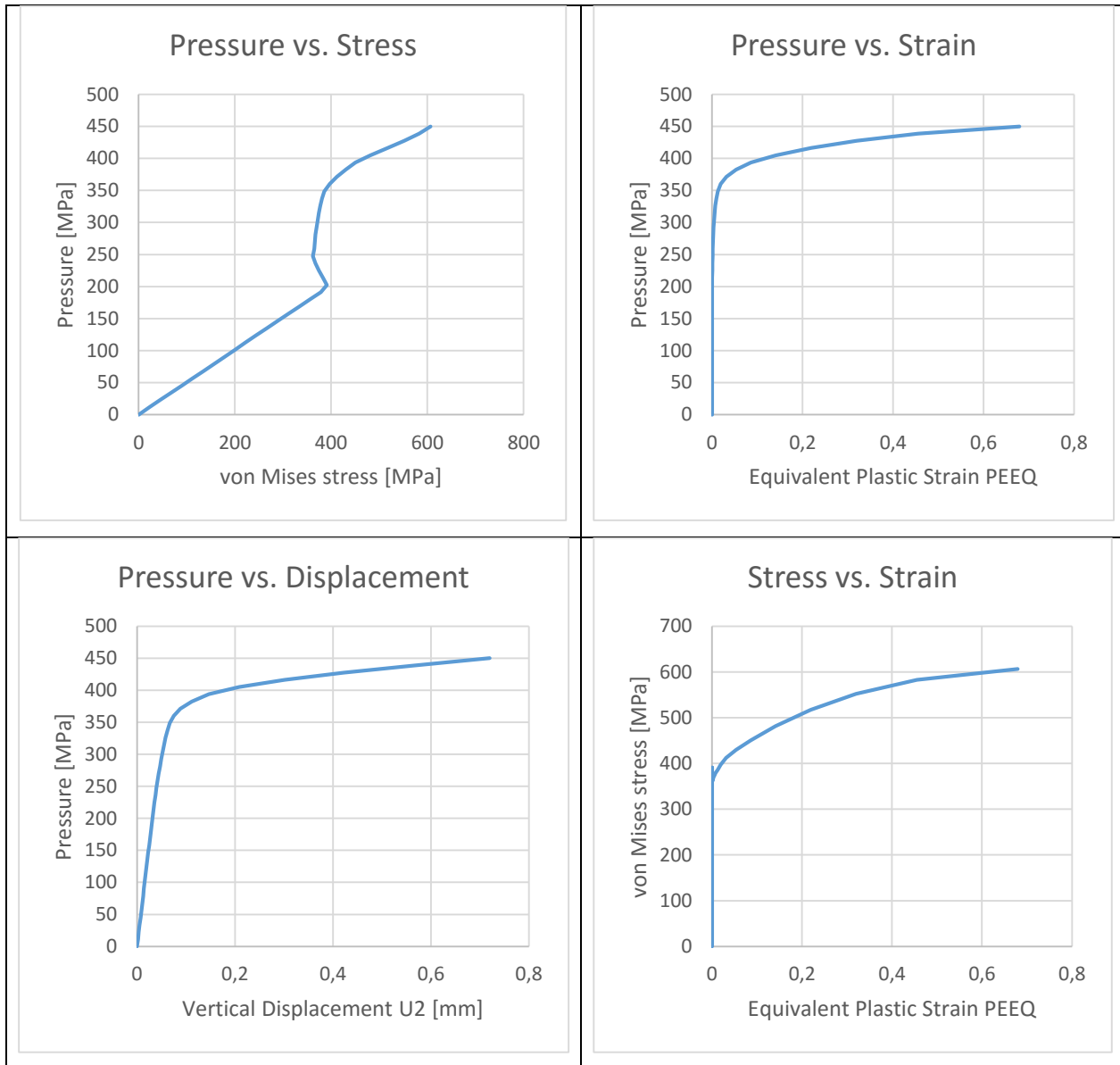
Table 4.13 shows that the capacity ($F_{failure}$) of the pad eye in "Test 6", in the case of pad eye without the plate, is equal to <u>21.904 tons,</u> and the corresponding vertical displacement (U2) is equal to <u>0.150 mm.</u>

For details, see APPENDIX D section "Test 6 (pad eye without the plate)."

Test 7: Pad eye <u>without</u> the plate.

Table 4.14 - Data diagrams of pad eye without the plate from Test 7
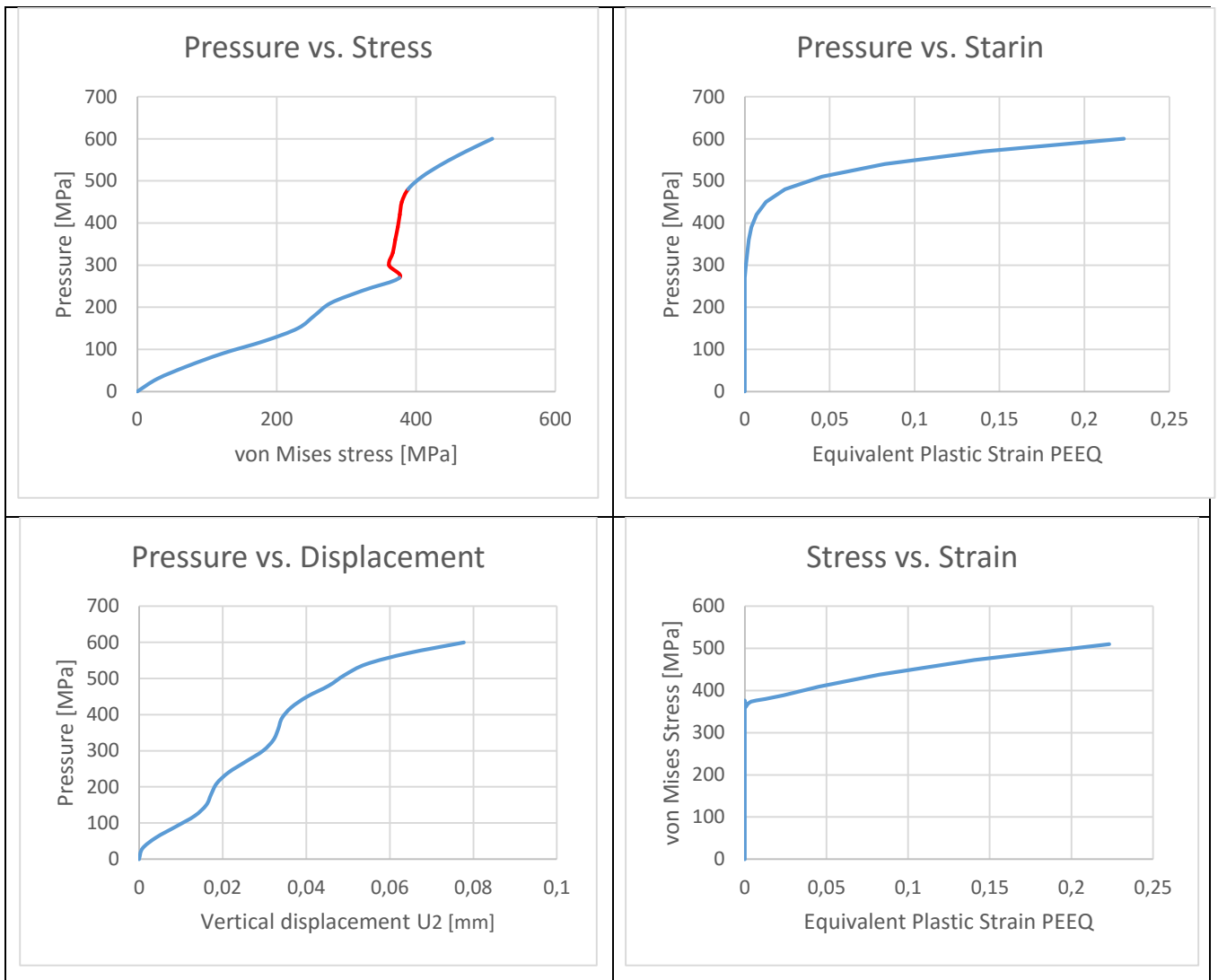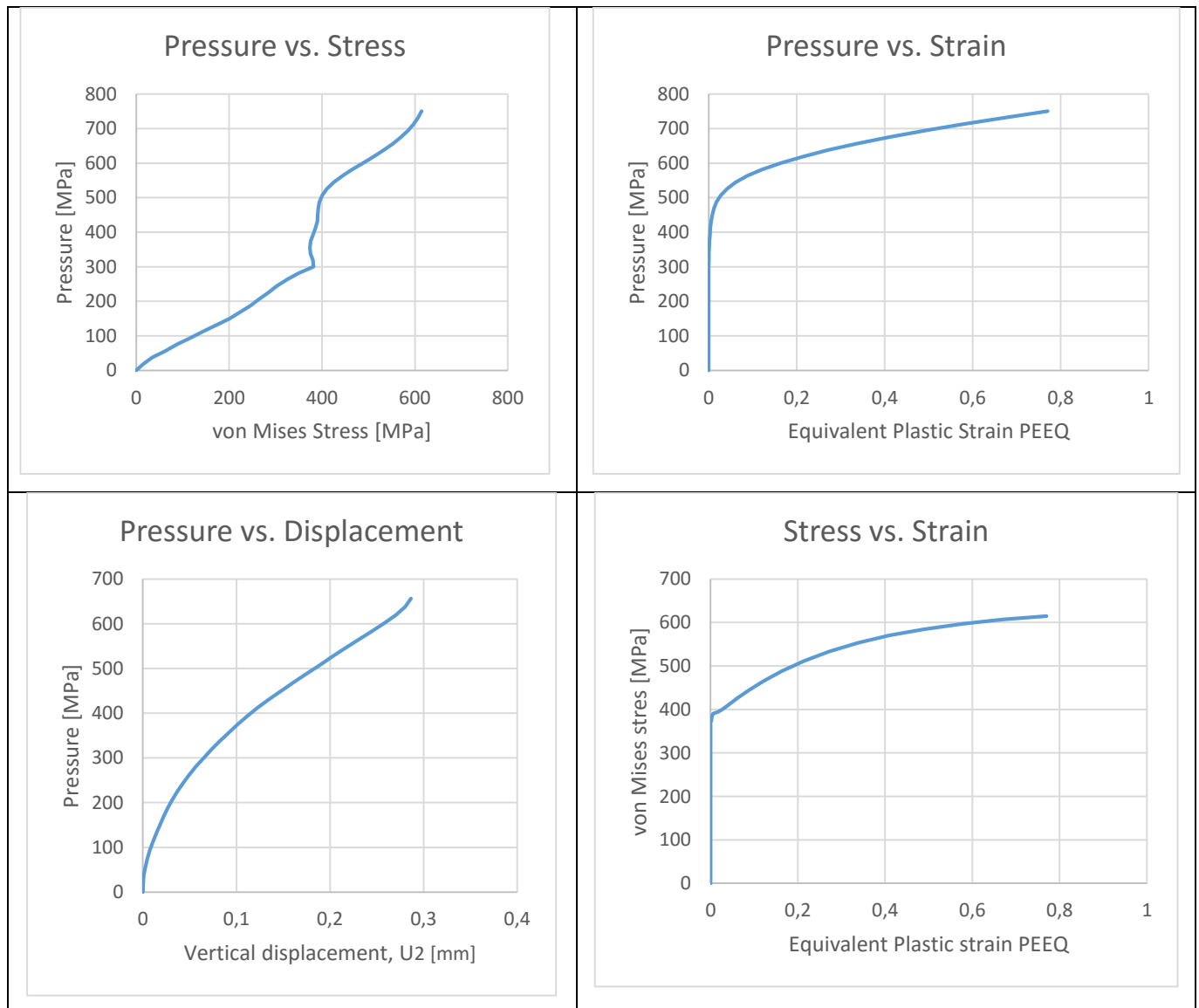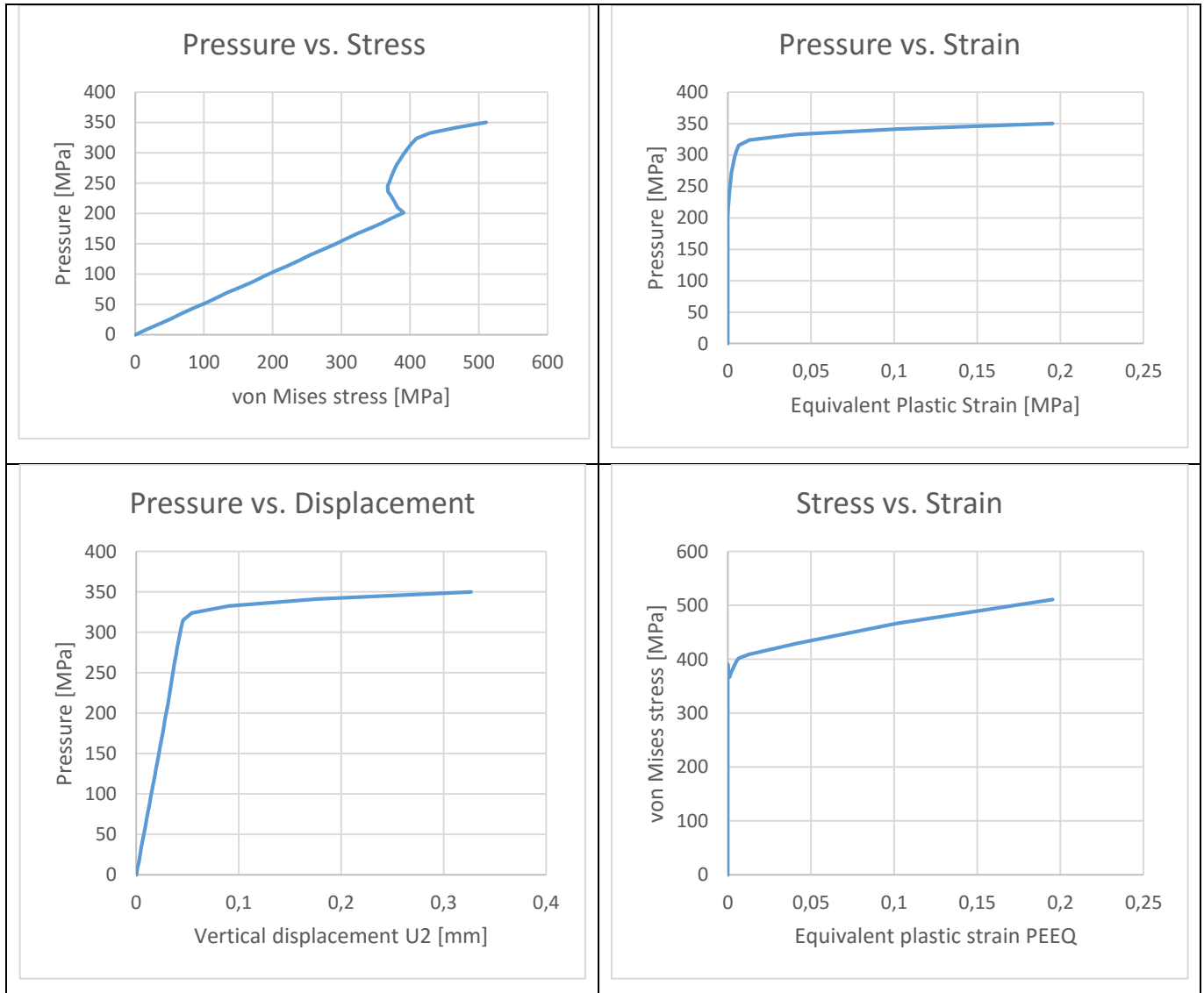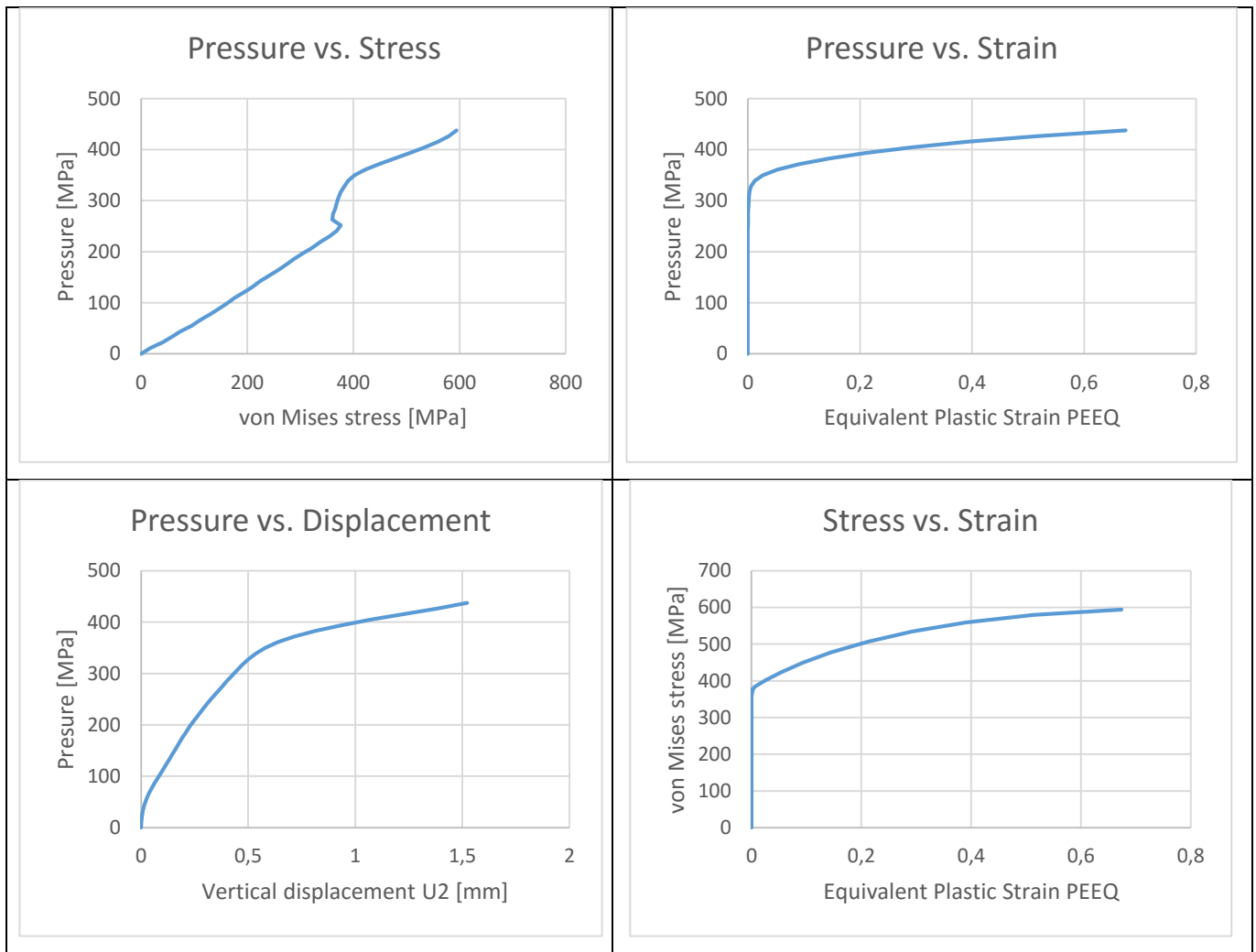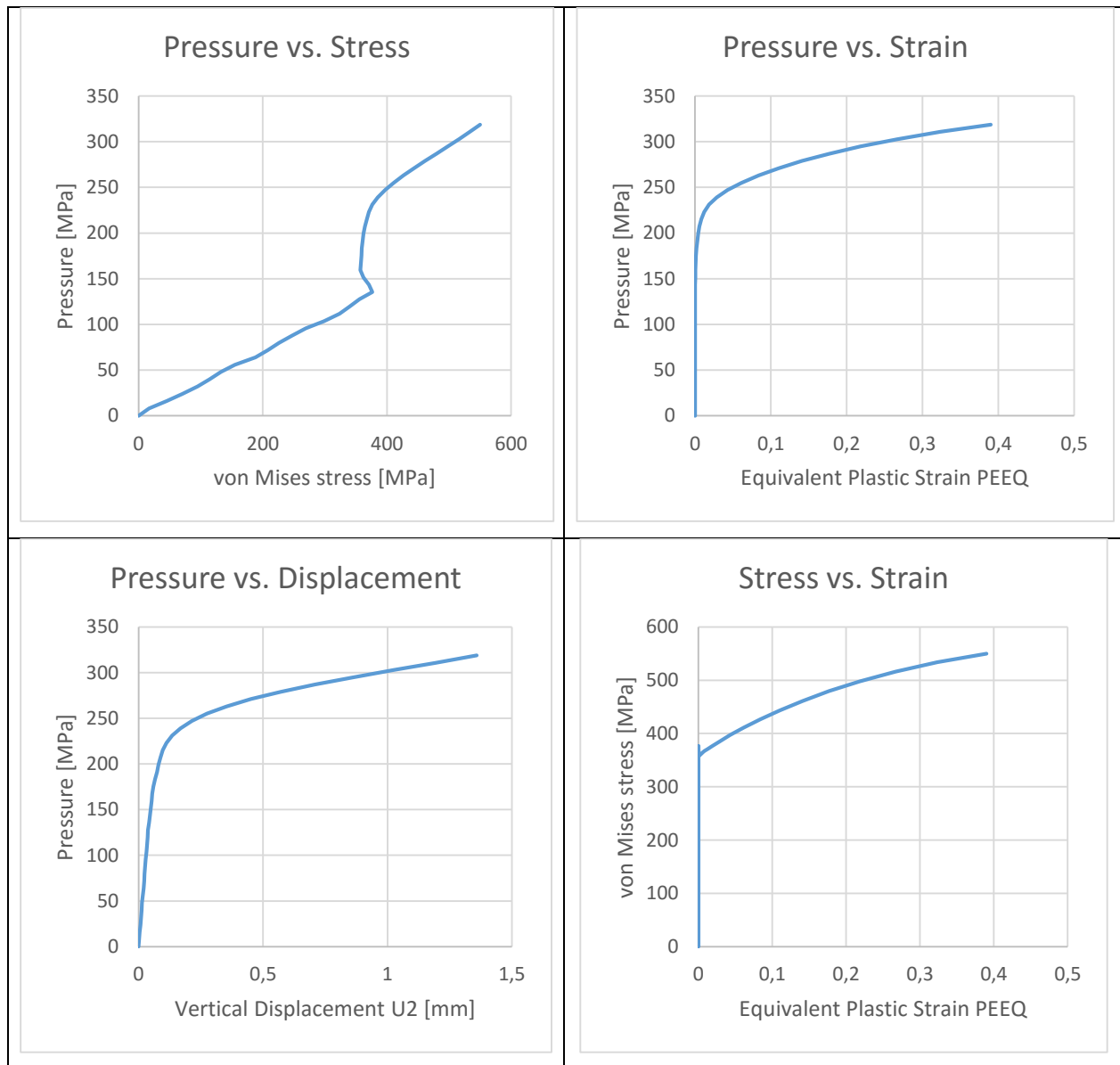

In Table 4.14 it is observed that the capacity ($F_{failure}$) of the pad eye in "Test 7", in the case of pad eye without the plate, is equal to <u>20.379 tons,</u> and the corresponding vertical displacement (U2) is equal to <u>0.600 mm.</u>

For details, see APPENDIX D section "Test 7 (pad eye without the plate)".

5 Comparison

5.1 Introduction

In this chapter, we will cover the objective of this thesis, which is the comparison between simulation results, done in this thesis, with the theoretical and experimental results from the previous thesis [1]. For this purpose, plastic analysis of the stresses, strains and displacements in the upper part of the pinhole were made for pad eyes in various tests. These analyses determined the capacities in the different pad eye tests, which we are going to use as our comparison basis.

5.2 Design load capacity – Theoretical results

The theoretical approach for determining the capacity of the pad eyes was described in section 3.3. The primary focus was on the pad eye calculations, but some calculations for shackles and beams were also done [1], which we are neglecting in this thesis as we only are intrested in the pad eye calculations. The theoretical calculations were conducted for the entire set of tests, which were ten. In this section, only the test results, which are relevant to our comparison, are considered. The relevant results from the theoretical calculations, for determination of the pad eye capacity, are shown in the table below:

Table 5.1 – Theoretical calculation results of the pad eye capacity [1]

Test number	Pinhole diameter of the pad eye [mm]	Load direction	Theoretical load capacity [Tonnes]
1	22	Vertical	26.2
3	32	Vertical	20.7
4	42	Vertical	15.3
5	22	Angular	26.2
6	32	Angular	20.7
7	42	Angular	15.3

5.3 Design load capacity – Experimental results

The experimental approach for determining the capacity of the pad eyes was described in section 3.43.3. Similar to the theoretical approach, the experimental approach in the previous thesis was also conducted for the entire set of tests, which were ten. Again, only six of those experimental tests for our comparison are considered. The relevant results from the experimental calculations, for determination of the pad eye capacity, are shown in the table below:

Table 5.2 - Experimental results of the pad eye capacity [1]

Test number	Pinhole diameter of the pad eye [mm]	Load direction	Experimental Load capacity [Tonnes]	Deformation remarks [mm]
1	22	Vertical	> 21	0.5
3	32	Vertical	> 21	3.5
4	42	Vertical	14.5	Large deformation
5	22	Angular	>14	Large deformation
6	32	Angular	>15	Large deformation
7	42	Angular	>14.5	Large deformation

We can see from Table 5.2 that the smallest deformations are observed in test one and test three. Test four from the experimental load capacity, with the largest pinhole diameter, is smaller than the theoretical load capacity, and therefore, is more subjected to fracture. For the tests specimens five, six and seven, which were subjected to angular loads, could withstand less loads than the theoretical design load, without them being subjected to local buckling. This concludes that:

- The pad eyes had less load capacity than theoretically predicted when the load direction was angled since the plate was most vulnerable to local buckling.
- The pad eyes, which were prepared according to the standard, could withstand larger forces than they were designed for, and got minimal deformations, which showed the importance of following the standards. While the pad eyes that were not prepared according to the specifications, got much larger deformations, and some of them even failed altogether.

The following pictures taken in the laboratory under the testing of the pad eye capacity [1], illustrates the values given in Table 5.2.

Table 5.3 – Experimental pad eye tests [1]

Test 1	Test 3	Test 4

Test 5

Test 6

Test 7

5.4 Design load capacity – FEA simulation results

In this section, our final FEA simulation results will be shown, which are based on the methodology in Chapter 4 "Design Load Capacity – Simulation Approach" These test results include six tests. The first three tests, test one, two and three, were conducted in two cases, which were the pad eyes with and without the plate. While for the last three cases, only the case of the pad eyes without the plates was done, because of time limitation. However, even though all of the simulation tests were not done, the scope of this thesis will still be covered and the conclusion of this thesis will still be made from the available simulation results as the undone simulation tests follows exactly the same procedure as the conducted tests. These simulation results, which are going to be compared to the experimental and theoretical results [1], are from the dynamic simulation part, from section 4.3.1 "Simulation results of the elastic-plastic analysis of the pad eye." where Abaqus /Explicit was used.

Table 5.4 – Design Load Capacity – Simulation Results

| Test number | Simulation Load Capacity | | | |
| | Pad eye with the plate | | Pad eye without the plate | |
	Load capacity [Tons]	Corresponding deformation [mm]	Load capacity [Tons]	Corresponding deformation [mm]
1	26.247	0.250	25.575	0.060
3	24.464	0.750	22.179	0.180
4	23.547	0.850	21.406	0.800
5	-	-	22.493	0.0085
6	-	-	21.904	0.150
7	-	-	20.379	0.600

5.5   Comparison and discussion

In this section, the comparisons of all of the three different types of approaches for designing load capacity of the pad eyes in this thesis are carried out. Where both the experimental, theoretical and finally simulation results of the capacity of the 3.25-ton pad eyes are organized in a table (Table 5.5). These results will then be explained and discussed. Each one of the six tests in the table below will be discussed and explained individually. Then in the next chapter, where the conclusion will be made, the results from these different tests will be explained as a whole, to be able to see and understand the big picture.

Table 5.5 – Final comparison of the design load capacities of pad eyes

Test number	Simulation Load Capacity				Theoretical load capacity	Experimental load capacity	
	Pad eye with the plate		Pad eye without the plate		Pad eye with plate	Pad eye with plate	
	Load capacity [Tons]	Corresponding deformation [mm]	Load capacity [Tons]	Corresponding deformation [mm]	Load Capacity [tons]	Load Capacity [tons]	Corresponding Deformation [mm]
1	26.247	0.250	25.575	0.060	26.2	> 21	0.5
3	24.464	0.750	22.179	0.180	20.7	> 21	3.5
4	23.547	0.850	21.406	0.800	15.3	14.5	Large deformation
5	-	-	22.493	0.0085	26.2	>14	Large deformation
6	-	-	21.904	0.150	20.7	>15	Large deformation
7	-	-	20.379	0.600	15.3	>14.5	Large deformation

We can see from Table 5.5 that:

- **In Test 1**, in the case where the pad eye is without the plate, the capacity from the FEA simulation load capacity is larger than both the theoretical and the experimental load capacities, while the displacements are much smaller than the experimental deformation. In the case of the pad eye with the addition of the plate, the test specimens can carry the same amount of load as the theoretical design load, without going to failure, and can withstand larger loads than the experimental. This shows that when following the standards (as the pad eye geometries which test 1 is based on, is in accordance with NORSOK R-002, [17], while tests two and three are not totally based on NORSOK R-002), very reliable and precise simulation results can be obtained. Moreover, it is observed from the table that the displacement for the pad eye with the plate is much larger and closer to the experimental results than for the pad eye without the plate, which is because that this deformation of the plate is now also a part of the global deformation of the pad eye. It can be seen from the table that the experimental load capacity has no particular value, as it is >21 tons, which means that it can carry more than 21 tons without being subjected to failure.

In Table 4.6, which represents the pad eye without the plate, in the "Pressure vs. Stress" graph, there is a red marking on the curve, which represents the start of the yielding in the pad eye. The "Pressure vs. Strain" graph shows that the yielding starts at a pressure value around 375 MPa. While in "Stress vs. Strain", the yielding begins at a von Mises stress value of approximately 360 MPa. In the "Pressure vs. Displacement" graph, it is observed that the displacement follows an approximate proportional incrimination, which is reasonable as the displacement should increase with increased applied pressure, until a certain point before it is subjected to fracture. In Table 4.7, which represent the pad eye with the plate, it is noticed an increment in the pressure applied to the pad eye, which was helpful to get the desired results, and at the same time did not lead to failure of the pad eyes. To obtain the wanted pressure, many tests were carried out to find the right amount of pressure. The increment in the pressure led to larger capacity in the pad eyes with the plates than in the pad eyes without the plates.

- **In Test 3**, in the case where the pad eye is without the plate, the capacity from the FEA simulation load capacity is larger than both the theoretical and the experimental, while the displacements are again far from the experimental. In the case of the pad eye with the plate, the simulation load capacity is even larger. Regarding the displacements, it is again observed that the displacement for the pad eye with the plate is much greater than for the pad eye without the plate, and are closer to the experimental result.

  In Table 4.8 and Table 4.9, the same patterns of graphs (except some small changes) are observed as in Table 4.6 and Table 4.7, which are described above.

- **In Test 4**, in the case where the pad eye is without the plate, the capacity from the FEA simulation load capacity is much larger than both the theoretical and the experimental. In the case of the pad eye with the plate, the simulation load capacity is even greater. Regarding the displacements, it is not possible to compare the results at this stage since there is no particular value of the deformation as it is only noted "large deformation."

  In Table 4.10 and Table 4.11, the same patterns of graphs (except some small changes) are observed as in Table 4.6 and Table 4.7, which are described above.

- **In Test 5**, which only contains the pad eye without plate, the capacity from the FEA simulation load capacity is smaller than the theoretical and larger than the experimental load capacities. It is also noticeable that the load capacity in Test 5 (22.493 tons), which is an angled loading, is smaller than the load capacity in Test 1 (25.575 tons), which is a vertical loading. In Table 4.12, the same patterns of graphs (except some small changes) are observed as in Table 4.6 , which are described above. The only difference is in the "Pressure vs. Displacement" graph, which shows an increment of the graph in a negative direction. The reason is that the angled loading has led to a strain which has caused the critical zone to move in the opposite direction of the loading direction U2, which is a negative vertical displacement.

- **In Test 6**, which only contains the pad eye without plate, the capacity from the FEA simulation load capacity is close to the theoretical and much larger than the experimental load capacities. In Table 4.12, the same patterns of graphs (except some small changes) are observed as in Table 4.6 , which are described above.

- **In Test 7**, which only contains the pad eye without plate, the capacity from the FEA simulation load capacity is much larger than both the theoretical and the experimental load capacities. In Table 4.12, the same patterns of graphs (except some small changes) are observed as in Table 4.6 , which are described above.

6 Conclusion

The primary purpose of this master's thesis was to show the difference between the design capacity results of the 3.25-ton pad eye, with different approaches, being the experimental, the theoretical, and the FE analysis simulation. The FEA simulation software, which was utilized to carry out the pad eye tests, was Abaqus/CAE. To get acquainted with the software, I started with a simple example, and then moved on the main problem, which was to design and to analyze the 3.25-ton pad eye in Abaqus(CAE. It took a lot of time to build a basic knowledge in Abaqus/CAE so that I could comfortably and successfully carry out the simulation tests that was based on the NORSOKS standard "Lifting Equipment" [17].

The comparison results showed positive signs to some extent, as some of the simulation results were very close to the theoretical and the experimental results, while others were a bit far from them. There are several factors which can be the cause of the deviation from the results of the three different approaches. The factors can be:

- In reality, the real material behavior can withstand more load than the than the assumptions made in the DNV standards generally, and more specifically, in our thesis, the DNV-RP-C208 [5]. The reason is that the requirements in the DNV standards include safety factors, which leads safer designs.
- The uncertainty of the material behavior may have caused these deviations.
- The uniform applied pressure acting on the upper part of the pinhole, instead of an actual pin, may also have caused the differences in the results.

Even though there was some deviation between the numerical results obtained from the different approaches, the result patterns were the same. It is observed in our comparisons that the capacity of the pad eyes reduces when the pinhole diameter size increase, which demonstrates the importance of following the standard requirements. Furthermore, the results show that the pad eyes with the base plate have greater capacity than the pad eyes without the plates. Finally, a reduction of the load capacity is recognized for the angled loading case when compared to the vertical loading case, even though the theoretical capacities provide the same results for both cases.

For further studies, it would be interesting to investigate the following cases:

- Because the uncertainty of material behavior may lead to deviations in the results, its is advisable to attend probabilistic FE simulation for more precise comparison as future studies.

- Although reasonably good results were obtained by applying the uniform pressure on the pad eye pinhole, it may give even better results if a multi-model pad eye were designed and analysed. Where both, the pad eye and the pin were designed and interacted with each other so that the pin is pulling the up (in a vertical or an angled direction) instead of the uniform pressure.

References

1.   Kvalvaag, R., *Offshore Hook-up project management*, in *Department of Mechanical and Structural Engineering/Offshore Construction*. 2014: University of Stavanger, Norway.
2.   Kvalvåg, R., A. Christerssion, and S.C. Siriwardane. *Testing for Load Capacity of Pad Eyes used in Offshore Lifting Operations*. in *IABSE Symposium Report*. 2015. International Association for Bridge and Structural Engineering.
3.   Bo, Z., L. Yujun, and J. Zhuoshang, *Robust stress check formula of lifting padeye.* Journal of Ship Research, 2010. **54**(1): p. 34-40.
4.   *NORSOK R-002, Lifting equipment*. September 2012, Standards Norway.
5.   Veritas, D.N., *DNV-RP-C208: Determination of Structural Capacity by Non-linear FE analysis Methods.* Det Norske Veritas, 2013.
6.   Young, W.C. and R.G. Budynas, *Roark's formulas for stress and strain*. Vol. 7. 2002: McGraw-Hill New York.
7.   Arthur P. Boresi, R.J.S., *Advanced Mechanics of Materials, Six Edition*. 2003, USA: John Wiley & Sons, Inc.
8.   Ling, Y., *Uniaxial true stress-strain after necking.* AMP Journal of Technology, 1996. **5**: p. 37-48.
9.   *Lug analysis*. 2015; Available from: https://mechanicalc.com/theory/lug-analysis#note-pin-size.
10.   *NORSOK N-004, Design of Steel Structures*, in *Standards Norway*. October 2004.
11.   Dhatt, G., E. Lefrançois, and G. Touzot, *Finite element method*. 2012: John Wiley & Sons.
12.   De, P.S. *MANE 4240/ CIVL 4240: Introduction to Finite Elements*. Available from: http://info.baustatik.uni-due.de/Lehre/CM-AOS/DocuCollection/Abaqus/Abaqus%20tutorial.pdf.
13.   Corp, D.S.S., *Abaqus/CAE 6.10 User's Manual*. 2010, Providence, RI, USA: Dassault Systèmes Simulia Corp.
14.   Boresi, A.P., *Advanced Mechanics of Materials* Sixth Edition ed. 2003: John Wiley and Sons, INC.
15.   *DNV Standard for Certification 2.7-1 "Offshore Containers"*. June 2013, Det norske veritas AS.
16.   Mitao Ohga, S.C.S., *Fatigue Life of Steel Structures under Service and Ultimate Loadings: Recent Concepts, Formulations and Case studies*. May 2011, USA: LAP LAMBERT Academic Publishing.
17.   *NORSOK R-002, "Lifting equipment"*. September 2012: Standards Norway.

APPENDIX A   DATA TABLES

Table A.1 - Yield strength of steel type S235 [5]

Table 4-2 Proposed non-linear properties for S235 steels (Engineering stress-strain)			
	S235		
Thickness [mm]	$t \leq 16$	$16 < t \leq 40$	$40 < t \leq 63$
E [MPa]	210000		
$\sigma_{prop}/\sigma_{yield}$	0.9		
E_{p1}/E	0.001		
σ_{prop} [MPa]	211.5	202.5	193.5
σ_{yield} [MPa]	235	225	215
σ_{yield2} [MPa]	238.4	228.4	218.4
σ_{ult} [MPa]	360	360	360
ε_{p_y1}	0.004		
ε_{p_y2}	0.02		
ε_{p_ult}	0.2		
E_{p2}/E	0.0032	0.0035	0.0037

Table A.2 - Yield strength of steel type S355 [5]

Table 4-3 Proposed non-linear properties for S355 steels (Engineering stress-strain)			
	S355		
Thickness [mm]	$t \leq 16$	$16 < t \leq 40$	$40 < t \leq 63$
E [MPa]	210000		
$\sigma_{prop}/\sigma_{yield}$	0.9		
E_{p1}/E	0.001		
σ_{prop} [MPa]	319.5	310.5	301.5
σ_{yield} [MPa]	355	345	335
σ_{yield2} [MPa]	358.4	348.4	338.4
σ_{ult} [MPa]	470	470	450
ε_{p_y1}	0.004		
ε_{p_y2}	0.02		
ε_{p_ult}	0.15		
E_{p2}/E	0.0041	0.0045	0.0041

APPENDIX B   FIGURES FROM ABAQUS/CAE

(a)

(b)

(c)

- (a) is the pad eye with 22 mm pinhole diameter
- (b) is the pad eye with 32 mm pinhole diameter
- (c) is the pad eye with 42 mm pinhole diameter

Assembly figures for the pad eyes without plate:

(d)

(e)

- (d) is the pad eye with 32 mm pinhole diameter
- (e) is the pad eye with 42 mm pinhole diameter
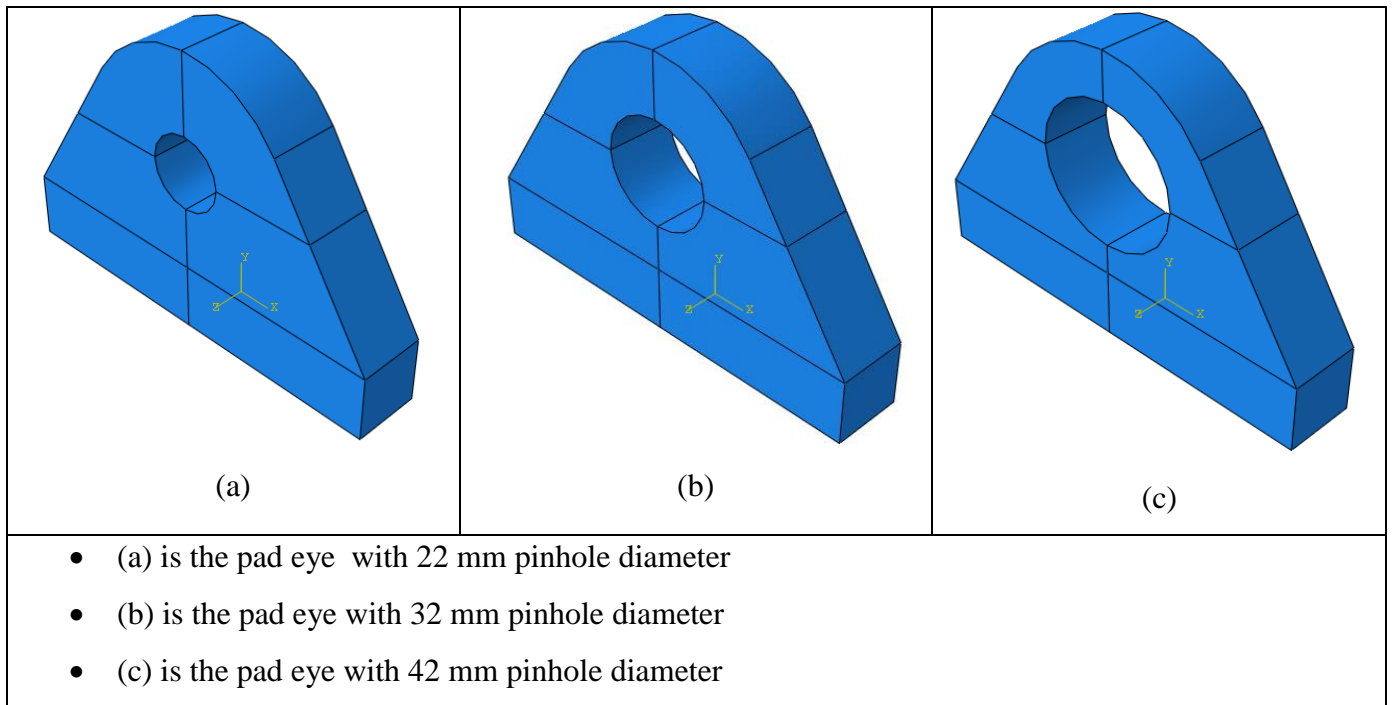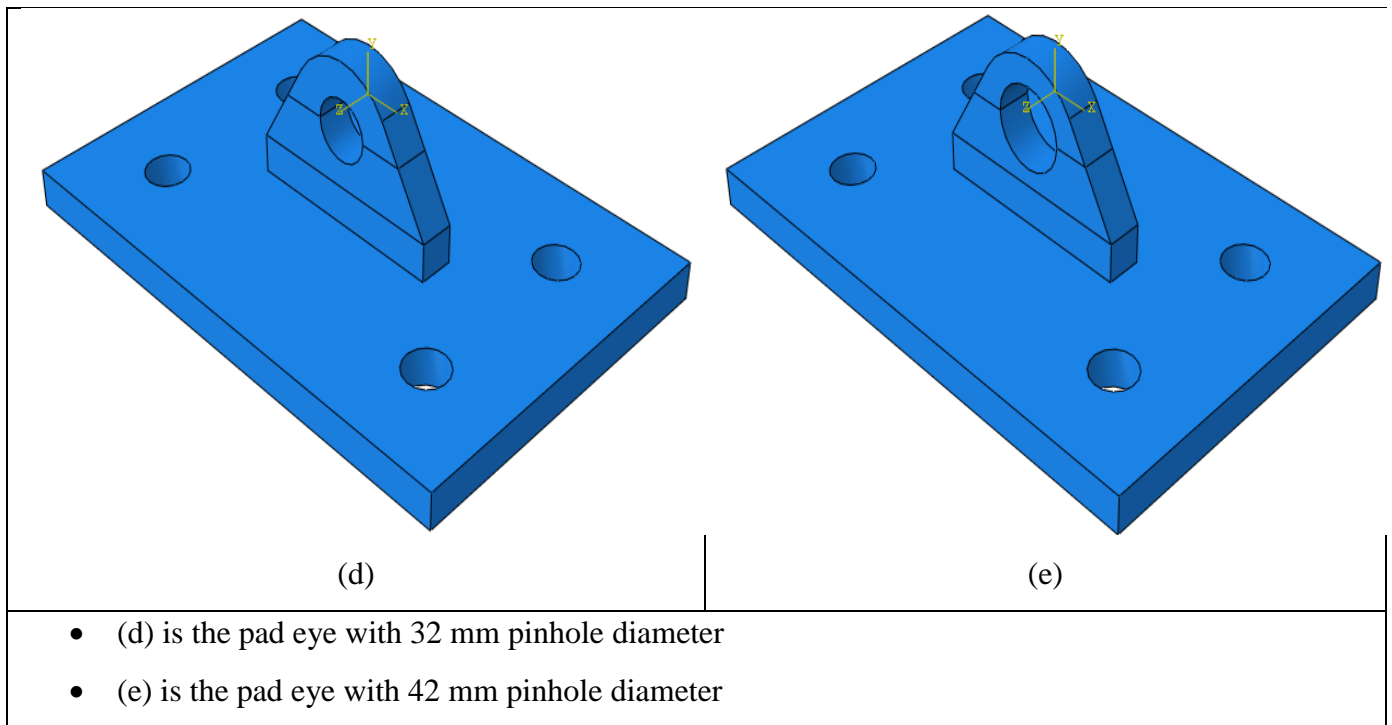
Assembly figures for the pad eyes with plate

B.2
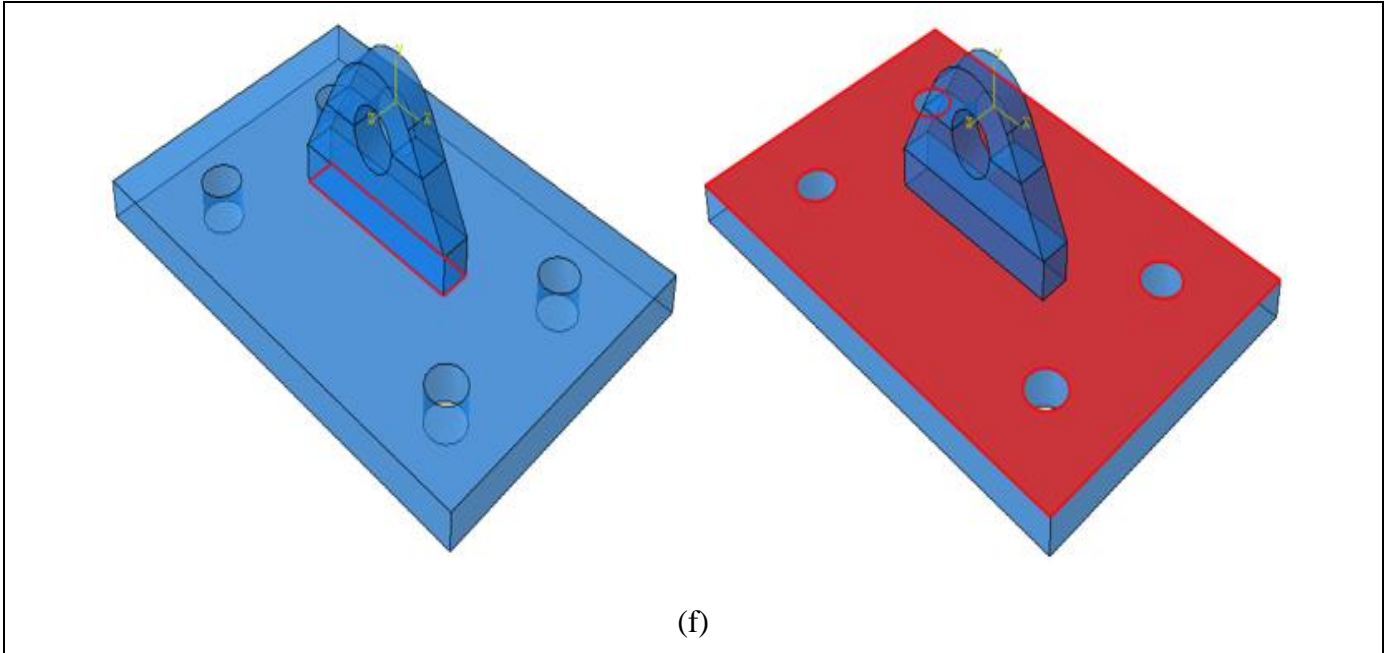
(f)
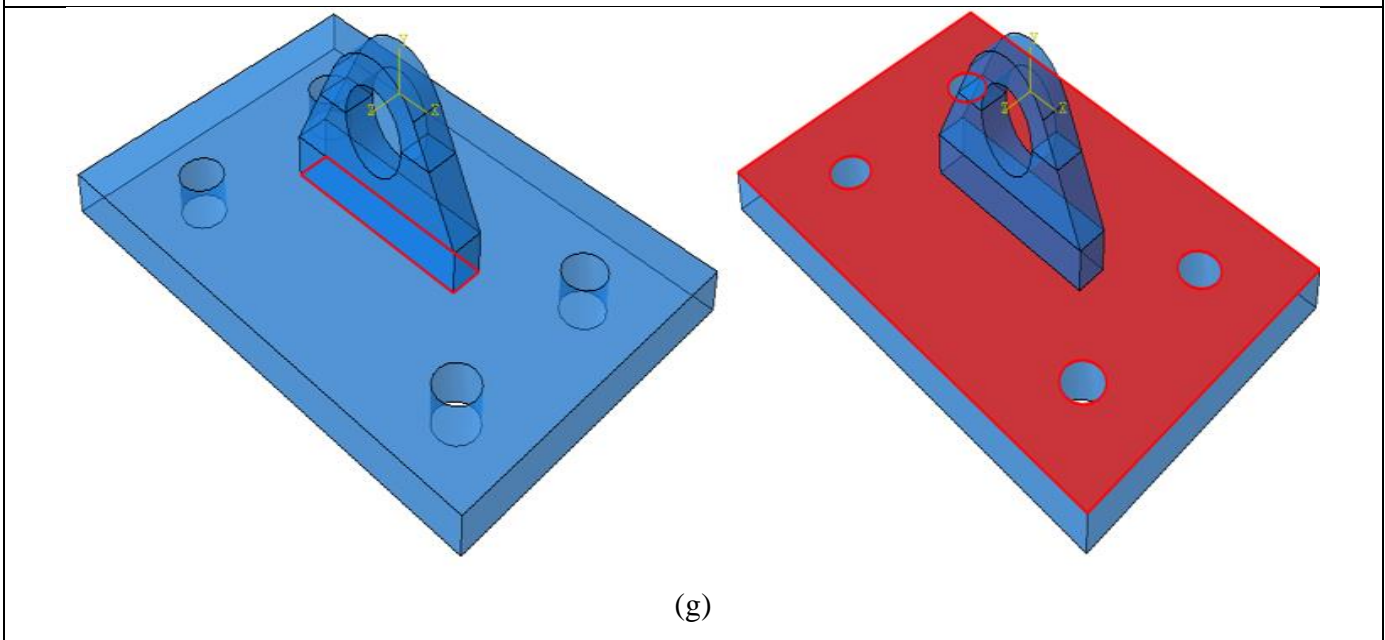
(g)

- (f) is the pad eye with 32 mm pinhole diameter

- (g) is the pad eye with 42 mm pinhole diameter

Surfaces of the pad eye with plate that we want to tie together firmly

B.3

(h)

(i)

- (h) is the pad eye with 32 mm pinhole diameter
- (i) is the pad eye with 42 mm pinhole diameter

Pad eyes without plate subjected to vertical uniform pressure and fixed BC

(j)

(k)

- (j) is the pad eye with 32 mm pinhole diameter
- (k) is the pad eye with 42 mm pinhole diameter
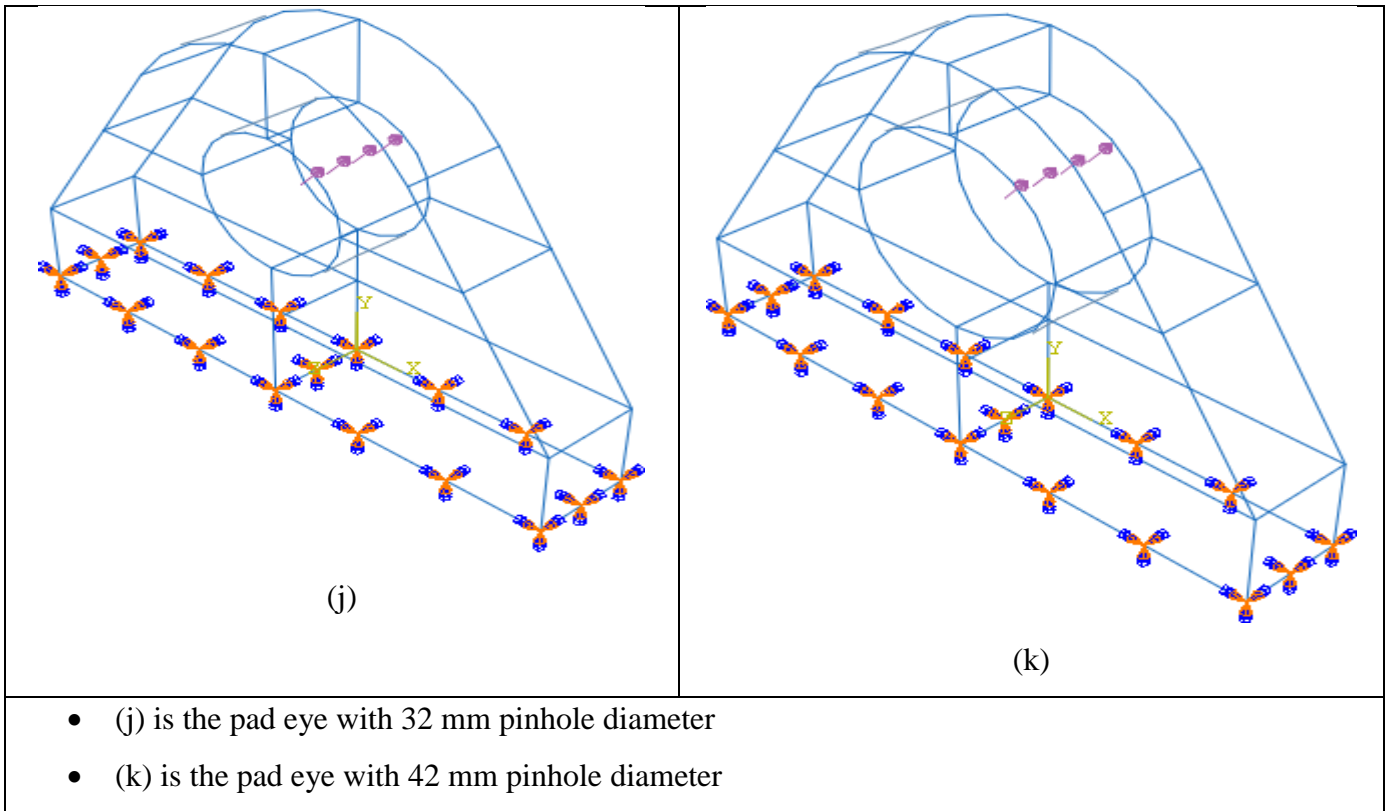
Pad eyes without plate subjected to angled uniform pressure and fixed BC

B.4

(l)	(m)

- (l) is the pad eye with 32 mm pinhole diameter
- (m) is the pad eye with 42 mm pinhole diameter
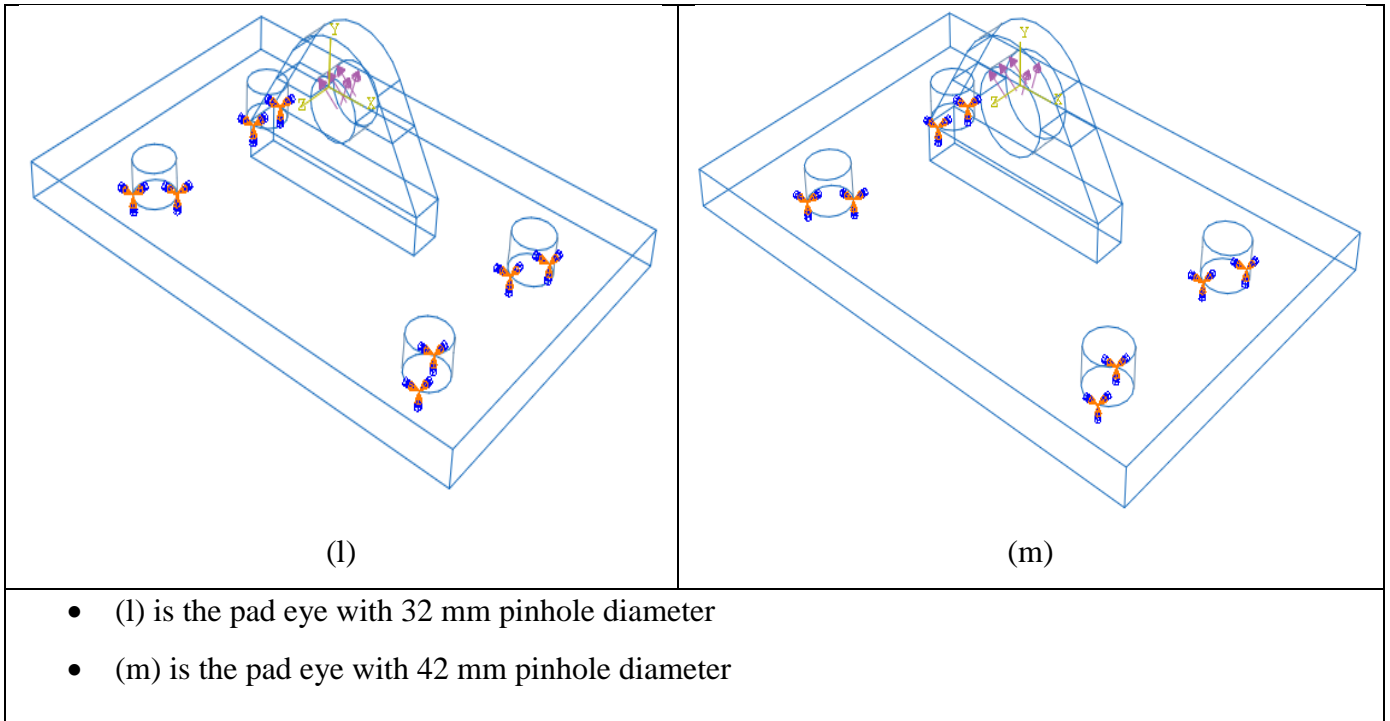
Pad eyes with plate subjected to vertical uniform pressure and fixed BC

Converting mass into <u>vertical</u> uniform pressure:

1 kilogram-force = 9.81 N

<u>Test 1:</u>

$$P = \frac{F}{D*t} = \frac{g*m}{D*t} = \frac{9.81N*21000kgf}{22mm*20mm} = 468.20\frac{N}{mm^2} = 468.20MPa \approx 500MPa$$

(since the capacity is >21 tons)

<u>Test 3:</u>

$$P = \frac{F}{D*t} = \frac{g*m}{D*t} = \frac{9.81N*21000kgf}{32mm*20mm} = 321.90\frac{N}{mm^2} = 321.90MPa \approx 350MPa$$

(since the capacity is >21 tons)

<u>Test 4:</u>

$$P = \frac{F}{D*t} = \frac{g*m}{D*t} = \frac{9.81N*14500kgf}{42mm*20mm} = 169.3\frac{N}{mm^2} = 169.3 \; MPa$$

Converting mass into <u>angled</u> uniform pressure:

<u>Test 5:</u>

$$P = \frac{F}{0.85*D*t} = \frac{g*m}{0.85*D*t} = \frac{9.81N*14000kgf}{0.85*22mm*20mm} = 367.22\frac{N}{mm^2} = 367.22 \; MPa \approx$$

$$400 \; MPa \; \text{(since the capacity is >14 tons)}$$

<u>Test 6:</u>

$$P = \frac{F}{0.85*D*t} = \frac{g*m}{0.85*D*t} = \frac{9.81N*15000kgf}{0.85*32mm*20mm} = 270.50\frac{N}{mm^2} = 270.5 \; MPa \approx$$
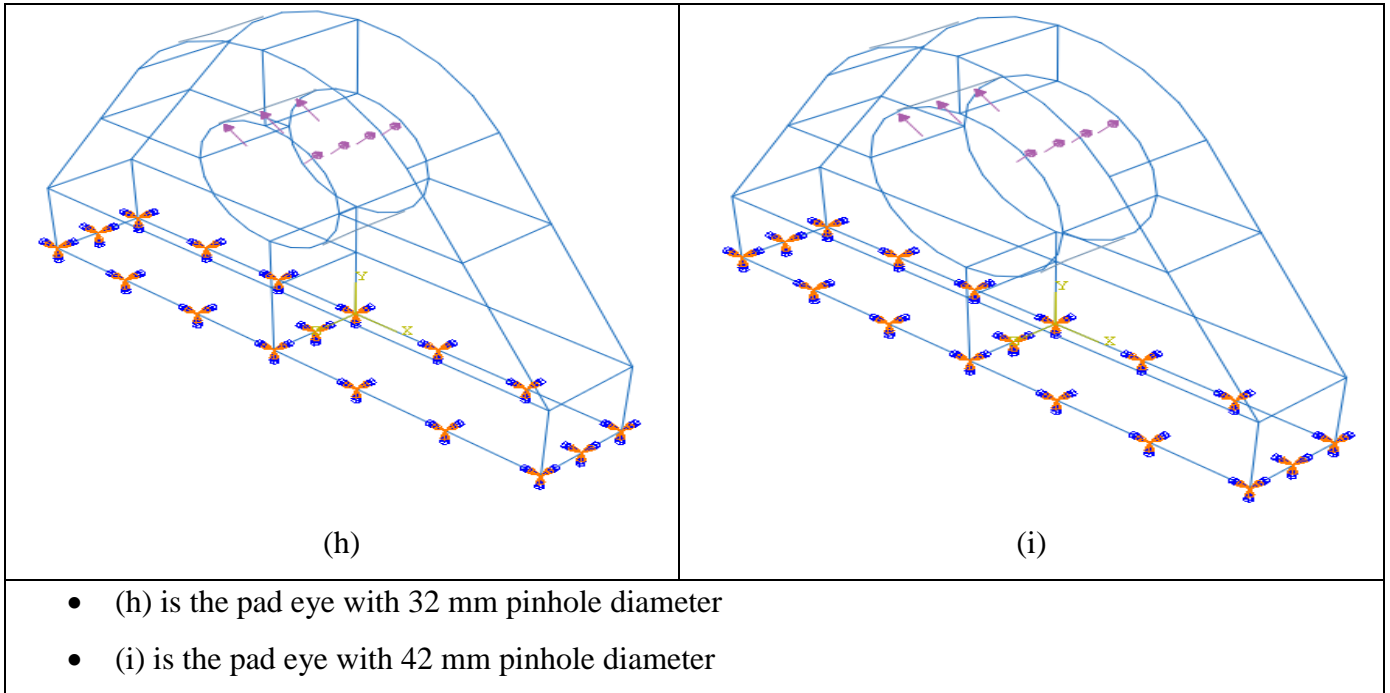
$$300 \; MPa \; \text{(since the capacity is >15 tons)}$$

<u>Test 7:</u>

$$P = \frac{F}{0.85*D*t} = \frac{g*m}{0.85*D*t} = \frac{9.81N*14500kgf}{0.85*42mm*20mm} = 199.22\frac{N}{mm^2} = 199.22 \; MPa \approx$$

$$250 \; MPa \; \text{(since the capacity is >14.5 tons)}$$

B.6

APPENDIX C   ELASTIC ANALYSIS RESULTS

Simulation results of the static analysis of the pad eyes using Abaqus/Standard.

<u>Test 1 (pad eye without plate):</u>

NB! The numbering of the figures in this appendix are based on

(a)

(d)

(b)

(c)

C.8

(e)

(f)

C.9
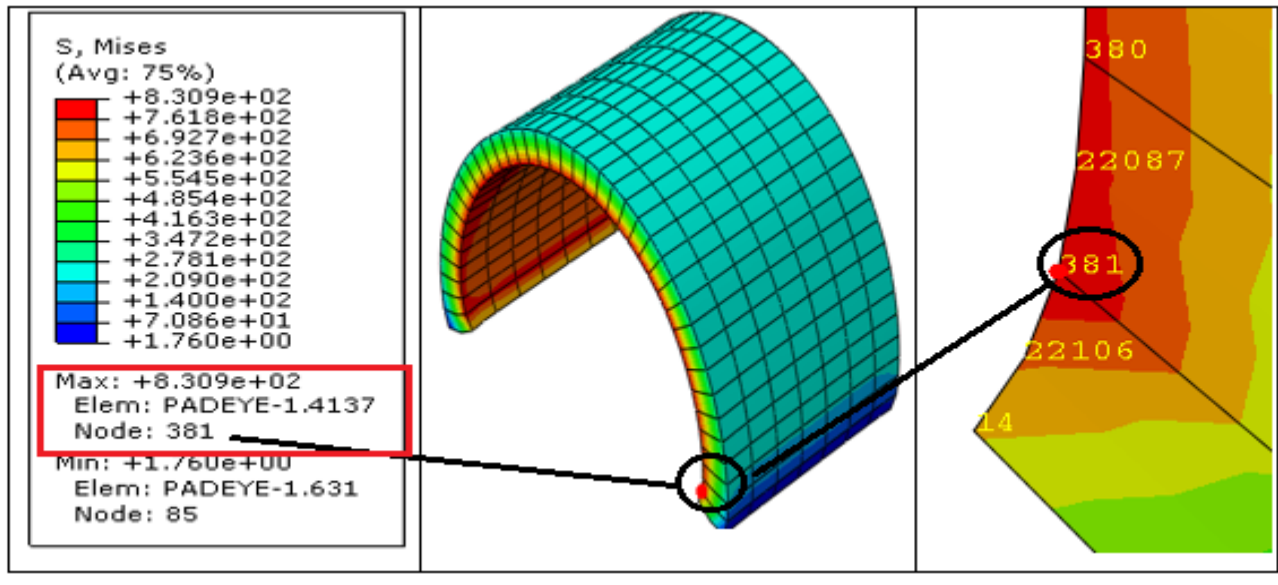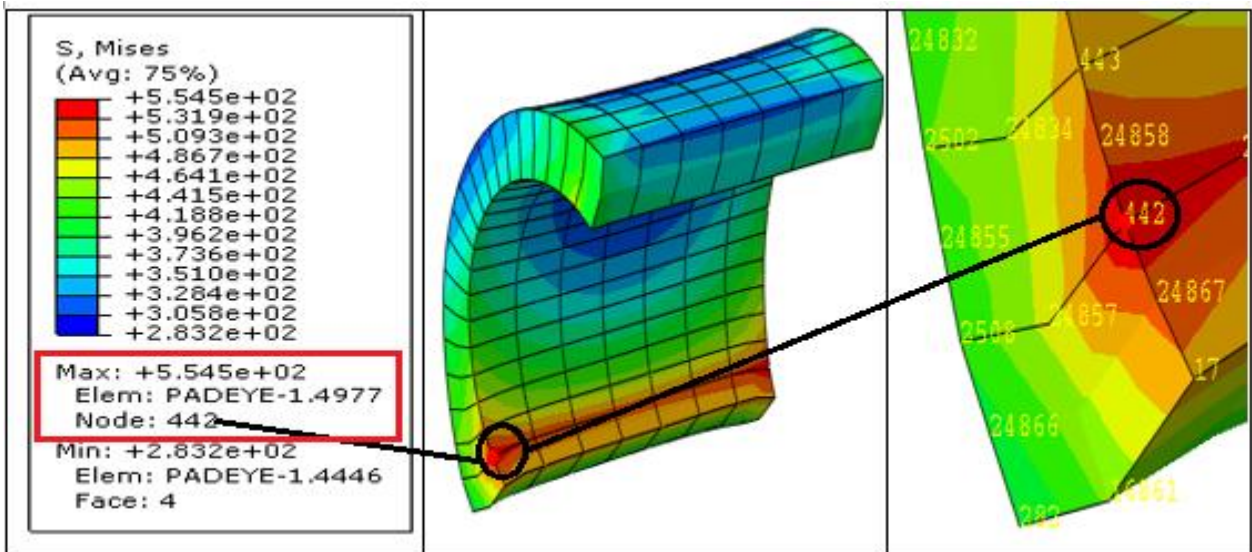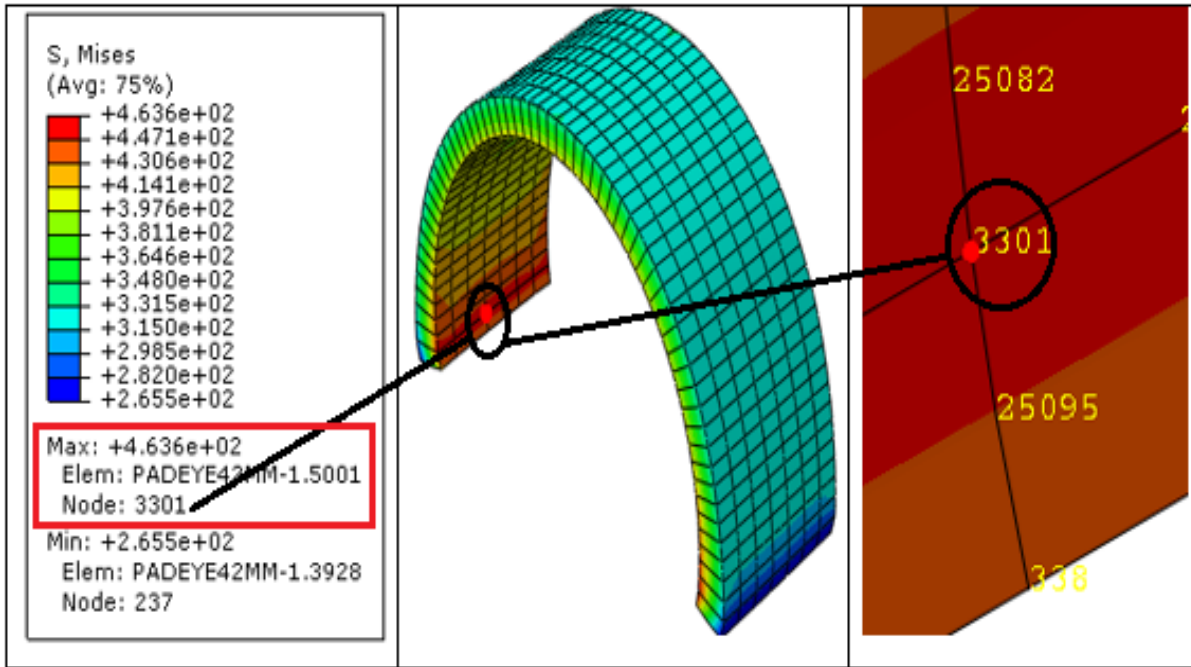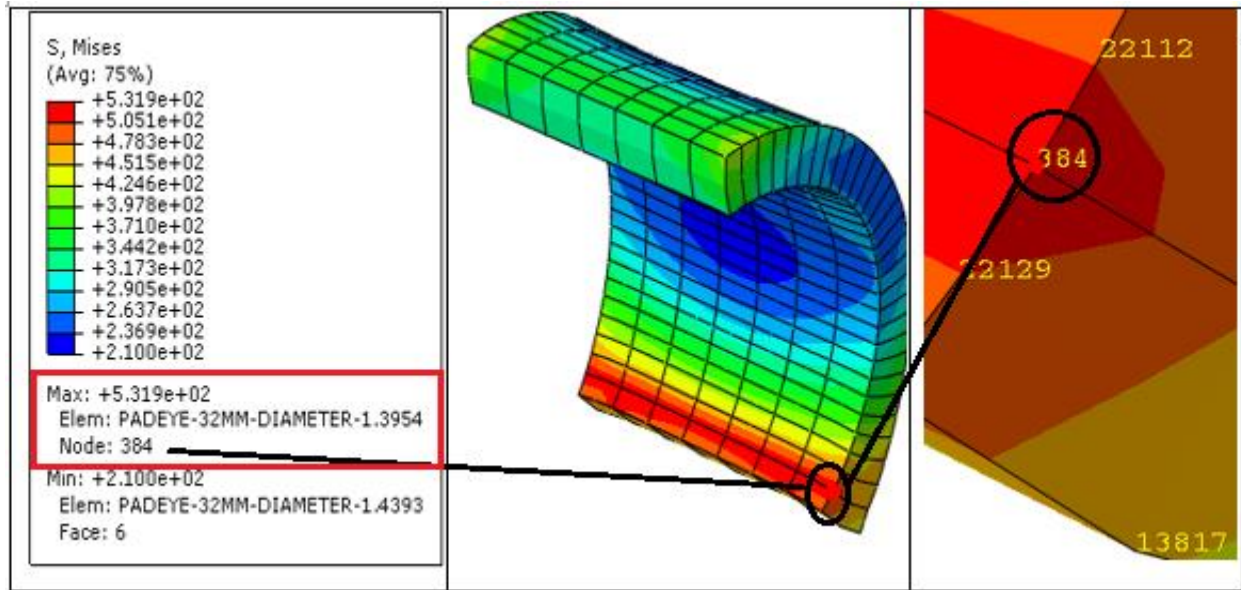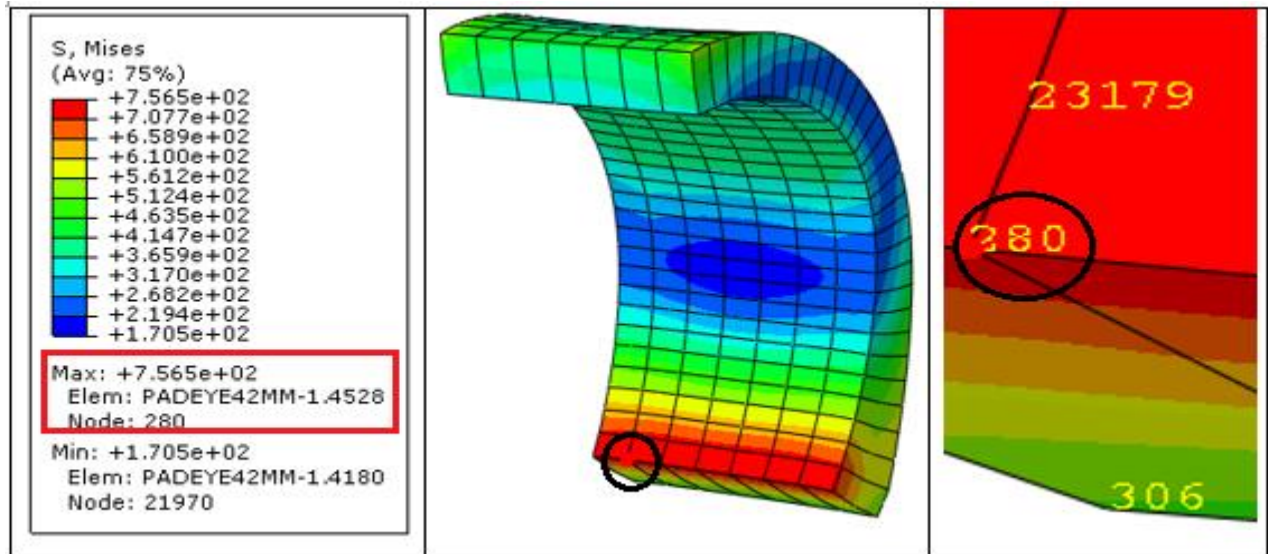
Second case: pad eyes with the plate

(g)

(h)

(i)

C.10
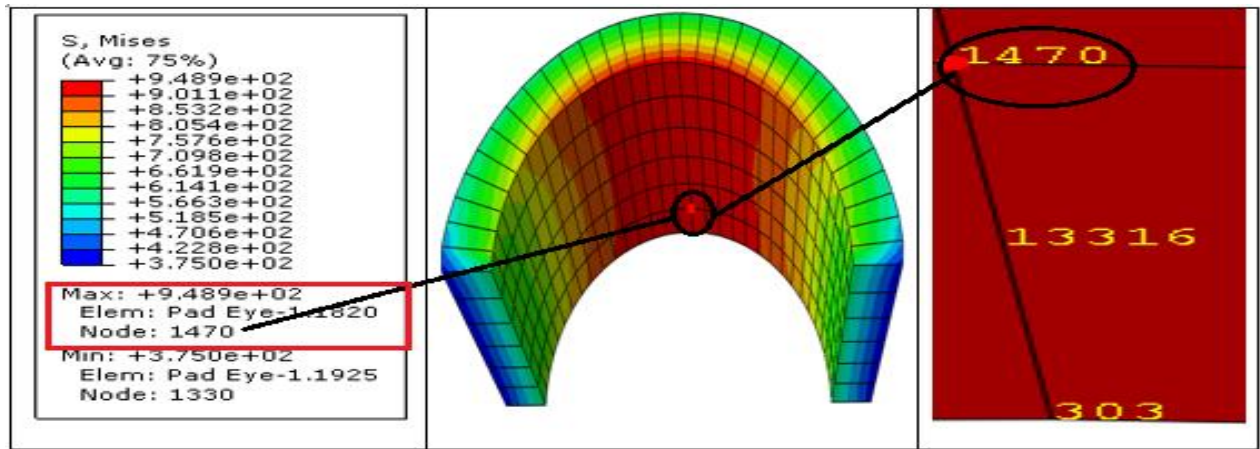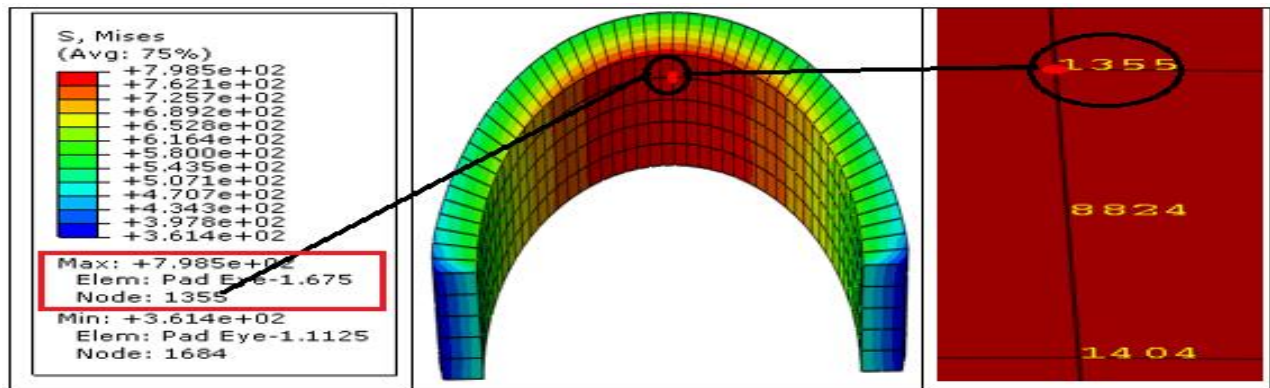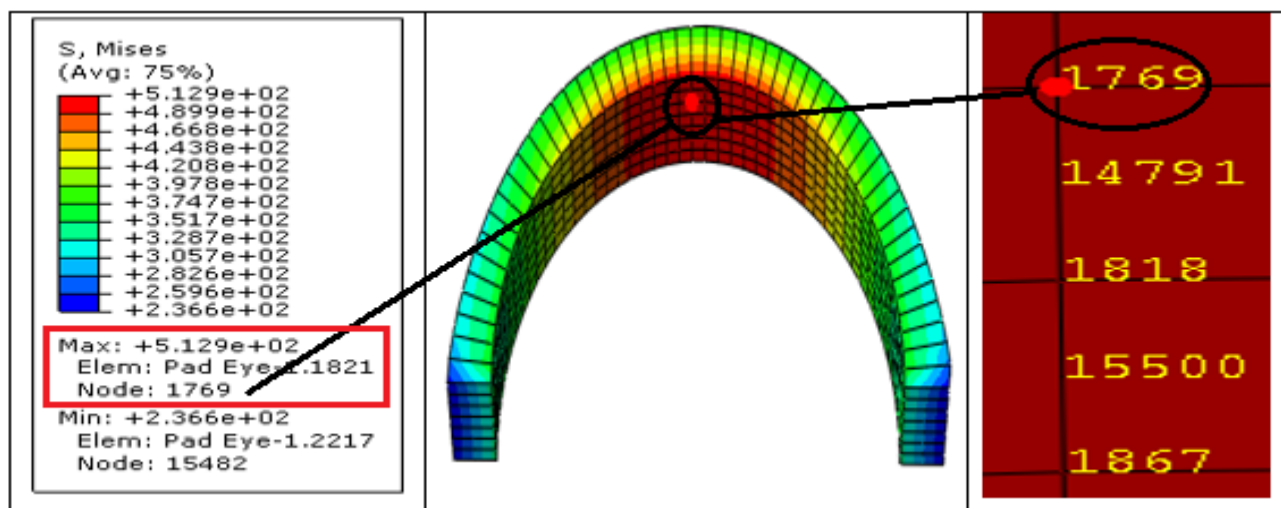
APPENDIX D   ELASTIC-PLASTIC ANALYSIS RESULTS

Simulation results of the dynamic analysis of the pad eyes using Abaqus/Explicit.
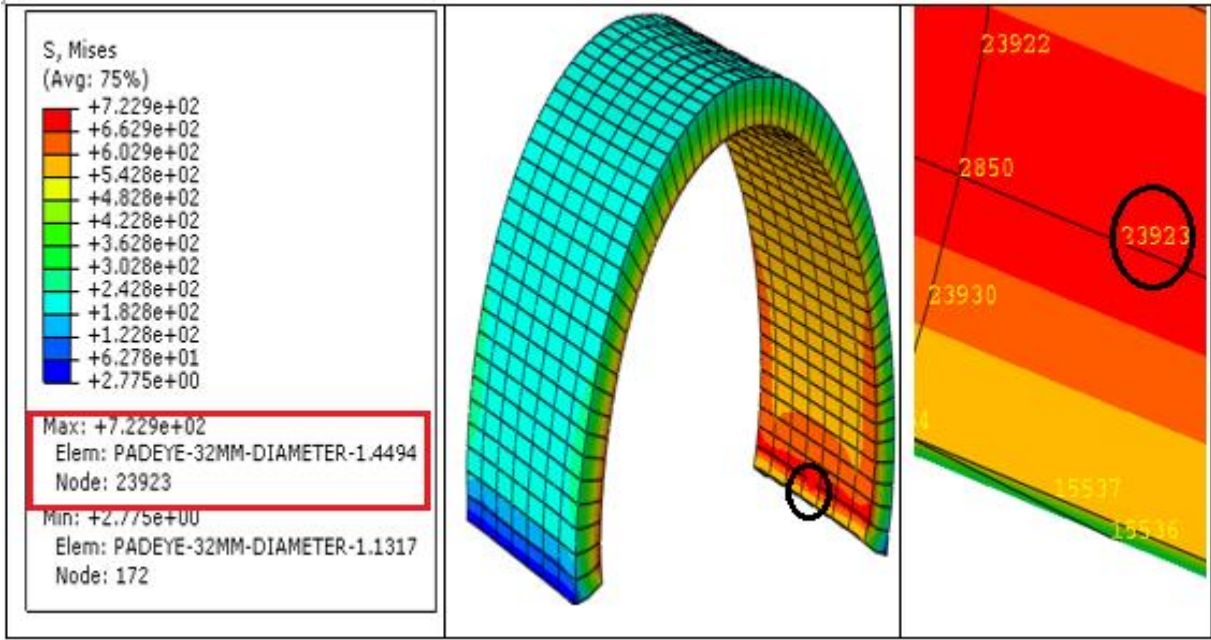
Test 1 (pad eye without plate):
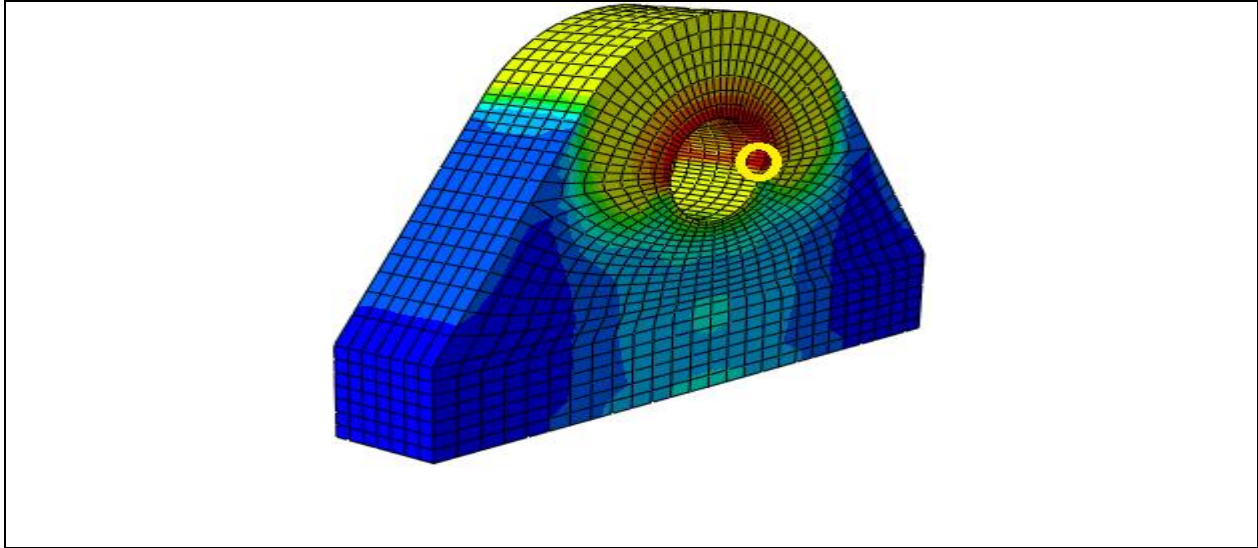
Critical zone (yellow circle) in pad eye pinhole, without plate (Test 1)

Pad eye pinhole, for pad eye without plate (Test 1)
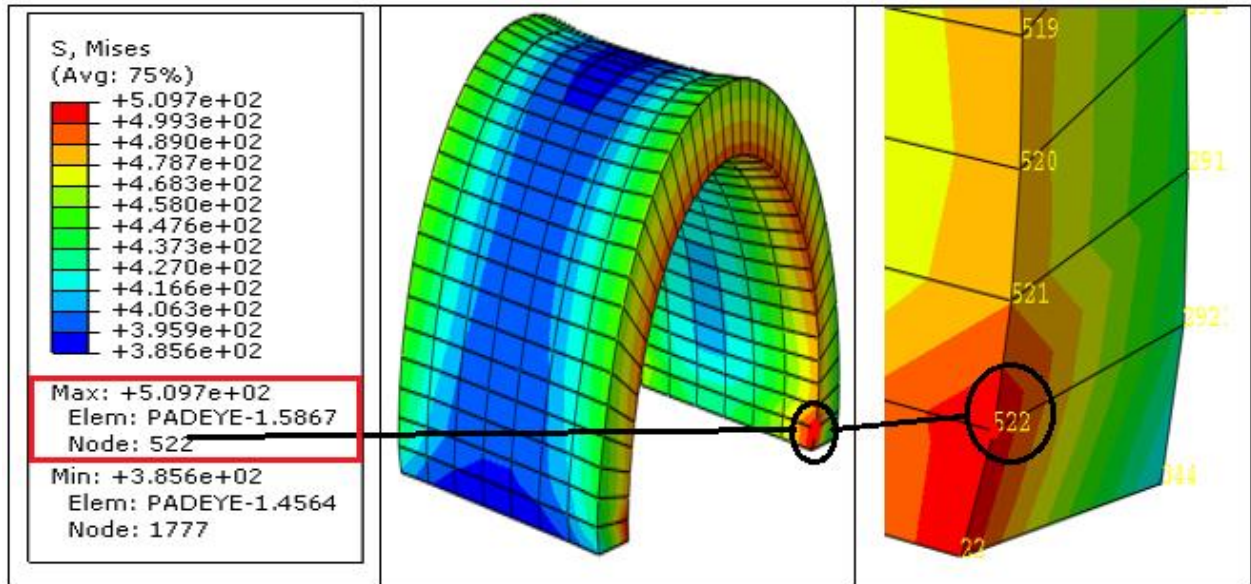
```
Field Output Report, written Wed Jun 08 18:18:40 2016

Source 1
---------

   ODB: C:/Temp/excel.odb
   Step: Padeye loading
   Frame: Increment     1848: Step Time =   6.0000E-03

Loc 1 : Nodal values from source 1

Output sorted by column "Node Label".

Field Output reported at nodes for part: PADEYE-1
   Computation algorithm: EXTRAPOLATE_COMPUTE_AVERAGE
   Averaged at nodes
   Averaging regions: ODB_REGIONS
```

Node Label	U.U2 @Loc 1	PEEQ @Loc 1	S.Mises @Loc 1	S.S11 @Loc 1	S.S22 @Loc 1	S.S33 @Loc 1
22	24.0645E-03	203.032E-03	507.364	-167.616	-93.8100	-41.5879
521	176.157E-03	187.994E-03	488.621	-486.749	-28.8464	-77.9734
522	77.7026E-03	223.204E-03	509.669	-371.574	-60.1862	-73.8064
1954	22.5417E-03	8.94123E-06	218.689	119.789	-14.5953	48.8221
Minimum	22.5417E-03	8.94123E-06	218.689	-486.749	-93.8100	-77.9734
At Node	1954	1954	1954	521	22	521
Maximum	176.157E-03	223.204E-03	509.669	119.789	-14.5953	48.8221
At Node	521	522	522	1954	1954	1954

Stress, Strain and Displacement values at node 522

Calculations based on graphs in Table 4.6

<u>Von Mises</u> (from Pressure vs. Stress graph)

1 Newton = 0.101972 Kilogram-force

$$F_{\text{max 1}} = P_{\text{max 1}} * D * t = 570\frac{N}{mm^2} * 22mm * 20mm = 250\ 800\ N = \underline{25.575\ tons}$$

<u>Plastic equivalent strain PEEQ</u> (from Pressure vs. Strain graph)

$$F_{\text{max 2}} = P_{\text{max 2}} * D * t = 580\frac{N}{mm^2} * 22mm * 20mm = 255\ 200\ N = \underline{26.023\ tons}$$

We can see from the calculations above that, F_{max1} is smaller than F_{max2}, which means:

$$F_{failure} = F_{\text{max 1}} = \underline{\textbf{25.575 tons}}\ \text{(Capacity)}$$

Vertical displacement, U_2 (From Pressure vs. Displacement graph) at pressure failure load $(P_{\text{max 1}} = 570\frac{N}{mm^2})$ is equal to **0.060 mm.**

D.12

Test 1 (pad eye with plate):

Although there might be higher stress values than the stresses in the yellow circle, for example in the bolt-holes, but we only highlight the critical zones in the upper part of the pad eye pinhole as it is our area of interest.

Critical zone (yellow circle) in pad eye with plate (Test 1)

Pad eye pinhole, for pad eye with plate (Test 1)

D.13

```
Source 1
---------

   ODB: C:/Temp/liri22mmpadeyeplate.odb
   Step: Apply load
   Frame: Increment      2198: Step Time =   6.0000E-03

Loc 1 : Nodal values from source 1

Output sorted by column "Node Label".

Field Output reported at nodes for part: Pad Eye-1
   Computation algorithm: EXTRAPOLATE_COMPUTE_AVERAGE
   Averaged at nodes
   Averaging regions: ODB_REGIONS

         Node          U.U2           PEEQ         S.Mises          S.S11          S.S22          S.S33
         Label        @Loc 1         @Loc 1        @Loc 1          @Loc 1         @Loc 1         @Loc 1
     --------------------------------------------------------------------------------------------------------
           11     147.784E-03    770.480E-03      614.599         -99.8984       -408.403       -103.313
          171     36.8447E-03    347.987E-03      559.290        -248.467       -285.466        -97.8729
          172     220.312E-03     1.00251         604.889        -446.887       -229.635       -213.883
         1188     156.259E-03    591.227E-03      585.137        -509.465       -156.965       -138.529


Minimum          36.8447E-03    347.987E-03      559.290        -509.465       -408.403       -213.883

   At Node             171            171            171            1188             11            172
Maximum          220.312E-03     1.00251         614.599         -99.8984       -156.965        -97.8729

   At Node             172            172             11              11           1188            171
```

Calculations based on graphs in Table 4.7

<u>Von Mises</u> (from Pressure vs. Stress graph)

1 Newton = 0.101972 Kilogram-force

$$F_{max\,1} = P_{max\,1} * D * t = 585\,\frac{N}{mm^2} * 22mm * 20mm = 257\,400\,N = \underline{26.247\;tons}$$

<u>Plastic equivalent strain PEEQ</u> (from Pressure vs. Strain graph)

$$F_{max\,2} = P_{max\,2} * D * t = 590\,\frac{N}{mm^2} * 22mm * 20mm = 259\,600\,N = \underline{26.471\;tons}$$
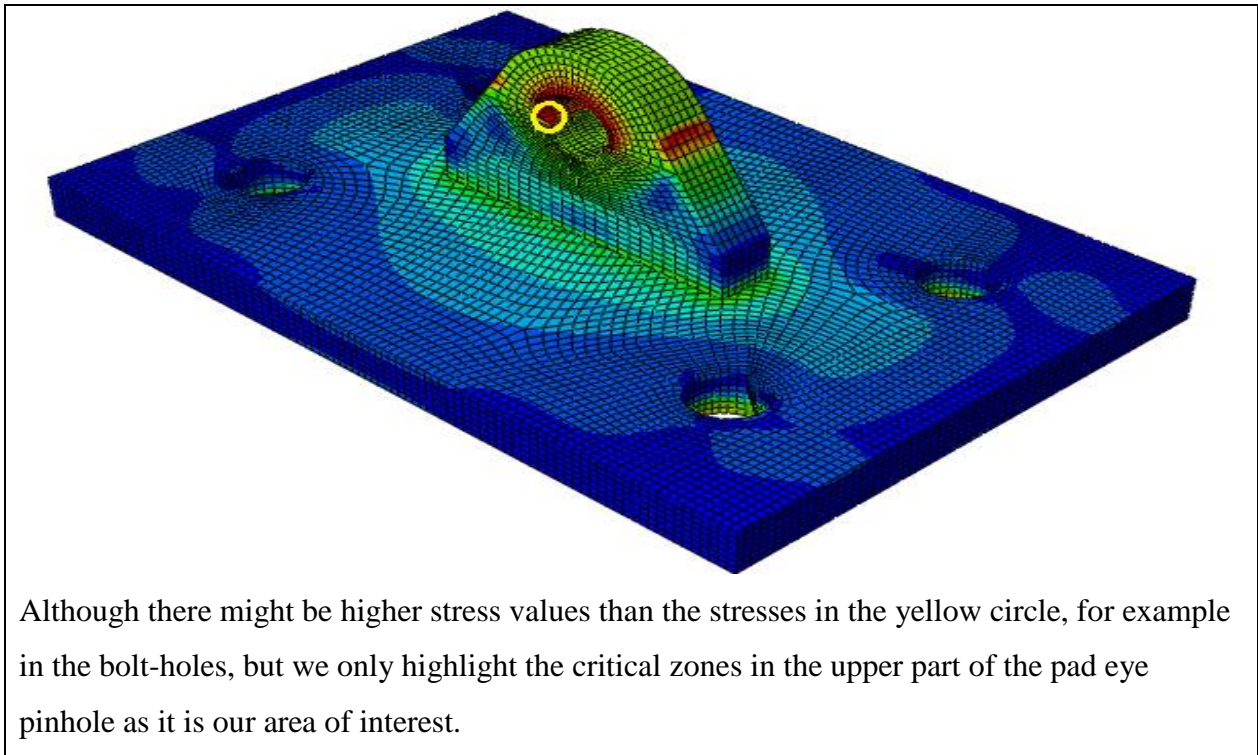
We can see from the calculations above that, F_{max1} is smaller than F_{max2}, which means:

$$F_{failure} = F_{max\,1} = \underline{\textbf{26.247 tons}}\text{ (Capacity)}$$
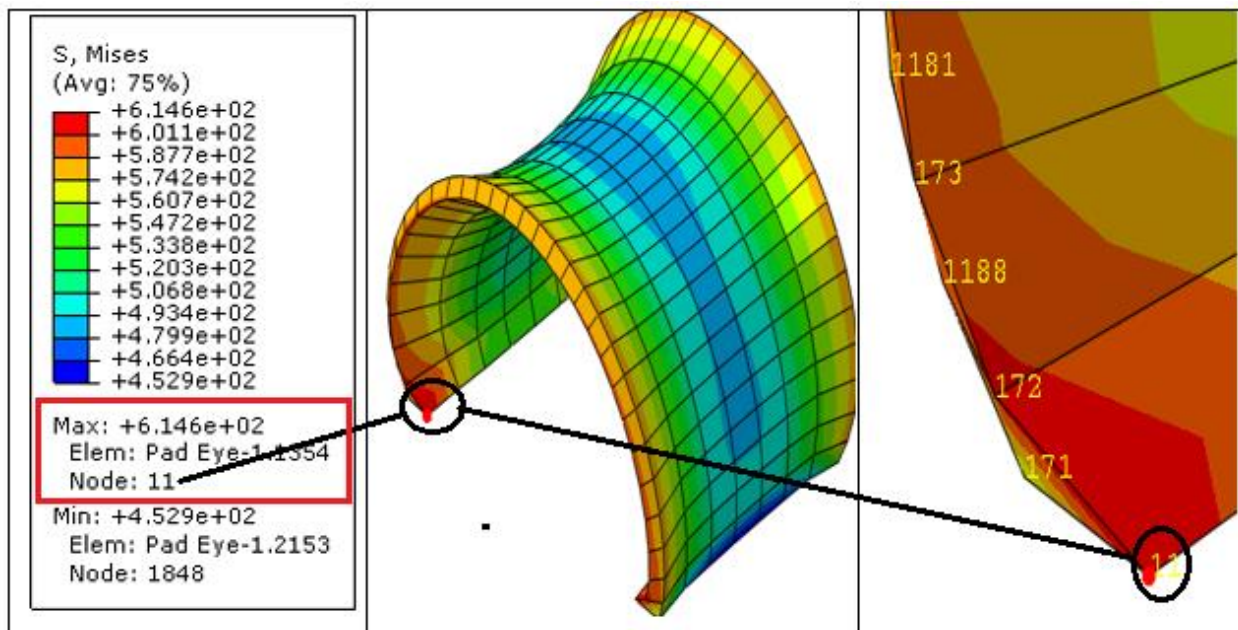
Vertical displacement, U_2 (From Pressure vs. Displacement graph) at pressure failure load

($P_{max\,1}$= 585$\frac{N}{mm^2}$) is equal to **0.25 mm.**
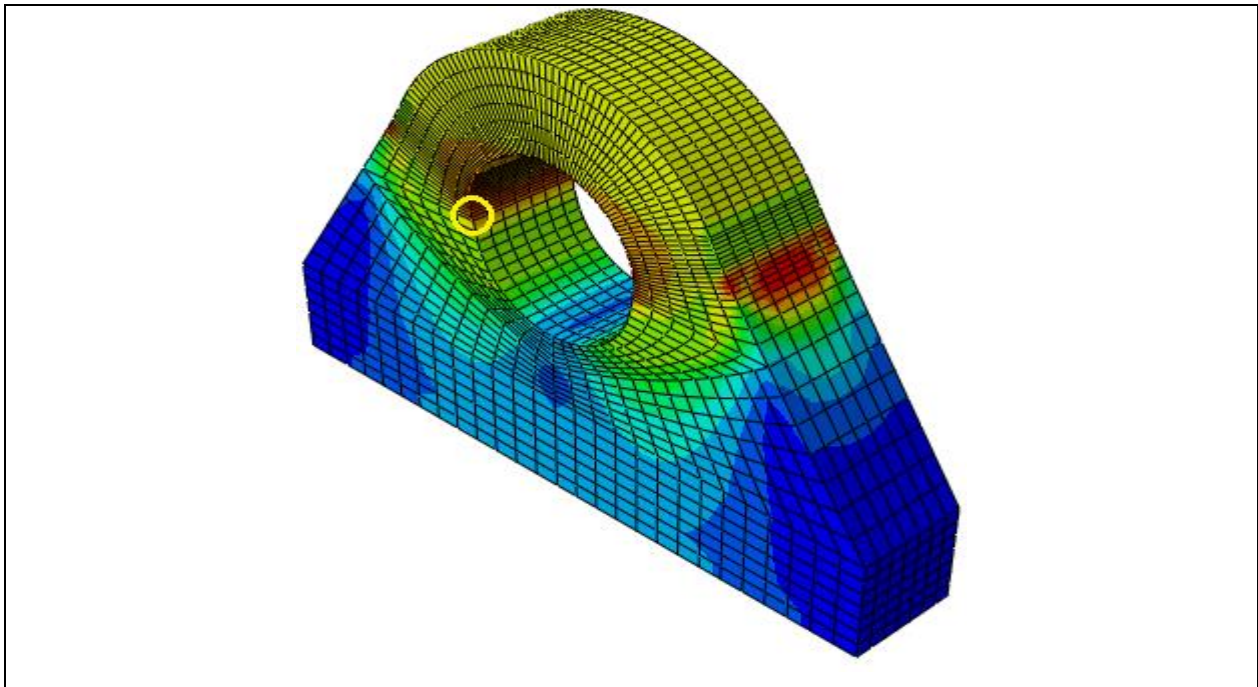
D.14

Test 3 (pad eye without plate):

Critical zone (yellow circle) in pad eye pinhole, without plate (Test 3)

Pad eye pinhole, for pad eye without plate (Test 3)

D.15
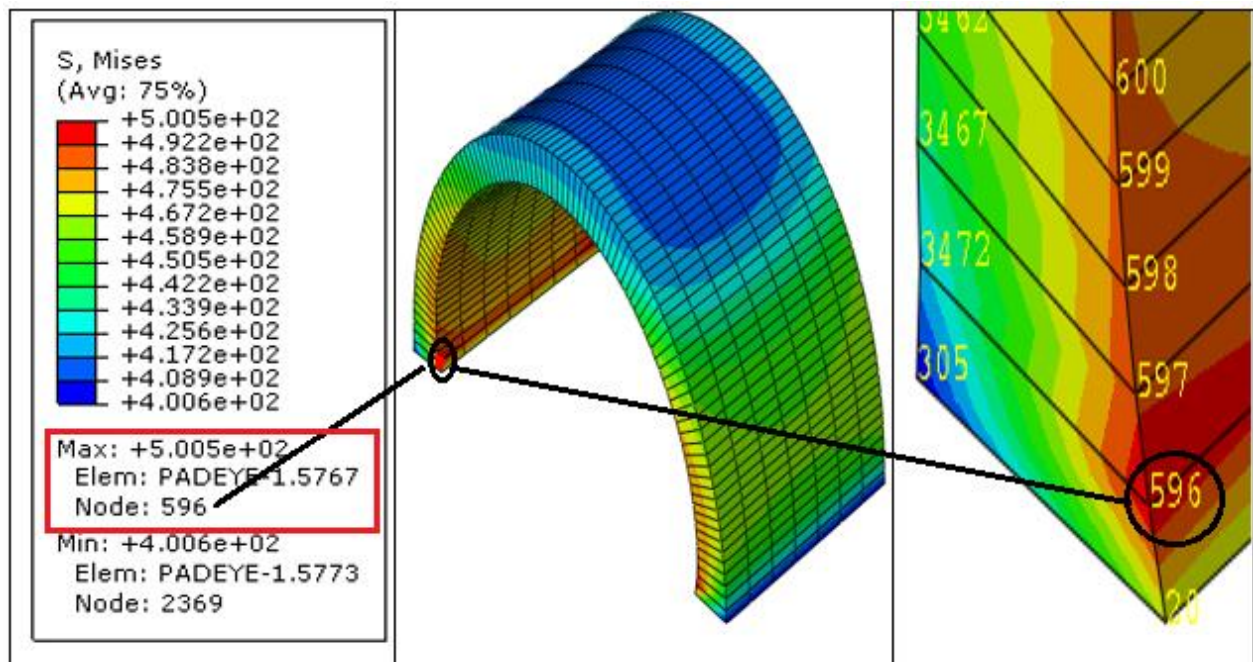
```
Source 1
---------

   ODB: C:/Temp/35STEPS+011.odb
   Step: Padeye loading
   Frame: Increment      38261: Step Time =    0.1000

Loc 1 : Nodal values from source 1

Output sorted by column "Node Label".

Field Output reported at nodes for part: PADEYE-1
   Computation algorithm: EXTRAPOLATE_COMPUTE_AVERAGE
   Averaged at nodes
   Averaging regions: ODB_REGIONS

          Node        U.U2          PEEQ        S.Mises       S.S11         S.S22         S.S33
          Label       @Loc 1       @Loc 1       @Loc 1       @Loc 1        @Loc 1        @Loc 1
       ------------------------------------------------------------------------------------------
            20     236.673E-03   134.404E-03    468.499      -65.8796      266.786       8.17879
           596     326.843E-03   193.903E-03    500.484     -148.648       252.733      -9.75081
           597     438.992E-03   198.372E-03    490.233     -231.890       264.400      -17.4009
          2369     79.3266E-03   32.9215E-03    400.574      -97.5582      289.700       43.6202


Minimum          79.3266E-03   32.9215E-03    400.574     -231.890       252.733      -17.4009

     At Node          2369          2369          2369          597           596           597
Maximum           438.992E-03   198.372E-03    500.484      -65.8796      289.700       43.6202

     At Node          597           597           596           20           2369          2369
```

Calculations based on graphs in Table 4.8

<u>Von Mises</u> (from Pressure vs. Stress graph)

$$F_{max\,1} = P_{max\,1} * D * t = 340\frac{N}{mm^2} * 32mm * 20mm = 217\ 600\ N = \underline{22.179\ tons}$$

<u>Plastic equivalent strain PEEQ</u> (from Pressure vs. Strain graph)

$$F_{max\,2} = P_{max\,2} * D * t = 350\frac{N}{mm^2} * 32mm * 20mm = 224\ 000\ N\ = \underline{22.831\ tons}$$

We can see from the calculations above that, F_{max1} is smaller than F_{max2}, which means:

$$F_{failure} = F_{max\,1} = \underline{\textbf{22.179 tons}}\ \text{(Capacity)}$$

Vertical displacement, U_2 (From Pressure vs. Displacement graph) at pressure failure load (P_{max1}= 340 $\frac{N}{mm^2}$) is equal to **0.180 mm.**

Test 3 (pad eye with plate):
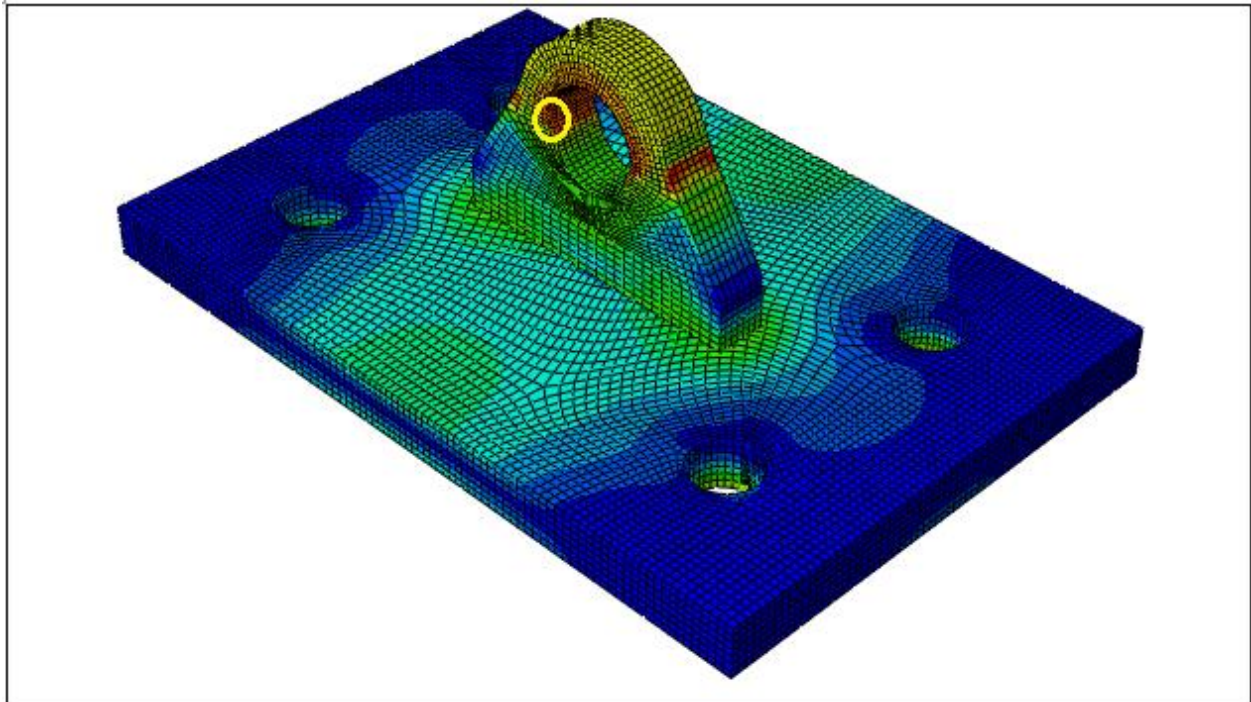
Critical zone (yellow circle) in pad eye with plate (Test 3)

Pad eye pinhole, for pad eye with plate (Test 3)

D.17
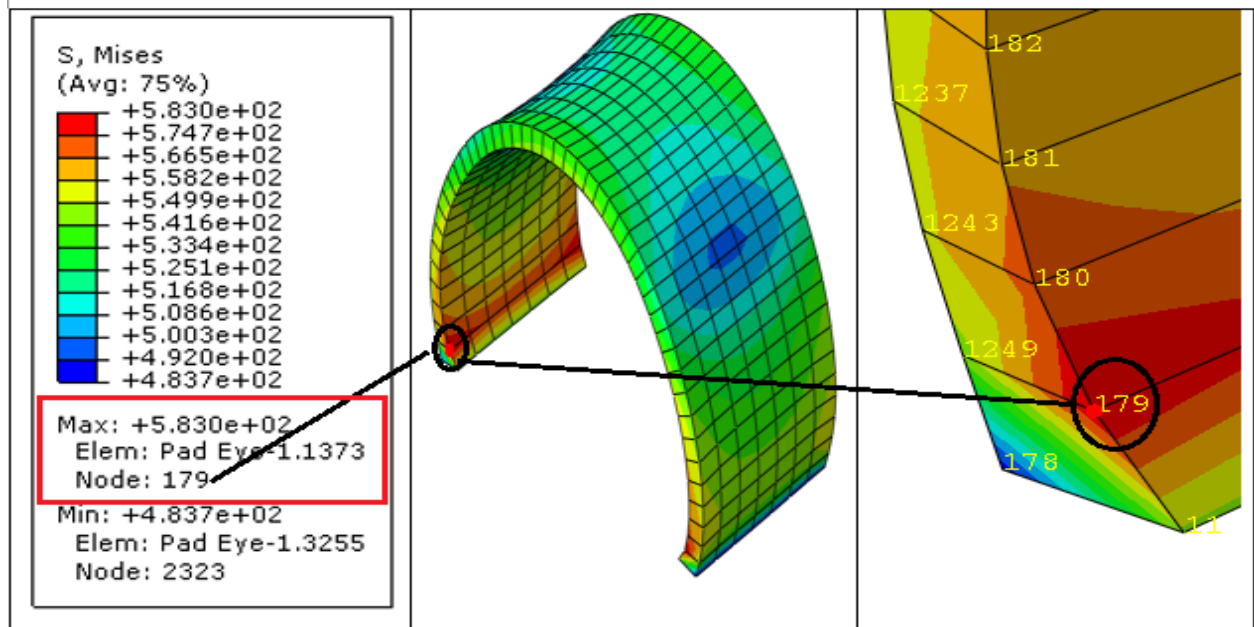
```
ODB: C:/Temp/0025+8steps.odb
Step: Apply load
Frame: Increment     8510: Step Time =   2.5000E-02

Loc 1 : Nodal values from source 1

Output sorted by column "Node Label".

Field Output reported at nodes for part: Pad Eye-1
   Computation algorithm: EXTRAPOLATE_COMPUTE_AVERAGE
   Averaged at nodes
   Averaging regions: ODB_REGIONS
```

Node Label	U.U2 @Loc 1	PEEQ @Loc 1	S.Mises @Loc 1	S.S11 @Loc 1	S.S22 @Loc 1	S.S33 @Loc 1
11	1.19170	406.729E-03	548.620	-3.37486	65.6654	4.83485
179	1.52217	633.949E-03	583.013	-186.351	114.360	-6.38940
180	2.12021	590.446E-03	570.320	-340.361	209.604	-25.6050
1782	912.126E-03	183.339E-03	483.806	-99.4071	194.230	1.98294
Minimum	912.126E-03	183.339E-03	483.806	-340.361	65.6654	-25.6050
At Node	1782	1782	1782	180	11	180
Maximum	2.12021	633.949E-03	583.013	-3.37486	209.604	4.83485
At Node	180	179	179	11	180	11

Calculations based on graphs in Table 4.9

<u>Von Mises</u> (from Pressure vs. Stress graph)

$$F_{max\,1} = P_{max\,1} * D * t = 375 \frac{N}{mm^2} * 32mm * 20mm = 240\,000\,N = \underline{24.464\,tons}$$

<u>Plastic equivalent strain PEEQ</u> (from Pressure vs. Strain graph)

$$F_{max\,2} = P_{max\,2} * D * t = 385 \frac{N}{mm^2} * 32mm * 20mm = 246\,400\,N = \underline{25.117\,tons}$$

We can see from the calculations above that, F_{max1} is smaller than F_{max2}, which means:

$$F_{failure} = F_{max\,1} = \underline{\textbf{24.464 tons}}\,(\text{Capacity})$$

Vertical displacement, U_2 (From Pressure vs. Displacement graph) at pressure failure load $(P_{max\,1} = 375 \frac{N}{mm^2})$ is equal to **0.750 mm.**

Test 4 (pad eye without plate):
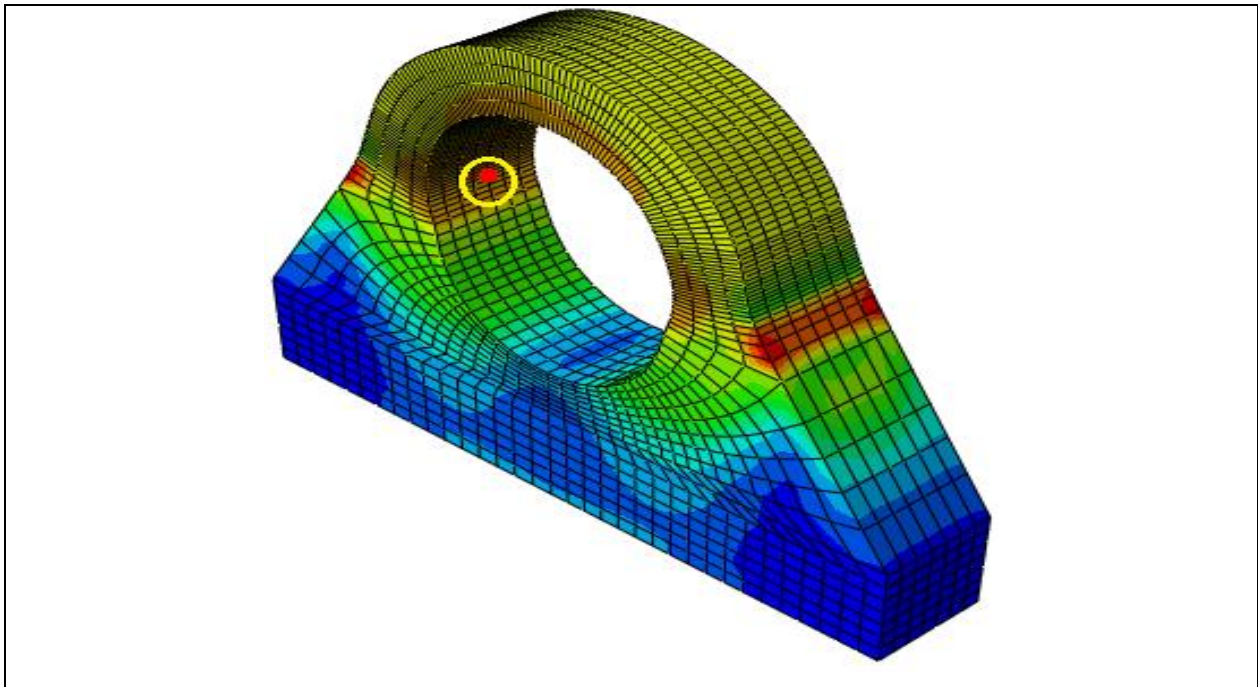
Critical zone (yellow circle) in pad eye pinhole, without plate (Test 4)
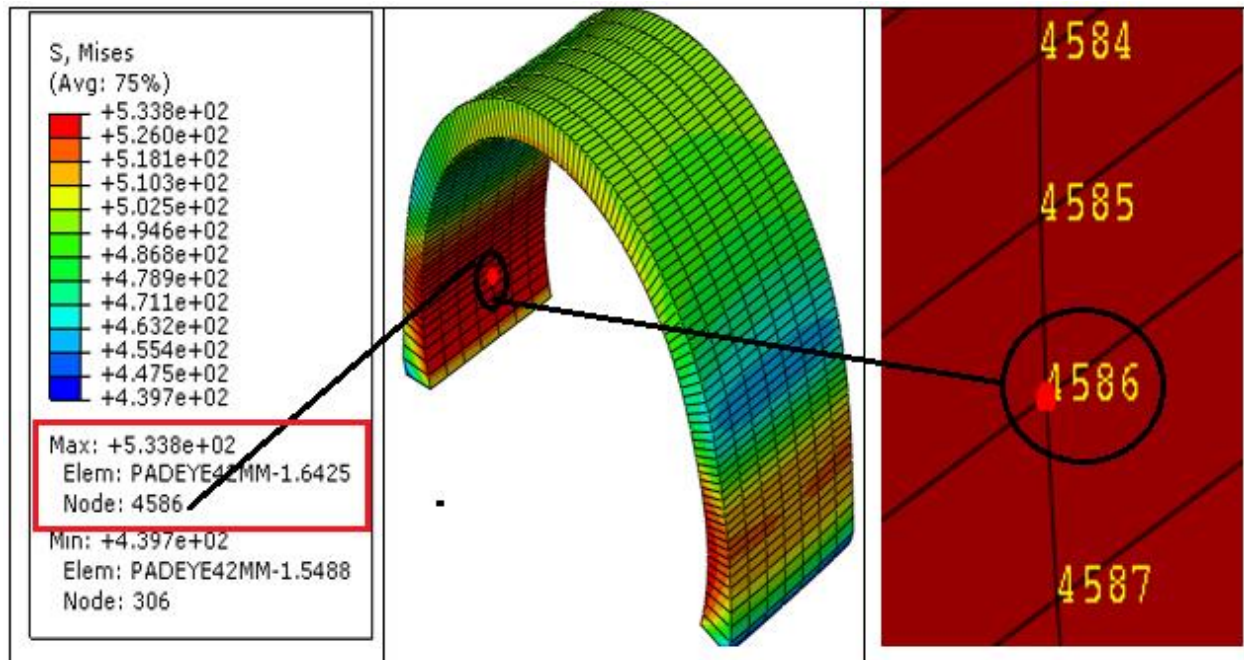
Pad eye pinhole, for pad eye without plate (Test 4)

```
ODB: C:/Temp/5step+00375.odb
Step: Padeye load
Frame: Increment      15155: Step Time =    3.7500E-02

Loc 1 : Nodal values from source 1

Output sorted by column "Node Label".

Field Output reported at nodes for part: PADEYE42MM-1
   Computation algorithm: EXTRAPOLATE_COMPUTE_AVERAGE
   Averaged at nodes
   Averaging regions: ODB_REGIONS

          Node        U.U2         PEEQ        S.Mises       S.S11        S.S22        S.S33
          Label      @Loc 1       @Loc 1       @Loc 1       @Loc 1       @Loc 1       @Loc 1
----------------------------------------------------------------------------------------------------
          4585      2.28137    352.156E-03    533.786      -212.745      394.070    281.154E-03
          4586      2.03786    351.769E-03    533.826      -210.019      395.242   -385.123E-03
          4587      1.77012    348.983E-03    533.486      -202.676      394.197      -1.80422
          9335    843.462E-03  242.188E-03    503.337      -147.872      408.550       37.3035
          9338    583.299E-03  204.486E-03    490.266      -123.249      399.051       45.2898


Minimum        583.299E-03  204.486E-03    490.266      -212.745      394.070      -1.80422

   At Node        9338         9338          9338          4585         4585          4587
Maximum           2.28137   352.156E-03    533.826      -123.249      408.550       45.2898

   At Node         4585         4585          4586          9338         9335          9338
```

Calculations based on graphs in Table 4.10

<u>Von Mises</u> (from Pressure vs. Stress graph)

$$F_{max\,1} = P_{max\,1} * D * t = 255\frac{N}{mm^2} * 42mm * 20mm = 214\,200\,N = \underline{21.834\;tons}$$

<u>Plastic equivalent strain PEEQ</u> (from Pressure vs. Strain graph)

$$F_{max\,2} = P_{max\,2} * D * t = 250\frac{N}{mm^2} * 42mm * 20mm = 210\,000\,N = \underline{21.406\;tons}$$

We can see from the calculations above that, F_{max2} is smaller than F_{max1}, which means:

$$F_{failure} = F_{max\,2} = \underline{\textbf{21.406\;tons}}\;(\text{Capacity})$$

Vertical displacement, U_2 (From Pressure vs. Displacement graph) at pressure failure load

$(P_{max\,1} = 250\frac{N}{mm^2})$ is equal to **0.800 mm.**

Test 4 (pad eye with plate):
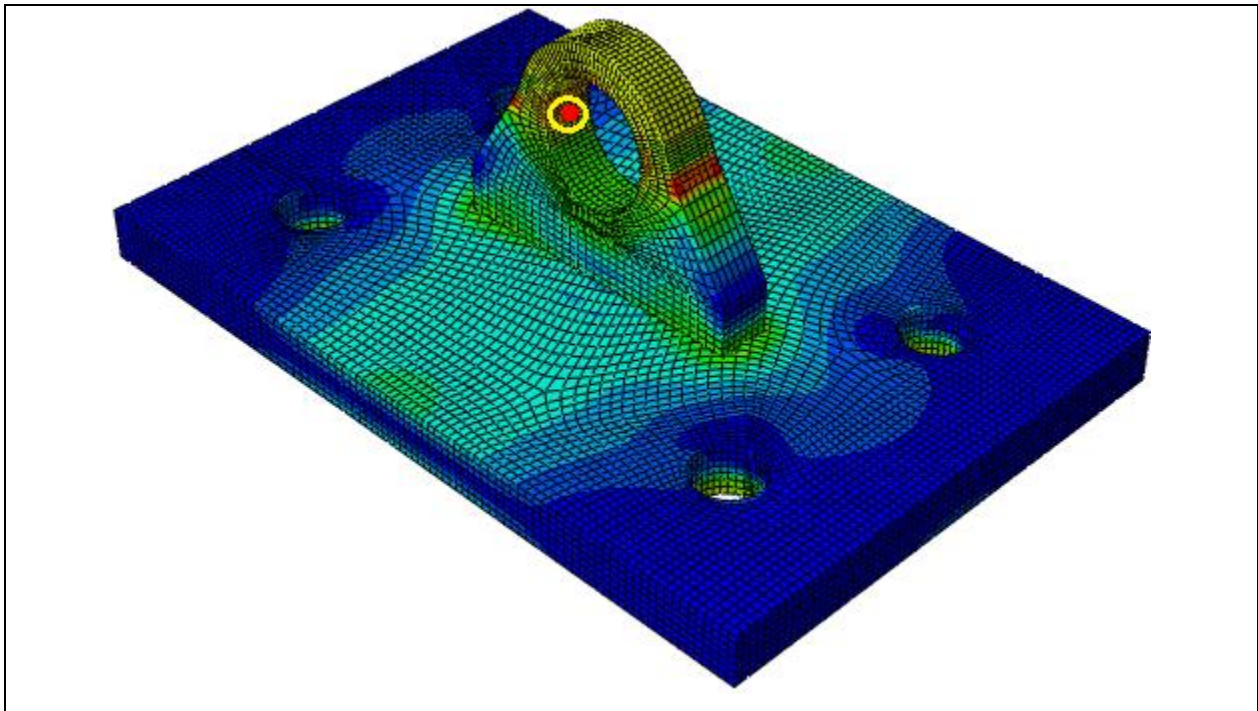
Critical zone (yellow circle) in pad eye pinhole, with plate (Test 4)

Pad eye pinhole, for pad eye without plate (Test 4)

D.21

```
ODB: C:/Temp/3steps+002+42mm.odb
Step: Apply load
Frame: Increment     6292: Step Time =   2.0000E-02

Loc 1 : Nodal values from source 1

Output sorted by column "Node Label".

Field Output reported at nodes for part: Pad Eye-1
   Computation algorithm: EXTRAPOLATE_COMPUTE_AVERAGE
   Averaged at nodes
   Averaging regions: ODB_REGIONS
```

Node Label	U.U2 @Loc 1	PEEQ @Loc 1	S.Mises @Loc 1	S.S11 @Loc 1	S.S22 @Loc 1	S.S33 @Loc 1
330	982.418E-03	200.674E-03	493.978	-50.2486	331.487	36.8722
1803	688.516E-03	84.6120E-03	431.118	-70.4635	344.079	50.9537
2041	1.64480	272.603E-03	513.103	-214.749	353.780	-13.8700
2042	1.27900	263.131E-03	515.171	-155.234	343.513	10.1992
Minimum	688.516E-03	84.6120E-03	431.118	-214.749	331.487	-13.8700
At Node	1803	1803	1803	2041	330	2041
Maximum	1.64480	272.603E-03	515.171	-50.2486	353.780	50.9537
At Node	2041	2041	2042	330	2041	1803

Calculations based on graphs in Table 4.11

<u>Von Mises</u> (from Pressure vs. Stress graph)

$$F_{max\,1} = P_{max\,1} * D * t = 275\frac{N}{mm^2} * 42mm * 20mm = 231\,000\,N = \underline{23.547\,tons}$$

<u>Plastic equivalent strain PEEQ</u> (from Pressure vs. Strain graph)

$$F_{max\,2} = P_{max\,2} * D * t = 280\frac{N}{mm^2} * 42mm * 20mm = 235\,200\,N = \underline{23.975\,tons}$$

We can see from the calculations above that, F_{max1} is smaller than F_{max2}, which means:

$$F_{failure} = F_{max\,2} = \underline{\textbf{23.547 tons}}\,(Capacity)$$
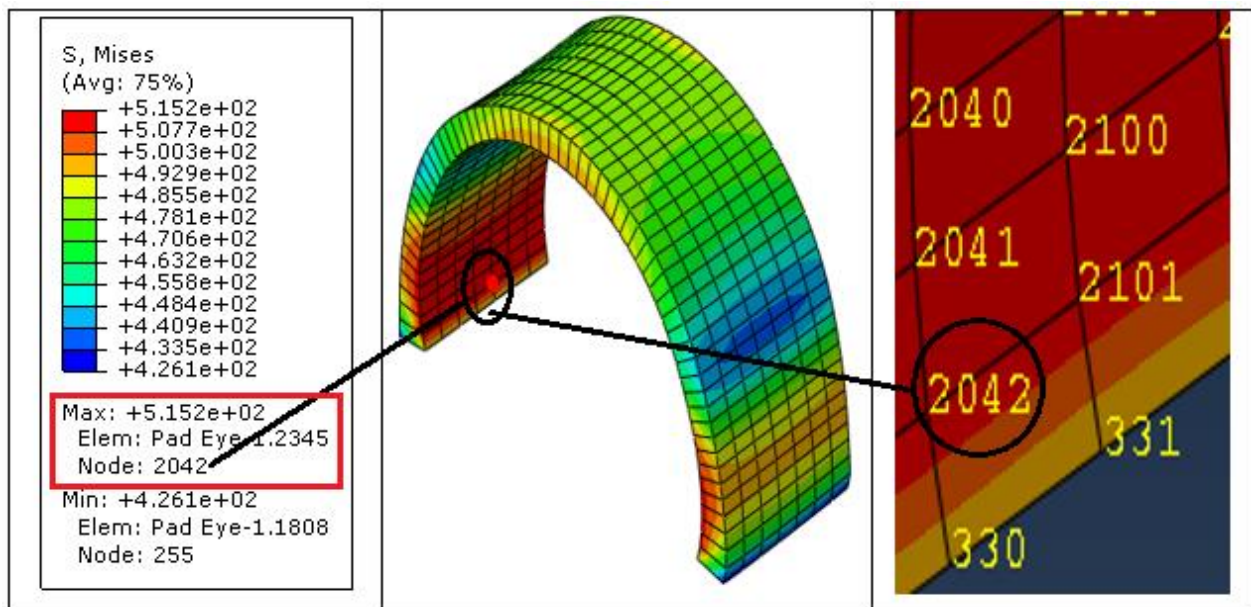
Vertical displacement, U_2 (From Pressure vs. Displacement graph) at pressure failure load $(P_{max\,1}= 275\frac{N}{mm^2})$ is equal to <u>**0.850 mm.**</u>

Test 5 (pad eye without plate):
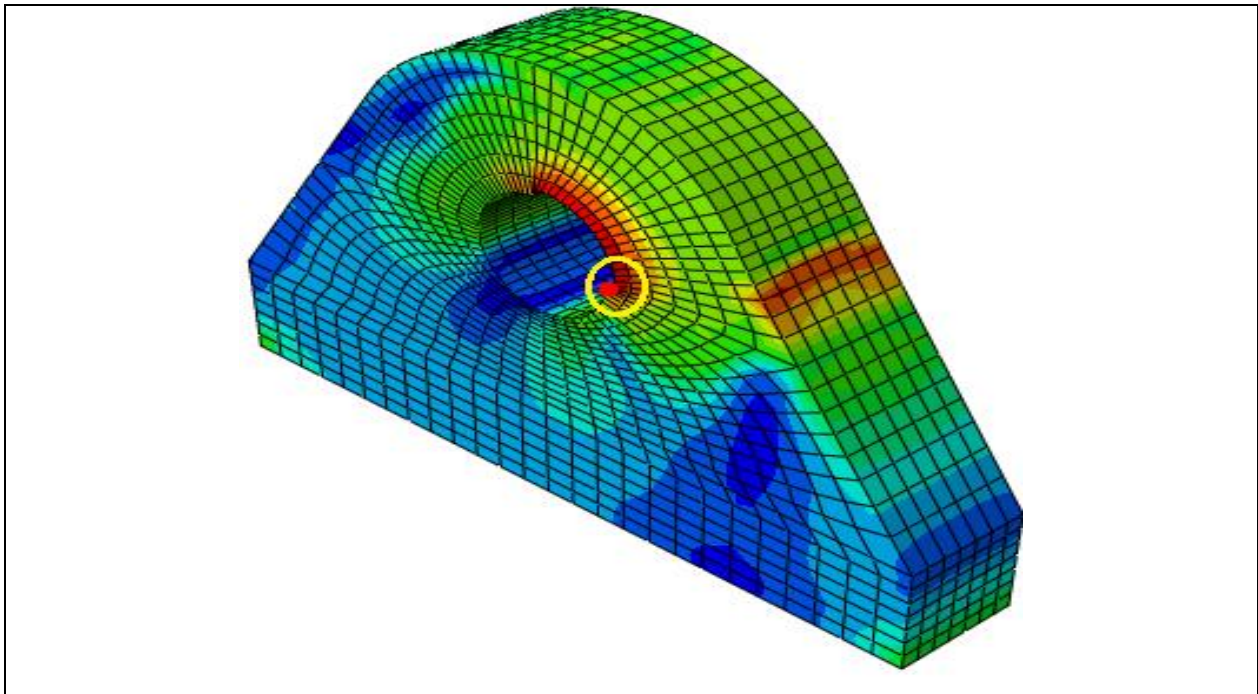
Critical zone (yellow circle) in pad eye pinhole, without plate (Test 5)

Pad eye pinhole, for pad eye without plate (Test 5)

D.23
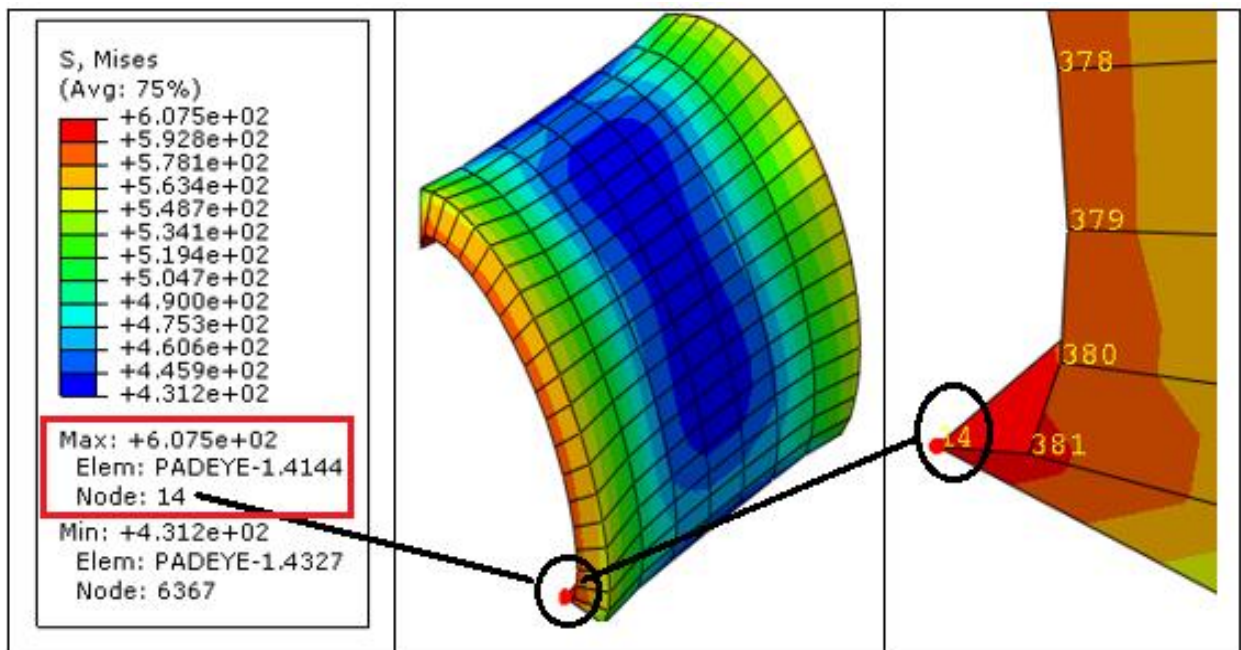
```
ODB: C:/Temp/angledloading22mmpdwithoutplate.odb
Step: Padeye loading
Frame: Increment    2771: Step Time =   9.0000E-03

Loc 1 : Nodal values from source 1

Output sorted by column "Node Label".

Field Output reported at nodes for part: PADEYE-1
  Computation algorithm: EXTRAPOLATE_COMPUTE_AVERAGE
  Averaged at nodes
  Averaging regions: ODB_REGIONS
```

Node Label	U.U1 @Loc 1	U.U2 @Loc 1	U.U3 @Loc 1	PEEQ @Loc 1	S.Mises @Loc 1	S.S11 @Loc 1	S.S22 @Loc 1	S.S33 @Loc 1
14	1.02876	-165.742E-03	486.335E-03	749.951E-03	607.500	-94.7948	-354.663	-73.5294
379	3.35082	470.890E-03	1.50037	653.233E-03	583.911	-598.501	-55.3616	-196.727
380	2.91416	117.764E-03	1.27193	681.800E-03	587.380	-536.596	-89.8036	-185.231
381	2.24291	-167.783E-03	940.964E-03	865.314E-03	597.793	-356.710	-222.716	-161.893
Minimum	1.02876	-167.783E-03	486.335E-03	653.233E-03	583.911	-598.501	-354.663	-196.727
At Node	14	381	14	379	379	379	14	379
Maximum	3.35082	470.890E-03	1.50037	865.314E-03	607.500	-94.7948	-55.3616	-73.5294
At Node	379	379	379	381	14	14	379	14

Calculations based on graphs in Table 4.12

<u>Von Mises</u> (from Pressure vs. Stress graph)

$$F_{max\,1} = 0.85 * P_{max\,1} * D * t = 0.85 * 590\,\frac{N}{mm^2} * 22mm * 20mm = 220\,660\,N = \underline{22.493\,tons}$$

<u>Plastic equivalent strain PEEQ</u> (from Pressure vs. Strain graph)

$$F_{max\,2} = 0.85 * P_{max\,2} * D * t = 595\,\frac{N}{mm^2} * 22mm * 20mm = 222\,530\,N = \underline{22.684\,tons}$$

We can see from the calculations above that, F_{max1} is smaller than F_{max2}, which means:

$$F_{failure} = F_{max\,2} = \underline{22.493\,tons}\,(\text{Capacity})$$

Vertical displacement, U_2 (From Pressure vs. Displacement graph) at pressure failure load $(P_{max\,1} = 590\,\frac{N}{mm^2})$ is equal to **0.0085 mm.**

Test 6 (pad eye without plate):
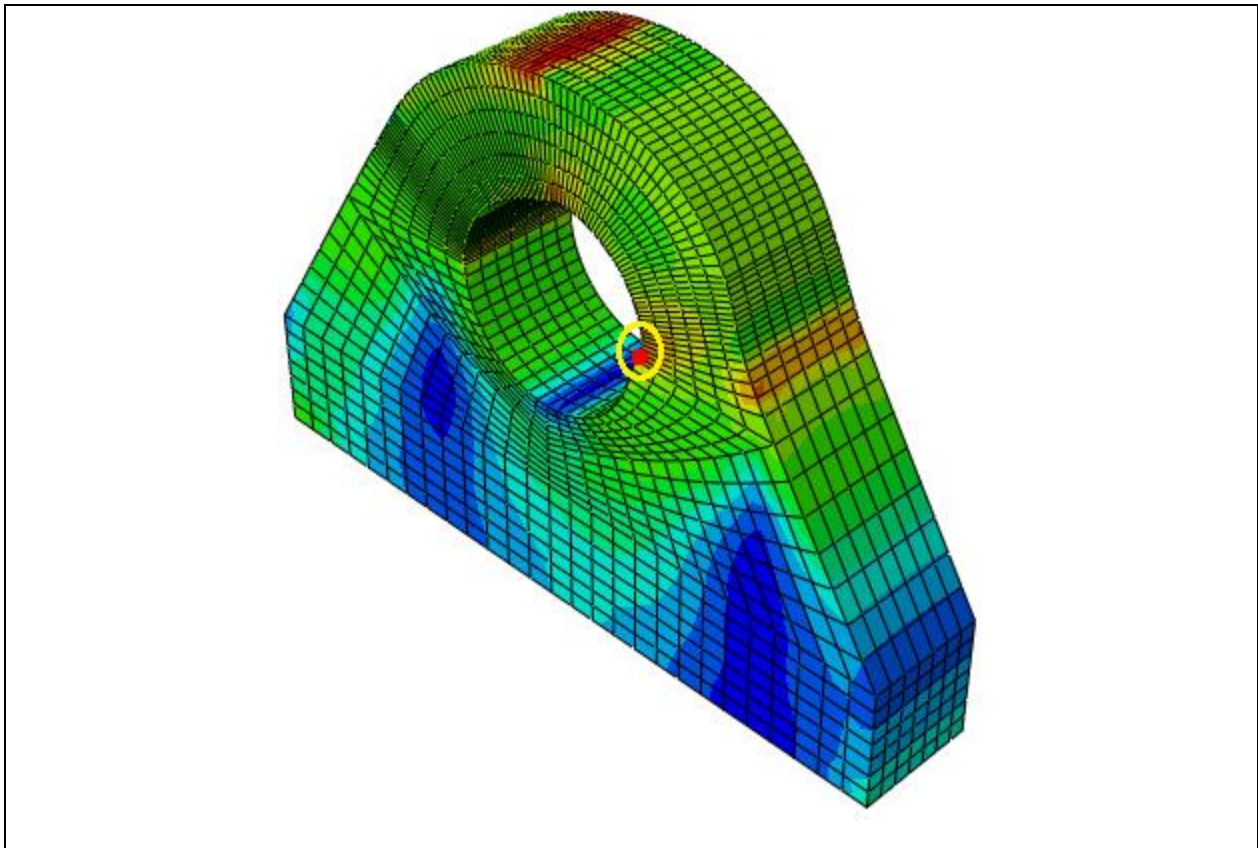
Critical zone (yellow circle) in pad eye pinhole, without plate (Test 6)
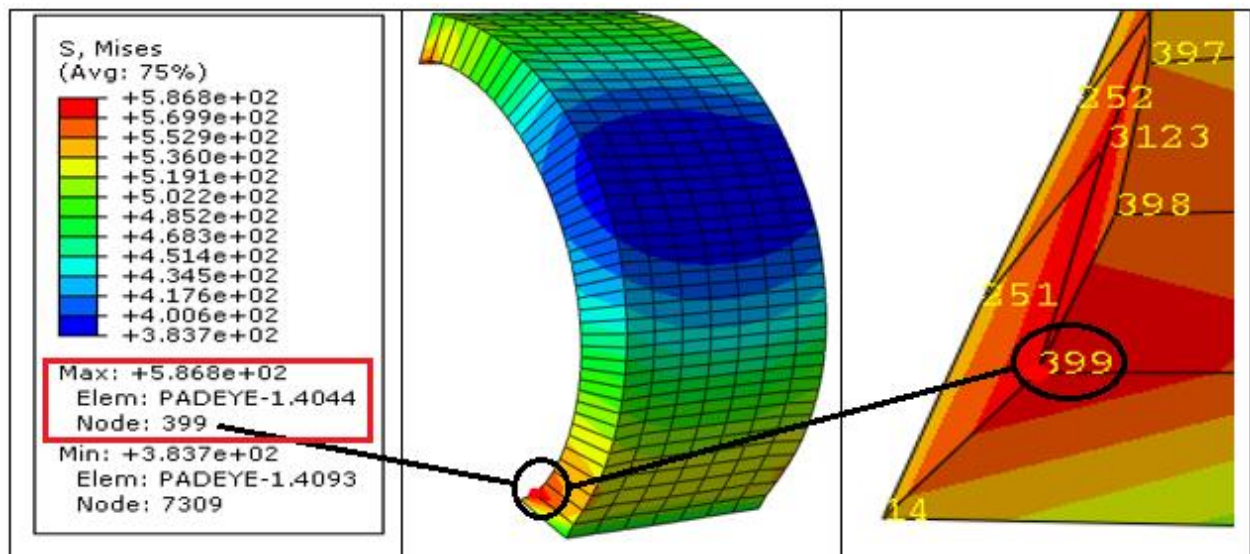
Pad eye pinhole, for pad eye without plate (Test 6)

```
ODB: C:/Temp/angled32mmwithoutplate.odb
Step: Padeye loading
Frame: Increment     58978: Step Time =   0.1500

Loc 1 : Nodal values from source 1

Output sorted by column "Node Label".

Field Output reported at nodes for part: PADEYE-1
  Computation algorithm: EXTRAPOLATE_COMPUTE_AVERAGE
  Averaged at nodes
  Averaging regions: ODB_REGIONS
```

Node Label	U.U1 @Loc 1	U.U2 @Loc 1	U.U3 @Loc 1	PEEQ @Loc 1	S.Mises @Loc 1	S.S11 @Loc 1	S.S22 @Loc 1	S.S33 @Loc 1
14	1.11715	532.533E-03	-183.073E-03	420.181E-03	547.147	15.8899	70.7929	17.4947
397	2.66671	1.26789	222.672E-03	454.497E-03	552.886	-343.795	227.579	-20.3519
398	2.36553	1.00233	116.427E-03	514.341E-03	562.535	-272.308	195.782	-16.7224
399	1.88771	719.850E-03	-32.1006E-03	604.895E-03	586.776	-106.864	104.104	-418.615E-03
Minimum	1.11715	532.533E-03	-183.073E-03	420.181E-03	547.147	-343.795	70.7929	-20.3519
At Node	14	14	14	14	14	397	14	397
Maximum	2.66671	1.26789	222.672E-03	604.895E-03	586.776	15.8899	227.579	17.4947
At Node	397	397	397	399	399	14	397	14

Calculations based on graphs in Table 4.13

<u>Von Mises</u> (from Pressure vs. Stress graph)

$$F_{max\,1} = 0.85 * P_{max\,1} * D * t = 0.85 * 395\,\frac{N}{mm^2} * 32mm * 20mm = 214\,880\,N = \underline{21.904\ tons}$$

<u>Plastic equivalent strain PEEQ</u> (from Pressure vs. Strain graph)

$$F_{max\,2} = 0.85 * P_{max\,2} * D * t = 405\,\frac{N}{mm^2} * 32mm * 20mm = 220\,320\,N = \underline{22.458\ tons}$$

We can see from the calculations above that, F_{max1} is smaller than F_{max2}, which means:

$$F_{failure} = F_{max\,2} = \underline{\textbf{21.904\ tons}}\,\text{(Capacity)}$$

Vertical displacement, U_2 (From Pressure vs. Displacement graph) at pressure failure load $(P_{max\,1}= 590\,\frac{N}{mm^2})$ is equal to <u>**0.150 mm.**</u>

Test 7: Pad eye without the plate
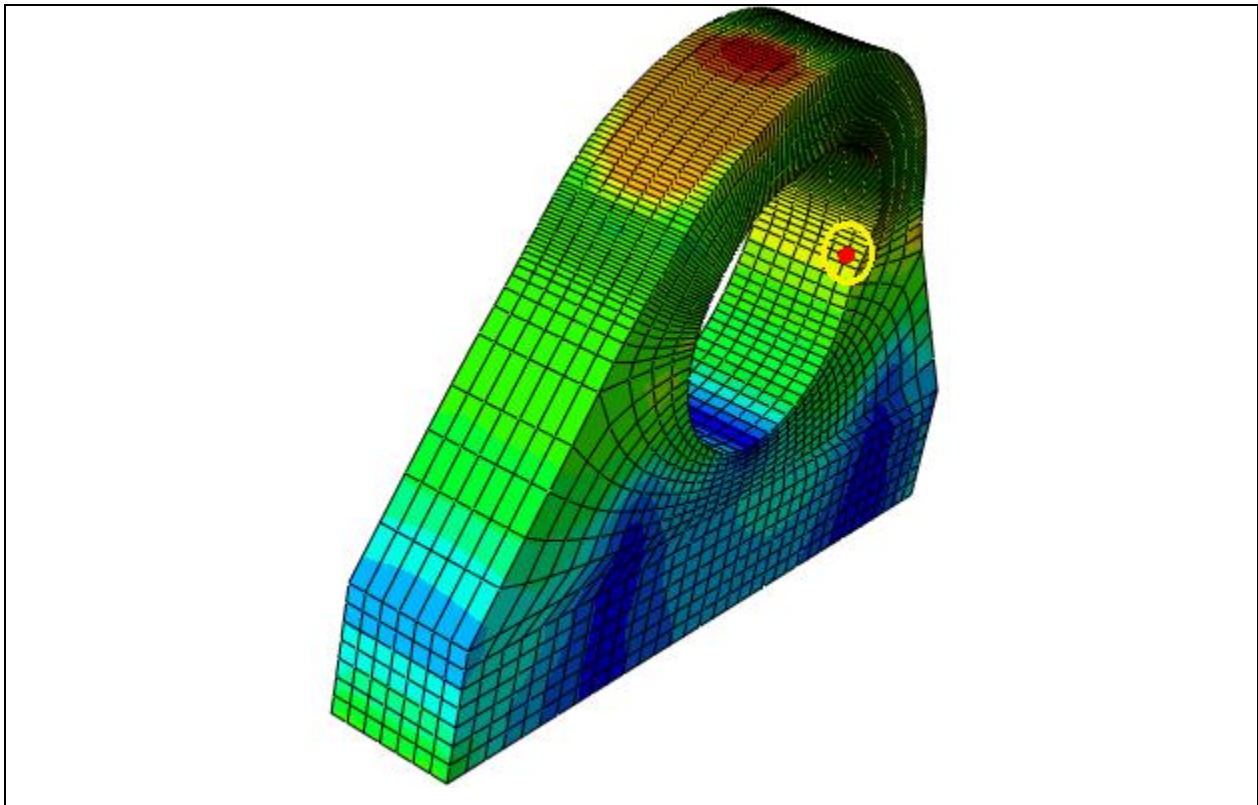
Critical zone (yellow circle) in pad eye pinhole, without plate (Test 7)
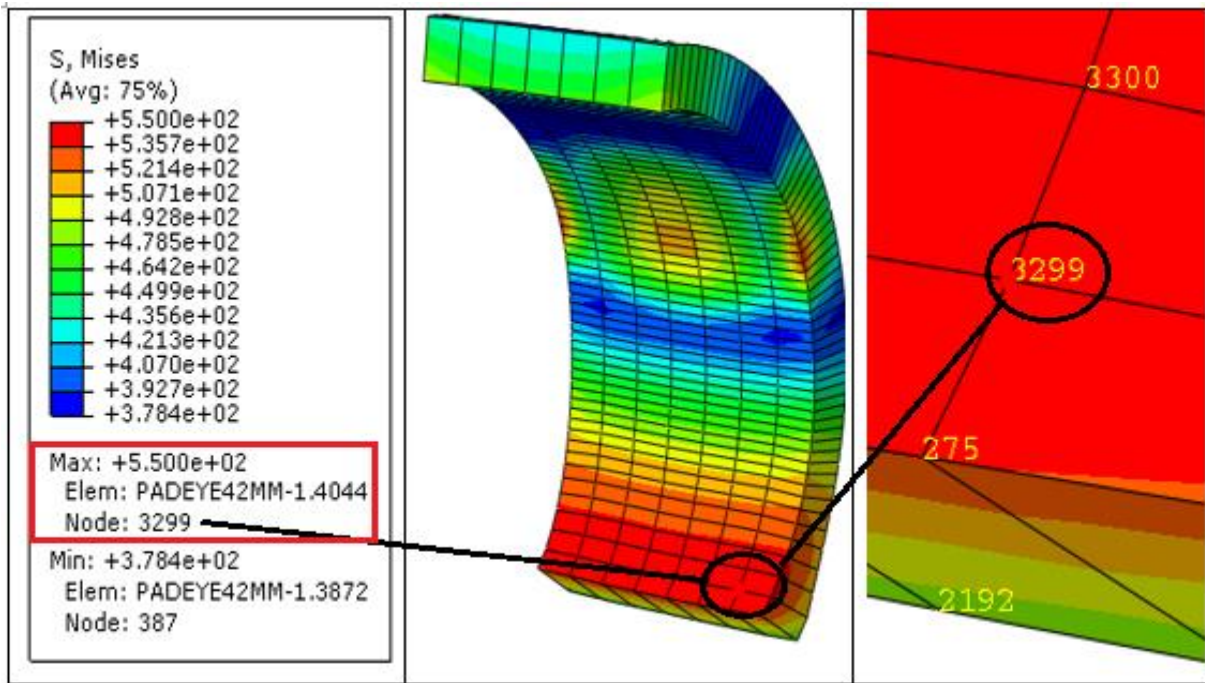
Pad eye pinhole, for pad eye without plate (Test 6)

```
ODB: C:/Temp/angled42mm.odb
Step: Padeye load
Frame: Increment     12928: Step Time =   3.0000E-02

Loc 1 : Nodal values from source 1

Output sorted by column "Node Label".

Field Output reported at nodes for part: PADEYE42MM-1
   Computation algorithm: EXTRAPOLATE_COMPUTE_AVERAGE
   Averaged at nodes
   Averaging regions: ODB_REGIONS

         Node        U.U1         U.U2         U.U3         PEEQ       S.Mises        S.S11        S.S22        S.S33
         Label      @Loc 1       @Loc 1       @Loc 1       @Loc 1      @Loc 1       @Loc 1       @Loc 1       @Loc 1
-----------------------------------------------------------------------------------------------------------------------
          275      1.55488      1.08441     -412.573E-03   311.594E-03   536.269      -12.3181      296.948       17.5005
         2192   864.972E-03   512.017E-03  -166.160E-03   185.112E-03   485.289      -49.3887      368.584       55.7724
         3299      2.08535      1.35867     -386.265E-03   389.909E-03   549.954      -94.1204      307.012       15.0478
         7750      1.11264   721.653E-03   -169.561E-03   249.622E-03   509.115      -84.2563      389.063       58.0944


Minimum       864.972E-03   512.017E-03  -412.573E-03   185.112E-03   485.289      -94.1204      296.948       15.0478

   At Node       2192         2192          275          2192         2192         3299          275          3299
Maximum          2.08535      1.35867     -166.160E-03   389.909E-03   549.954      -12.3181      389.063       58.0944

   At Node       3299         3299          2192         3299         3299          275         7750          7750
```

Calculations based on graphs in Table 4.14

Von Mises (from Pressure vs. Stress graph)

$$F_{\max 1} = 0.85 * P_{\max 1} * D * t = 0.85 * 280\,\frac{N}{mm^2} * 42mm * 20mm = 199\,920\,N = \underline{20.379\ tons}$$

Plastic equivalent strain PEEQ (from Pressure vs. Strain graph)

$$F_{\max 1} = 0.85 * P_{\max 1} * D * t = 0.85 * 280\,\frac{N}{mm^2} * 42mm * 20mm = 199\,920\,N = \underline{20.379\ tons}$$

We can see from the calculations above that, F$_{max1}$ is equally large as F$_{max2}$, which means:

$$F_{failure} = F_{\max 1} = F_{\max 2} = \underline{\mathbf{20.379\ tons}}\ (\text{Capacity})$$

Vertical displacement, U$_2$ (From Pressure vs. Displacement graph) at pressure failure load
($P_{\max 1} = 280\,\frac{N}{mm^2}$) is equal to **0.600 mm.**

D.28